

# Searching for substellar companion candidates with Gaia.

## III. Search for companions to members of young associations

A.-M. Lagrange<sup>1,2</sup>, F. Kiefer<sup>1</sup>, P. Rubini<sup>3</sup>, V. Squicciarini<sup>1,4</sup>, A. Chomez<sup>1,2</sup>, J. Milli<sup>2</sup>, A. Zurlo<sup>5,6</sup>, J. Bouvier<sup>2</sup>, P. Delorme<sup>2</sup>, H. Beust<sup>2</sup>, J. Mazoyer<sup>1</sup>, O. Flasseur<sup>7</sup>, N. Meunier<sup>2</sup>, L. Mignon<sup>2</sup>, G. Chauvin<sup>8</sup>, and P. Palma-Bifani<sup>8,1</sup>

<sup>1</sup> LIRA, CNRS, Observatoire de Paris, Université PSL, 92190 Meudon, France\*

<sup>2</sup> Univ. Grenoble Alpes, CNRS, IPAG, F-38000 Grenoble, France

<sup>3</sup> Pixyl, 5 Avenue du Grand Sablon, 38700 La Tronche, France

<sup>4</sup> INAF – Osservatorio Astronomico di Padova, Vicolo dell’Osservatorio 5, I-35122, Padova, Italy

<sup>5</sup> Instituto de Estudios Astrofísicos, Facultad de Ingeniería y Ciencias, Universidad Diego Portales, Av. Ejército Libertador 441, Santiago, Chile

<sup>6</sup> Millennium Nucleus on Young Exoplanets and their Moons (YEMS), Chile

<sup>7</sup> Univ. Lyon, Univ. Lyon1, ENS de Lyon, CNRS, Centre de Recherche Astrophysique de Lyon (CRAL) UMR5574, F-69230 Saint-Genis-Laval, France

<sup>8</sup> Université Côte d’Azur, OCA, CNRS, Lagrange, 96 Bd de l’Observatoire, 06300 Nice, France

Received ; accepted

### ABSTRACT

*Context.* Absolute astrometry with Gaia is expected to detect and characterize the orbits of thousands of exoplanets in the coming years. A tool, GaiaPMEX, was recently developed to characterize multiple systems based on two binarity indicators derived from the DR3 astrometric solution: the astrometric signature  $\alpha_{\text{true}}$  in linear motion residuals in Gaia-only data, and, when the sources were also observed by Hipparcos, the astrometric signature  $\alpha_{\text{PMa}}$  in the Gaia-Hipparcos proper motion anomaly (PMa).

*Aims.* Our aim is to identify close (less than typ. 20 au) (sub)stellar companion candidates to star members of close-by young associations previously monitored in radial velocity (RV) surveys. We wish to compare the detection capabilities of absolute astrometry and spectroscopy, and to characterize planetary-mass companions, combining the astrometric data with direct imaging and RV data.

*Methods.* We use GaiaPMEX to identify binary stars members of close young associations and constrain the mass and semi-major axes (sma) of possible companions. For companion masses possibly in the planetary range, we use direct imaging and when possible, RV data as well, to further constrain their nature and orbital properties.

*Results.* For each of our targets, we provide a diagnosis on its binarity based on absolute astrometry. When no binary is detected, GaiaPMEX provides detection limits in the (sma, mass) space. We identify several companions with possible masses down to the brown dwarfs (BD; 50+) or planetary masses (13). Around the M-type star G80-21, we detected a new companion orbiting at less than 1-2 au. Adding RV and high contrast imaging data shows this companion is a giant planet. In other two cases, AB Pic and HD 14082 B, we confirm the presence of substellar companions, and determine the first robust solutions for their mass and orbital properties. We further identified 9 potentially interesting candidates for planetary mass companions, which remain to be studied. Finally, a detailed treatment of noises in Gaia astrometric measurements shows that there are no evidence at a  $2\text{-}\sigma$  level of two exoplanet detections that were previously announced based on the same set of data.

*Conclusions.* Our approach allows to detect all stellar mass companions with sma in the range 0.1-10 au. For separations below 0.1 au, however, spectroscopy outperforms absolute astrometry. Combining GaiaPMEX and RV data is therefore perfectly adapted for a full exploration of the 0.01-10 au sma range when searching for stellar companions, and increases the expected rate of detections derived from RV surveys. Moreover, in the 0.5 to 5 au domain, GaiaPMEX has an excellent sensitivity to BDs, and a good sensitivity to planetary mass planets as well for this sample.

**Key words.** exoplanets detection ; astrometry ; radial velocities

### 1. Introduction

Planet formation is one of the most challenging questions in today’s astronomy. From an observational point of view, the search for low-mass companions (planets, BDs) of stars has driven a lot of efforts in the last decades, to contain statistical information on planets’ properties or to characterize exoplanets individually. In both cases, the results are compared to model outputs: population synthesis outputs for surveys, and interiors or atmospheric

models for individual objects, which in turn allow further constraining the models.

The conditions in which planetary systems form are key information that motivates, in particular, studies of stellar multiplicity. Indeed, binarity or multiplicity plays a major role in the formation and evolution of planetary systems through protoplanetary disk truncation and shape, disk lifetime, star-planet interactions, etc. The identification and characterization of multiple systems in star-forming regions or in young stellar associations have then motivated many observational efforts for decades. We refer to Offner et al. (2023) for a recent review.

\* Please send any request to anne-marie.lagrange@obspm.fr

So far, most estimates of stellar binary occurrence rates for small semi-major axis ( $\lesssim 1\text{-}10$  au) have been obtained using ground based spectroscopic surveys (see results in Offner et al. 2023). However, such surveys are biased towards nearly equal mass binaries (companion-to-star mass ratio – hereafter,  $q$  – close to 1), towards periods less than a few years, and towards inclined systems, as the "projected" radial velocity (RV) amplitude, and therefore the survey sensitivity, increases as  $\sin i$ , with  $i$  the inclination of the companion's orbital momentum with respect to the line of sight. Interferometric surveys can also detect close binaries (see ref. in Offner et al. 2023). They are also biased towards a  $q$ -ratio close to 1. High contrast imaging allows identifying companion stars with a low  $q$ -ratio, typically at separations down to 10-20 au (depending on the  $q$ -ratio). Absolute astrometry with Gaia is well suited to identify and characterize stellar multiplicity in the intermediate region (1-10 au), down to brown dwarfs companions (small  $q$ -ratio), as well as planetary mass companions (Perryman et al. 2014; Sahlmann et al. 2015; Holl et al. 2022; Gaia Collaboration et al. 2023a; Holl et al. 2023).<sup>1</sup>

Using proper motion anomalies (PMa) estimated from both Gaia and Hipparcos (hereafter PMa; see Kervella et al. 2019a; Brandt 2021a; Kervella et al. 2022) data has allowed to identify previously unknown substellar companions. Gaia data, on its own, provide information that allows both identifying companions that the PMa alone cannot detect, and lifting degeneracies in the solutions found using the PMa only. Recently, we developed GaiaExplore, a tool designed to identify binaries by analyzing the observed excess astrometric Gaia signal. Additionally, it leverages available data on PMa from both Gaia and Hipparcos data. Complementing GaiaExplore is GaiaPMEX, that allows to constrain the candidate companion mass and sma axis using the same information. GaiaPMEX is described in Kiefer et al. (2024a) (hereafter K24). It has been used already to identify planetary companion candidates around solar-type stars in Kiefer et al. (2024b).

In this paper, we use GaiaExplore and GaiaPMEX to search for companions to star members of young and close-by associations that were already surveyed in RV. Such associations have been studied in detail in the last decades as they are ideal sites to study planetary systems formation and early evolution. The young age of these associations allows us to make the best use of direct imaging to search for planetary mass companions at separations typically larger than 10 au. We identify new stellar binary systems, compare the respective sensitivities of GaiaPMEX and spectroscopic surveys, and identify possible BD and planetary mass candidates. We further vet the planetary mass candidates.

We present our approach in Section 2. We analyze the output of GaiaPMEX in Section 3, and present the results related to binarity in Section 4. We analyze the 13 systems identified with possible planetary mass companions based on Gaia and PMa data in Section 5, and further characterize three "Gaia" planets in Sections 6.2 and 6.3. Grounded on our method, we discuss in Sect. 7 the status of some candidate planets around stars from the present survey, recently detected from PMa measurements. A brief conclusion is provided in Section 8.

<sup>1</sup> Gaia spectroscopy also revealed very close companions with periods in the 1-1000d (see ref. above), but no statistical results have been derived yet.

**Table 1.** Young Moving Groups (YMG) considered in the present study, with approximate ages and distances ( $d$ ).

| YMG   | Age               | $d$ | $N_{bf}$   | $N$ | ref.        |
|-------|-------------------|-----|------------|-----|-------------|
|       | Myr               | pc  |            |     |             |
| ECH   | $\sim 5$          | 100 | 36         | 17  | (1),(1),(2) |
| TWA   | $10 \pm 3$        | 50  | 67         | 17  | (3),(1),(4) |
| BPC   | $24 \pm 3$        | 50  | $\sim 200$ | 42  | (3),(1),(5) |
| THA   | $45 \pm 4$        | 50  | 142        | 76  | (3),(6),(7) |
| COL   | $42^{+6}_{-4}$    | 50  | 50         | 43  | (3),(6),(3) |
| OCT   | $35 \pm 5$        | 130 | 48         | 16  | (8),(6),(8) |
| ARG   | $45 \pm 5$        | 70  | 40         | 30  | (3),(9),(3) |
| ABDor | $150^{+50}_{-19}$ | 30  | 89         | 46  | (3),(6),(3) |

**Notes.**  $N_{bf}$  indicates the number of bona-fide members of these groups, and  $N$  indicates the number of stars found in ZF21. References, respectively, for distance, age and  $N_{bf}$  are provided as well. (1): Kastner & Principe (2022), (2): Dickson-Vandervelde et al. (2021), (3): Bell et al. (2015), (4): Luhman (2023), (5): Shkolnik et al. (2017), (6): Gagné et al. (2018), (7): Kraus et al. (2014), (8): Murphy & Lawson (2015), (9): Zuckerman (2019).

## 2. Approach

### 2.1. Sample

We first considered the sample gathered by Zúñiga-Fernández et al. (2021) (hereafter ZF21) for their census of spectroscopic binary systems among close associations and moving groups (MG, see Table 1):  $\beta$  Pictoris (BPC), Octans (OCT),  $\epsilon$  Chamaeleontis (ECH), TW Hya (TWA), Argus (ARG), AB Doradus (ABDor), Columba (COL) and Tucana-Horologium (THA). Their primary membership assessment relies on the SACY approach, described in Torres et al. (2006) and in Torres et al. (2008). They also use the BANYAN  $\Sigma$  classification<sup>2</sup> (hereafter BANYAN) based on Gaia DR2 (Gagné et al. 2018). The SACY and BANYAN classifications do not always agree; in particular, 60 targets have a BANYAN-based membership but no SACY-based membership.<sup>3</sup> ZF21 considered both classifications in their analysis, and so did we. An additional criterion in their selection process was that at least one spectrum or one radial velocity (either coming from ground-based surveys or from Gaia DR2) with an uncertainty of less than 3 km/s had to be available. This ensured a first data point to their spectroscopic survey, aiming at identifying companions.

The initial ZF21 list contains 410 targets. Many targets are, however, not members of one of the above-mentioned associations, according to either SACY or BANYAN classification. We do not consider them in the present study, and we keep only the 328 members of these associations according to SACY or BANYAN. They are listed in Table B.1<sup>4</sup>. For each star, we provide the SACY and/or BANYAN parent association, together with relevant information.

The moving group (MG) ages range between 3 Myr and more than 100 Myr. Each MG contains between 16 and 75 members for the SACY classification and between 12 and 58 targets

<sup>2</sup> [https://github.com/jgagneastro/banyan\\_sigma](https://github.com/jgagneastro/banyan_sigma)

<sup>3</sup> Whether these conclusions would be changed once using Gaia DR3 instead of Gaia DR2 for the BANYAN classification is certainly to be tested, but is beyond the scope of this paper, as it would not allow us to compare our results with theirs any longer.

<sup>4</sup> Table B.1 is only available in electronic form at the CDS via anonymous ftp to cdsarc.u-strasbg.fr

for the BANYAN classification. Most of the stars have masses (as provided by ZF21) between 0.7 and 1.2  $M_{\odot}$  (median 0.9  $M_{\odot}$ ) and distances as estimated by ZF21 between 10 and 200 pc (median 67 pc), see Figure 1<sup>5</sup>. Finally, we note that, due to the selection process adopted by ZF21, the present sample gathers only a fraction of the known members of the considered associations.

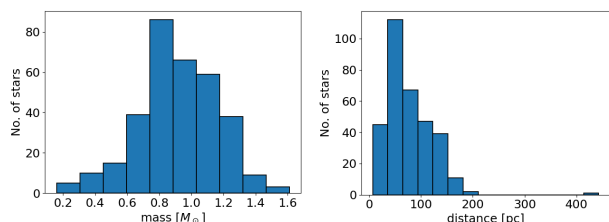


**Fig. 1.** Histogram of the sample stars masses and distances.

## 2.2. Absolute astrometry analysis

GaiaPMEX (for Gaia DR3 Proper Motion anomaly and astrometric noise EXcess) uses the Gaia DR3 database to characterize the properties of companions around any star that was observed with Gaia (K24). Starting from the Renormalised Unit Weight Error (ruwe), it calculates the astrometric signature  $\alpha_{\text{ruwe}}$ , that is the angular wandering of the photocenter beyond proper motion, parallax and noise<sup>6</sup>. When available, it also calculates the astrometric signature  $\alpha_{\text{PMa}}$ , that is the part of proper motion anomaly (PMA) in excess of the expected PMA of a single star with astrometric noise. The PMA is taken from Kervella et al. (2022). Both astrometric information may provide constraints on a possible companion orbiting the target star. A large number of astrometric models of ruwe – and PMA if relevant – are calculated at each node of a grid of mass and sma of a hypothetical companion. At any of those nodes, the companion and orbital parameters, as well as parallax and stellar mass, are taken randomly, following the prior distributions shown in Table 2. The resulting distributions of ruwe – and PMA – are then used to calculate the likelihood of the corresponding observed data given the model – i.e. mass and sma of the companion. Through Bayesian inversion, this likelihood is used to calculate the confidence region of the companion’s mass and sma given the data. When the PMA is available, we also combine its constraints with those from the ruwe, leading to narrower confidence regions on mass and sma.

Moreover, comparing the observed value of  $\alpha_{\text{ruwe}}$  – and  $\alpha_{\text{PMa}}$  – to the distributions they should follow if a star were single, led us to define the significance of these data. Formally, we calculate the significance of  $\alpha_{\text{ruwe}}$  or  $\alpha_{\text{PMa}}$  from their  $p$ -value in the distributions based on the null hypothesis of the star being single. We translate this  $p$ -value into an  $N$ - $\sigma$  significance level by using the normal law, such that  $p=0.046$  is equivalent to a  $2$ - $\sigma$  significance. In the following, we will note the significance as  $N$ - $\sigma_{\text{ruwe}}$  and  $N$ - $\sigma_{\text{PMa}}$  for the various related quantities, and we will use the  $2$ - $\sigma$  significance as the thresholds for identification of binaries.

Note that a similar analysis can be made using the AEN instead of the RUWE. In exceptional cases where we use the AEN,

<sup>5</sup> Note that CD-621197, classified an ARG member according to SACY ( $p = 0.8$ ), and as a field star according to BANYAN, has a distance of more than 400 pc; it is probably an outlier.

<sup>6</sup> Noise levels in the data are estimated for any source of a given  $G$ ,  $B_p - R_p$ , ra and dec, from a statistical study of the whole Gaia database of sources with  $G < 16$ . This is thoroughly demonstrated in K24.

the astrometric signature relative to the AEN will be noted  $\alpha_{\text{AEN}}$ . Similarly, we will note the significance as  $N$ - $\sigma_{\text{AEN}}$  when relative to the AEN.

**Table 2.** Distribution of parameters sampled at each tested bin of the mass-sma grid.

| parameter         | type                | bounds or law                                    |
|-------------------|---------------------|--|
| $\log M_{c,omp}$  | uniform             | $\log M_c \pm \Delta \log M_c$                   |
| $\log \text{sma}$ | uniform             | $\log \text{sma} \pm \Delta \log \text{sma}$     |
| $e$               | uniform             | 0–0.9  |
| $\omega$          | uniform             | 0– $\pi$   |
| $\Omega$          | uniform             | 0– $2\pi$  |
| $\phi$            | uniform             | 0–1  |
| $I_c$             | uniform or $\sin i$ | 0– $\pi/2$                                       |
| $\varpi$          | normal              | $\mathcal{N}(\text{PLX}, \sigma_{\text{PLX}}^2)$ |
| $M_{\star}$       | normal              | $\mathcal{N}(M_{\star}, \sigma_{M_{\star}}^2)$   |

In addition to GaiaPMEX, which aims at characterizing the mass and sma of the binaries, we also built GaiaExplore, that just aims at quickly identifying sources with a significance beyond the  $2$ - $\sigma$  threshold adopted above. This allows splitting split the faster detection phase and the slower characterization phase of our analysis. For any list of sources, it searches online archives to gather Simbad, Gaia DR3, and, if available, Hipparcos-2 data (van Leeuwen 2007) and PMA data from (Kervella et al. 2022). Then it calculates, as explained above, the astrometric signature from the RUWE and its significance, as well as, when Hipparcos-2 data are available, the significance of the PMA. We note that a 5-parameters fit is necessary on a given source’s astrometry in the Gaia DR3 (astrometric\_params\_solved = 31 or 95, see Z24). For some sources, only a 2-parameters (sky RA and DEC coordinates) fit solution is released in the Gaia DR3. In such cases, GaiaPMEX cannot be used, since it requires that parallax and proper motion be also fitted.

## 2.3. Limitations of GaiaPMEX

One of the most stringent limitations of GaiaPMEX is the source magnitude, as the calibration and AL-scan measurement noises were only determined for sources with  $G < 16$ . This is nonetheless with a weak impact on studies, such as this work, based on RV surveys that are strictly limited to  $V$ -mag  $< 15$ .

For the sources with  $G < 16$ , the determination of calibration and AL-scan measurements noises are certainly only approximative, assuming constancy of noise levels over time, and cannot model systematic non-Gaussian wanderings of astrometric signals, if any, beyond single Keplerian motion. We thus assume that "in average" any source behaves well over time, that is within the typical behavior of single sources of the same category in  $G$  and  $B_p - R_p$  magnitudes, which consists in calibration noise and AL-scan measurement error.

Although this tool can apply, within the above-mentioned limitations, to most sources, the interpretation of the AEN, ruwe and PMA and their respective GaiaPMEX curves, is limited by the possible presence of additional unmodeled signals, beyond single Keplerian orbit, including for instance stellar activity, disk accretion, and multiplicity – as discussed in Section 2.4 below – as well as blended PSF due to visual binary companions or background sources. The presence of a binary stellar companion with a separation typically 200 mas or more (up to 1000 mas) may impact the Gaia PSF, depending on the brightness ratio between the two components (Holl

et al. 2023). In such a case, the (sma, mass) solutions found by GaiaPMEX can be impacted, and should be taken with care. In practice, the *IPD\_frac\_multi\_peak* (hereafter *Frac*) and *IPD\_gof\_harmonic\_amplitude* (hereafter *GoF*) are two useful indicators of such a situation determined by the Image parameter determination (IPD) of Gaia. The first one indicates that multiple peaks are occasionally detected in the PSF and removed from the aperture window, and the second one measures the amplitude of the goodness-of-fit variations when fitting the PSF by a single source model, as a function of the position angle of the scan direction. Note, however, that multiple peaks can both be due to background stars, or physical companions, and thus is not a strong indicator multiplicity.

#### 2.4. Note on the origin of the GaiaPMEX signal

In our approach, we implicitly assume that  $N\sigma_{\text{ruwe}} \geq 2$  or  $N\sigma_{\text{PMa}} \geq 2$  indicates the presence of one companion. The rationale for assuming a single companion instead of several is that such rudimentary astrometric data, basically two points – ruwe and PMa – cannot, on its own, disentangle signals from different companions. Assuming that both the Gaia astrometric excess and PMa are due to a single companion is an additional hypothesis, also taken for the sake of parsimony.

Finally, we identified three other effects, besides a companion, that could a priori produce an astrometric signal: stellar activity, and in the case of young systems, accretion and disks. They are discussed below.

##### 2.4.1. Spots

Low-mass to solar-type stars show various types of activity (see e.g. Meunier 2021, for a review) that can, a priori, induce shifts in the star’s photocenter. This is the case, in particular, for dark spots and bright faculae. The astrometric jitter (AJ, defined as the rms of the induced shifts of the photocenter) expected from the Sun seen at 10 pc is less than 0.1  $\mu\text{as}$  for spots only (Lagrange et al. 2011). This translates into an astrometric jitter of 0.04  $\mu\text{as}$  for a Sun-twin at 50 pc. For such a star, the relation between the RV semi-amplitude (RVSA) and the astrometric jitter (AJ) was found to be:  $\text{AJ}(\mu\text{as}) = 0.2 \times \text{RVSA} \text{ (m/s)}$ . For close-by FGK-type stars, simulations yield astrometric jitters less than 0.5  $\mu\text{as}$  (Meunier & Lagrange 2022). Such values are orders of magnitudes smaller than the values (typ. 0.1 mas) associated to binaries.

The activity of young stars is, however, much more intense than the Sun’s one, as reflected by their  $\log(R'_{\text{HK}})$ , down to  $-4.2$  to be compared to that of the Sun, which varies between  $-4.93$  and  $-5.03$  (Hall et al. 2007). It is dominated by a smaller amount of dark spots or bright structures with sizes larger than those of their older counterparts (Berdyugina & Järvinen 2005; Lockwood et al. 2007). The temperature difference between the structures and the star’s surface is up to a few hundred of degrees. In the case of the nearby (9.7 pc) M1-type star AU Mic, known for decades to show intense magnetic activity clearly seen in photometry and in spectroscopy (Lannier et al. 2017; Zicher et al. 2022; Mignon et al. 2023), the amplitude of these long-term photometric variations is of the order of 5%. These variations are best reproduced by one dominating, long-lived structure that in-

duces RV variations due to stellar rotation modulation, with an amplitude of 600 m/s, plus a smaller one (Martoli et al. 2021)<sup>7</sup>.

A rough estimate of the impact of spots/faculae on the astrometric jitter can be made as follows. We assume a single, large and fully dark spot that produces a flux variation of 5 % of the star flux (as in the extreme case of AU Mic). Note that multiple structures spread over the star longitudes would decrease the astrometric jitter. The maximum shift of the photocenter is obtained when the spot is located at the edge of the stellar disk and is  $\approx 0.05 \times R_*$ . We computed the induced photometric shift for all our targets, taking into account their estimated radius, their distance, and assuming such a spot. To estimate the stellar radii, we employed the MADYS tool (Squicciarini & Bonavita 2022) for stellar parameter determination based on isochrone fitting: the conversion between observed Gaia DR3 (Gaia Collaboration et al. 2023b) and 2MASS (Skrutskie et al. 2006) photometry and stellar parameter was mediated by PARSEC isochrones (Nguyen et al. 2022) with solar metallicity, under the assumption of moving groups’ ages.

For all targets, the induced shifts are found to lead to  $\alpha_{\text{ruwe}}$  and  $\alpha_{\text{PMa}}$  significances much smaller than the thresholds used for companion detection: indeed, the median value of the induced shifts is about 0.003 mas, while all  $\alpha_{\text{ruwe}}$  are larger than 0.05 mas. Hence, we conclude that the jitters due to stellar activity are negligible in the context of the present study.

##### 2.4.2. Accretion and circumstellar extinction

In the case of very young (a few Myr) stars, the photocenter shifts can have other origins than a companion. This is potentially the case when stars are still accreting material from their disks. For classical T Tauri members of Taurus, Lupus, or Chameleon, the accretion luminosity may be as high as the star luminosity itself (Alcalá et al. 2021; Gangi et al. 2022). The accretion luminosity is dominated by the accretion spot at the stellar surface but regions within au from the stars may also contribute to this luminosity. Also, scattered light from dust in the non homogeneous disk, variable in time, can also contribute to the photometric budget. In such cases, attributing the astrometric variations to a companion may then be incorrect.

Episodic extinction by the inner disk (dippers, see e.g. McGinnis et al. 2015) may also occur in the case of accreting stars seen with a high inclination (greater than typically 55 degrees). Such effects cannot be estimated without a dedicated modeling of the systems. Hence, in the case of accreting stars, the Gaia signal cannot be straightforwardly attributed only to companions.

Most of the stars considered in the present paper are older than 10 Myr, i.e. much older than classical T Tauri stars. Yet, some members of the youngest associations, eps Cha and TWA do show signs of accretion or of being still embedded in massive disks.

With an age of 3-5 Myr, eps Cha is the youngest nearby moving group in our sample. Three members of Eps Cha in our sample are actually known to be surrounded by accretion disks: DX Cha (HD 104237A), a Herbig AeBe star which forms, together with the T Tauri-type companion HD 104237B a close binary system, surrounded by a CO-rich circumbinary disk Hales et al. (2014), and two CTT stars, MP Mus (PDS 66, CPD-681894) and T Cha (Kastner et al. 2010; Sacco

<sup>7</sup> Note that we do not consider the impact of the flares that produce additional, high amplitude photometric variations because they are spurious and very short-lived.

et al. 2014). We will therefore not consider these targets in our study. Six do not show IR excesses indicative of accretion disks (Dickson-Vandervelde et al. 2021). Among the remaining ones, RXJ 10053-7749, and [K2001c] 17 are reported as weak-line T Tauri stars (WTTs) by Wahhaj et al. (2010); we therefore do not expect accretion to be active for these stars.

None of our TWA targets, except TWA 3A, belongs to the list of the 14 confirmed or putative TWA members showing evidence of dense circumstellar material from mid-infrared excess in Spitzer/IRAC or WISE bands (Venuti et al. 2019). We furthermore note that for those 14 accretors, the accretion luminosity is 100 to 1000 times lower than stellar luminosity. Hence, we can assume that the astrometric signal will probably not be impacted by accretion for our TWA targets, but the results have to be taken with caution because of this risk.

For the remaining stars, we collected AllWISE (Cutri et al. 2021) photometry to look for evidence of infrared excess. Assuming ages corresponding to their respective moving group, we computed expected AllWISE magnitudes based on PARSEC isochrones, and then compared the synthetic  $G - W_i$ ,  $\forall i \in [1, 4]$  colors with the observed ones. Whereas the above-mentioned T Cha and DX Cha show a significant ( $\Delta(G - W_i) > 2$ ) IR excess in all bands, other stars only show infrared disks in W3 and W4 bands, indicative of a more evolved disk: in addition to the already mentioned TWA 3A (TWA according to SACY; ? according to Banyan), to this list belong TW Hya (TWA), DZ Cha (ECHA), HD 98800 (TWA), HD 319139 (BPC) and CPD-68 1894 (ECHA according to SACY; LCC according to BANYAN classifications). For the sake of precaution, in the following, we will not consider these stars for the GaiaPMEX analysis, except HD 319139 given its older age.

### 3. GaiaPMEX overall results

#### 3.1. GaiaPMEX maps

Figure 2 shows examples of GaiaPMEX results on five stars members of the BPC according to SACY and BANYAN classifications, when using our ruwe analysis (left column), when using the PMA only (middle column), and when combining both constraints from ruwe and PMA (right column). Five different cases are considered: no detection of companions (AU Mic, 1st row), detection of a less-than-3-au-sma companion, which, on the basis of the present astrometric data only, can be either a star or a BD (HD 3221, 2nd row), detection of a very-well-constrained-sma companion (HD 139084, 3rd row), detection of a "large"-sma (larger than typically 2-3 au) companion which, on the basis of the present astrometric data only, can be either a star or a BD (PZ Tel, 4th row), and detection of a large sma companion which, on the basis of the present astrometric data only, can be either a star, or a BD, or a planet (AF Lep, 5th row). Note that the companion of HD 3221 is actually known to be a star, thanks to RV data (Vogt et al. 2015) and that HD 139084 is classified as a SB1 spectroscopic binary in ZF21. Also, PZ Tel has a BD companion directly imaged (Biller et al. 2010; Mugrauer et al. 2010); its dynamical mass and sma parameters found by ? are compatible with the GaiaPMEX solutions. AF Lep has a planetary mass companion also directly imaged with high contrast imaging (Mesa et al. 2023a; De Rosa et al. 2023; Franson et al. 2023), and the mass and sma found for this planet are compatible with GaiaPMEX solutions.

As expected, when a companion is detected, the (mass, sma) solutions are, in most cases, degenerate when considering ruwe only or PMA only. Combining the constraints from ruwe and

PMA significantly reduces the (sma, mass) solution ranges in case of detection, and improves the detection limits in case of non-detection. In very few cases like HD 139084, the (sma, mass) domain is very well constrained with ruwe and PMA constraints. Most of the time, though, the (mass, sma) domain of the companion is still degenerate, and additional data such as RV or high contrast imaging data are needed to fully constrain the companions' mass and orbital properties. This was the case for PZ Tel and AF Lep (see above).

When a companion is detected, we can distinguish different types of degeneracies, as described in K24:

- the solutions are on both parts of the V-shape locus, with possible sma ranging from a fraction of au to a several (sometimes dozens of) au. This may happen happens when Gaia data only are considered or when only PMA are considered or when they are both considered. Examples can be seen in Figure 2: HD 138084 (left) and PZ Tel or AF Lep (middle).
- all solutions are in the left part of the V-shape locus of solutions only, forming thus a L-shape. All have sma below typ. 1-3 au. The companion mass is often above  $13 M_{Jup}$ . This can happen only when both Gaia and Hipparcos data are available. An example can be seen in Figure 2: HD 3221 (right).
- all solutions are located in the right part of the V-shape locus of solutions. All have sma greater than typ. 1-3 au. Depending on the stars, the sma can extend to dozens of au. The companion mass can be as low as 2-3  $M_{Jup}$ . This can happen only when both ruwe and PMA are available. Examples can be seen in Figure 2: HD 138084, PZ Tel, or AF Lep (right).

#### 3.2. GaiaPMEX sensitivity

When no companion is detected, the (mass, sma) maps (either based from the ruwe analysis or PMA only or considering both constraints from ruwe and PMA) obtained provide valuable detection limits. An example can be seen in Fig. 2 in the case of AU Mic, and other examples are provided in subsequent figures. The sensitivity domain corresponds to the white/clear upper parts of the maps on the left column (ruwe analysis only) or on the middle (PMA analysis only) on the right column (ruwe + PMA). These areas give the (sma, mass) of companions that can be excluded as they would have been detected if present around the stars. Of course, the sensitivity domain depends on the star's properties (distance and mass, magnitudes, and colors).

At a given distance, the sensitivity domain increases with decreasing star mass. The effect is, yet, rather limited for most of our targets, given the limited range of masses considered in the present analysis (see Figure 1). This is illustrated in Figure 3 where we show the maps obtained for CD-351167 ( $0.7 M_{\odot}$ ) and HD 13246 ( $1.2 M_{\odot}$ ), both members of THA (according to both classifications), and with similar parallaxes ( $\approx 22$  mas).

For a star with a given mass, the sensitivity domain increases with decreasing distance. This is illustrated in Figure 4 where we show the obtained maps for HD 23208 ( $0.9 M_{\odot}$ ,  $\pi = 17.6$  mas), TYC 7066-1037-1 ( $0.8 M_{\odot}$ ,  $\pi = 7.4$  mas), two members of OCT according to both SACY and BANYAN classifications, and HD 105 ( $1.1 M_{\odot}$ ,  $\pi = 25$  mas) and HD 47875 ( $1.1 M_{\odot}$ ,  $\pi = 14$  mas), two members of THA according to both SACY and BANYAN.

From the inspection of all the GaiaPMEX maps obtained, we conclude that the survey is sensitive to all stellar mass companions in the  $\approx 0.1$  to  $\approx 10$  au range for all but 6 (resp. 2, 2, 1, 5, 5, 1, 0) stars members of COL (resp. THA, BPC, OCT, ABD, ARG, TWA, ECH). The sensitivity to BDs is also remarkably good in the  $\approx 1$  to  $\approx 3$  au range.

For sma below 0.1 au, and above 10-20 au, the sensitivity is, as expected, limited. The  $\leq 0.1$  au domain can be well explored by spectroscopy, while the  $\geq 10$  au domain can be well covered by high contrast imaging, for stellar and massive BDs companions. Finally, this survey is also sensitive to planetary-mass companions, as detailed in Section 5.

## 4. Astrometric binaries

### 4.1. GaiaPMEX detections (all masses)

Table C.1<sup>8</sup> provides the binary status found for each target of our sample. For each target, we indicate its  $N\text{-}\sigma_{\text{ruwe}}$  and  $N\text{-}\sigma_{\text{PMa}}$ . As mentioned above, a binary status is attributed when one of these parameters is larger than 2. For comparison purposes, we also indicate the conclusions on their binary status based on spectroscopic diagnostics using ZF21, as well as other indicators of binarity from the literature: *WDS flag*, *SB9 flag*, and *NSS flag* (see Appendix C). We also provide the Frac given by Gaia. In case of a 5 or 6 parameters fit, Frac greater than typically 20-30 indicates a stellar pair (companion or background) with a projected separation of about 400-1000 mas (Holl et al. 2023). In case of a 2-parameter solution, a Frac greater than typically 20 indicates a stellar pair with a projected separation of about 200 mas, while a Frac greater of 30-60 indicates a stellar pair with a projected separation of about 200-400 mas. Finally, a Frac of about 0 associated with a GoF greater than 0.2 is indicative of a galaxy (such a situation is not present in our sample) or a bright binary companion with separation  $< 200$  mas. The GoF is below 0.2 for all our targets except two targets, CD-431395 and HD161460, which have also high Frac, and have 3 parameters-solved so no GaiaPMEX computation. Therefore, we do not report the individual values of this indicator. We finally flag, for information, the targets for which companions were detected in direct imaging by Bonavita et al. (2022).

Table C.1 also reports the sma at minimum mass value, and the maximum masses of the GaiaPMEX solutions for each target. The minimum masses vary significantly (between stellar masses to planetary masses) from one target to the other. The maximum sma is often smaller than about 20 au, but may in some cases be as high as to a few dozen of au.

In the SACY classification, 126 targets are found to be binaries. A similar number is found in the BANYAN classification. When removing the two youngest associations, eps Cha and TWA according to SACY classification, GaiaPMEX finds 60 binaries based on the ruwe only, 13 on PMa only, and 10 on ruwe + PMa. Note we also find 4 targets: CD-471999 (OCT), HD 55279 (COL), VXRSPC16a (ARG), and HD217379A (ABDor) with  $N\text{-}\sigma_{\text{ruwe}}$  lower than but close to 2 (1.8, 1.7, 1.8, 1.7, respectively), and  $N\text{-}\sigma_{\text{AEN}}$  (see K24) greater than 2. We consider them as interesting candidates.

Finally, Table 3 summarizes the number of targets for these associations, as well as the number of binaries found using the ruwe only, PMa only, and ruwe or PMa. These numbers are given for both the SACY and the BANYAN classifications. We note that most detections are with  $N\text{-}\sigma_{\text{ruwe}}$  or  $N\text{-}\sigma_{\text{PMa}} > 3$ . In addition, we note that many of the targets detected with  $N\text{-}\sigma_{\text{ruwe}}$  or  $N\text{-}\sigma_{\text{PMa}}$  between 2 and 3, are known as binaries based on other criteria.

**Table 3.** Summary of detections and associated binary rates. SACY classification.

|   | THA         | OCT | COL            | BPC            | ARG | ABDor          |
|---|-------------|-----|----------------|----------------|-----|----------------|
| Sample  | 76          | 16  | 43             | 42             | 30  | 46             |
| $N\text{-}\sigma_{\text{ruwe}} \geq 2$        | 20          | 8   | 8              | 14             | 6   | 15             |
| $2 \leq N\text{-}\sigma_{\text{ruwe}} \leq 3$ | 5           | 0   | 1 (1 known)    | 5 (4 known)    | 2   | 1              |
| $N\text{-}\sigma_{\text{PMa}} \geq 2$         | 5           | 1   | 4              | 6              | 0   | 7              |
| $2 \leq N\text{-}\sigma_{\text{ruwe}} \leq 3$ | 2 (2 known) | 0   | 0              | 0              | 0   | 0              |
| Astrom. bin. (total)                          | 22          | 9   | 12             | 18             | 6   | 17             |
| $2 \leq N\text{-}\sigma \leq 3$               | 6 (3 known) | 1   | 1 (1 known)    | 5 (4 known)    | 2   | 1              |
| Spec. bin. ZF21                               | 13          | 2   | 1              | 11             | 1   | 4              |
| Spec. bin. ZF21 only                          | 6           | 0   | 1              | 4              | 1   | 2              |
| Binary (total)                                | 28          | 9   | 13             | 22             | 7   | 19             |
| Astrom. bin. rate                             | $29 \pm 6$  |     | $28 \pm 8$     | $43 \pm 10$    |     | $37 \pm 9$     |
| Binary rate                                   | $37 \pm 6$  |     | $30 \pm 8$     | $52 \pm 10$    |     | $41 \pm 9$     |
| Nbr Planets/light BD                          |             |     | 1 <sup>a</sup> | 3 <sup>b</sup> |     | 1 <sup>c</sup> |

**Notes.** Note that binaries and binary rates include stars, BD, and planets. 1st row: number of astrometric binaries with  $N\text{-}\sigma_{\text{ruwe}} \geq 2$ ; 2nd row: number of astrometric binaries with  $2 \leq N\text{-}\sigma_{\text{ruwe}} \leq 3$ ; 3rd row: number of astrometric binaries with  $N\text{-}\sigma_{\text{PMa}} \geq 2$ ; 4th row: number of astrometric binaries with  $2 \leq N\text{-}\sigma_{\text{PMa}} \leq 3$ ; 5th row: total number of astrom. binaries (this work); 6th row: number of astrom. binaries with  $2 \leq N\text{-}\sigma \leq 3$ . In parenthesis, the number of already known binaries, independently of the astrometric data. The following lines provide respectively the number of SB or SB? listed by ZF21, the number of spec. binaries not found as astrometric binaries among the spectroscopic binaries listed in the previous row, the rate of astrom. binaries, the rate of astrom+spec. binaries, and the number of known planets/light BDs among the sample. (a): AB Pic, (b): PZ Tel, AF Lep, HD 14082B b, (c) G80-21.

### 4.2. Comparison with ZF21 survey

ZF21 lists 0 binaries in OCT (among 15 targets)<sup>9</sup>, 8 binaries in BPC (40 targets), 10 in THA (75 targets), 0 in OCT, 0 in ARG (29 targets), 1 in COL (44 targets), and 3 in AB Dor (40 targets). The 22 binaries are flagged as SB or SB1, SB2, SB?, SB1?, SB2?, SB3 when classifications can be applied, or as ? when no conclusion was drawn from their analysis. These numbers can be compared to the numbers of binaries with sma unambiguously less than 10 au found by GaiaPMEX: 6, 7, 6, 3, 7, and 5 in the same associations (total of 28) (Table 3). Hence, GaiaPMEX finds more binaries (28) with sma unambiguously less than 10 au than ZF21 (22). Note that additional binaries identified by GaiaPMEX with sma up to a few dozens of au could actually have their sma in this range as well. The larger sensitivity to binary can be explained by the fact that GaiaPMEX is sensitive to binaries with larger sma, and with lower mass ratio than spectroscopy. Also, spectroscopic detection relies on favorable inclinations of the companion orbital plane, while absolute astrometry does not.

Fourteen of the stars identified by ZF21 as binaries or possible binaries are not found as binaries by GaiaPMEX given our detection criteria using ruwe or PMa. One of them, HD 217379A, reported as an SB3 by ZF21 on the basis of Elliott et al. (2014) results, and characterized by Tokovinin (2016) is just below the  $2\text{-}\sigma_{\text{RUWE}}$  detection limit and just above the  $2\text{-}\sigma_{\text{AEN}}$  one. We discuss these thirteen stars below, and show in Fig. 5 their GaiaPMEX maps, when available.

- HD 86356 (THA) is reported as an SB2 by ZF21. It was classified as a THA member by Torres et al. (2006) but was later classified as a PMS member of Chameleon (Lopez Martí et al. 2013), and then newly rediscovered as a THA member (Elliott et al. 2016). An SB2? status was tentatively proposed

<sup>8</sup> Table C.1 is only available in electronic form at the CDS via anonymous ftp to cdsarc.u-strasbg.fr

<sup>9</sup> HD 155177 is flagged as a SB2 on the basis of three RV by ZF21, though.

- by James et al. (2006) on the basis of CCF analysis, but according to these authors, new data were needed for confirmation. Yet, James et al. (2016) did not confirm its SB2 status. No new data were available to ZF21. The Frac is 0. GaiaPMEX excludes all stellar companions with sma in the range of 0.2 to 4 au, and all BDs in with sma in the range of 1 to 2 au. Depending on their masses, stellar or BD companions can also be excluded outside these boundaries (see Fig. 5). We conclude that the binary status of this star is not assessed.
- CD -42 3328 (THA) is reported as an SB2 by ZF21, but no RV could be found in their paper or in the literature to assess this classification. The Frac is 0. GaiaPMEX excludes all stellar companions with sma in the range 0.2 to 3 au, and all BDs in with sma in the range 1 to 3 au. Depending on their masses, stellar or BD companions can also be excluded outside these boundaries (see Fig. 5). We conclude that the binary status of this star is not assessed.
  - HD 13183 (THA) is mentioned as a SB1 by ZF21 but not reported in their Table 3. This target was flagged as an SB1 by Cutispoto et al. (2002) on the basis of RV variations. Yet, ZF21 do not confirm the RV variations but find an asymmetrical CCF profile. Note that it is classified as a WDS with a large separation (700+ as), but the wide companion cannot explain a SB1 status. The Frac is 0. GaiaPMEX excludes all stellar companions with sma in the range 0.1 to more than 10 au, and all BDs in with sma in the range 1 to 10 au. Depending on their masses, stellar or BD companions can also be excluded outside these boundaries (see Fig. 5). Notably, no companion around this star is reported in Gratton et al. (2024). We conclude that the binary status of this star is not assessed.
  - HD 22213 (THA) is flagged as SB1 by ZF21 on the basis of 2 UVES RV at 8 and 14 km/s, while the target is a relatively fast rotator ( $v \sin i$  about 41 km/s). A visual binary (0.9 and 0.5  $M_{\odot}$ ) with a projected separation of 1.7" ( $\approx 85$  au) was reported by Hagelberg et al. (2020). The Frac is low. GaiaPMEX is not sensitive to this visual binary. GaiaPMEX excludes all stellar companions with sma in the range 0.1 to 4 au, and all BDs in with sma in the range 1 to 2 au. Depending on their masses, stellar or BD companions can also be excluded outside these boundaries (see Fig. 5).
  - HD 32195 (THA) is classified as an SB? by ZF21, but it has a high  $v \sin i$ , more than 45 km/s. UVES data reveal variations with 1 km/s amplitude. The Frac is 0. This star was reported as a PMa binary by Kervella et al. (2019b), but GaiaPMEX does not confirm this status. GaiaPMEX excludes all stellar companions with sma in the range 0.3 to more than 10 au, and all BDs in with sma in the range 2 to 10 au. Depending on their masses, stellar or BD companions can also be excluded outside these boundaries (see Fig. 5). No companion around this star is reported in Gratton et al. (2024). We conclude that the binary status of this star is not assessed.
  - HD 17250 (THA) is classified as a SB by ZF21. Three UVES data separated by 5 and 14 days show variations of 0.3 and 0.5 km/s but it has a high  $v \sin(i)$  of 42 km/s. SOPHIE data also show variations on days timescales which can be compatible either with a companion or with pulsations. It is classified as a less than 2" (120 au) binary in the WDS catalogue. Tokovinin & Horch (2016) report a SB for this star member of a quadruple system but without references. Frac is 0. GaiaPMEX excludes all stellar companions with sma in the range of 0.3 to more than 10 au, and all BDs in with sma in the range of 2 to 4 au. Additional stellar or BD companions can be excluded from these boundaries, depending on their masses (see Fig.5). Additional data are needed to assess the SB status.
  - HD 36329 (COL) is classified by Torres et al. (2006) as an SB2. Frac is 0. GaiaPMEX excludes all stellar companions with sma in the range 0.3 to more than 10 au, and all BDs in with sma in the range 2 to 4 au. Depending on their masses, stellar or BD companions can also be excluded outside these boundaries (see Fig. 5). It is classified as a non single star by Gaia.
  - HD 161460 (BPC) is reported as a SB2 (Torres et al. 2006). HD 161460 is a SB2 (KOIV + KIIV), observed only twice, one near conjunction and in the other spectrum the lines are not very well resolved, but both Li lines are strong. An almost equal mass ( $q \approx 0.9$ ) stellar companion at  $\sim 8$  au is reported in Gratton et al. (2024). GaiaPMEX cannot find a solution because the Gaia DR3 archive only reports a 2-parameters fit (`astrometric_params_solved=3`). Frac is 35, indicating a possible pair. The absence of a 5-parameters fit solution in the DR3 leads to suspect a possibly unidentified issue with the 5-parameters fit previously performed in the DR2.
  - HD 191089 is classified as SB1? by ZF21. Yet, our HARPS data recorded over more than 1000 days do not reveal any hint of binarity and show rather pulsations (Grandjean et al. 2020). It is classified as a visual binary in the WDS catalog, but all companions are unbound. Frac is 0. GaiaPMEX excludes all stellar companions with sma in the range 0.3 to more than 10 au, and all BDs in with sma in the range 1.5 to 6 au. Depending on their masses, stellar or BD companions can also be excluded outside these boundaries (see Fig.5). Furthermore, no companion is reported in the analysis by Gratton et al. (2024).
  - CD -27 11535 is classified as an SB1 by ZF21 and was recently found as a member of a very close resolved system by Thomas et al. (2023). The latter, however, cannot reconcile the orbital fit results and the luminosity constraints based on the Gaia DR3 data, maybe due to a discrepant parallax measurement from Gaia attributed by the authors to variability, or to the presence of an additional unresolved companion to one of the two components. No companion around this star is reported in Gratton et al. (2024). GaiaPMEX cannot find a solution because the Gaia DR3 archive only reports a 2-parameters fit (`astrometric_params_solved=3`). Frac is 19, indicating possibly a possible pair. The absence of a 5-parameters fit solution in the DR3 leads to suspect a possibly unidentified issue with the 5-parameters fit previously performed in the DR2. It is thus likely that the DR2 reported an anomalous parallax.
  - V\* V1005 Ori (BPC) is an M-type star classified as a SB by ZF21, from the publication of Elliott et al. (2014) based on "literature RV". However, ZF21 do not confirm RV variations with their data. Our HARPS data, spread over 3000 days, do reveal RV variations (amplitude 300 m/s), but also significant (100 m/s) bissector variations indicative of stellar activity, well correlated with the RV variations, indicative of stellar activity. They do not show direct indication of a stellar binary. V\* V1005 Ori is classified as a very wide visual binary, a fact that cannot account for an SB status. Frac is 0. GaiaPMEX excludes all stellar companions with sma in the range 0.03 to more than 10 au, and all BDs in with sma in the range 0.2 to more than 10 au. Depending on their masses, stellar or BD companions can also be excluded outside these boundaries (see Fig. 5). Such limits leave very little room for

a close stellar companion, except at very short separations, but there are today no evidence for such a companion in the available RV data.

- V\*V379 Vel (ARG) is classified as a SB? by ZF21 on the basis of two epochs available with two instruments, and a variation of 3.2 km/s. Its  $v \sin i$  is about 14 km/s. Frac is 0. GaiaPMEX excludes most stellar companions with sma between 0.1 and 8 au, and most BD companions with sma between 0.5 and 3 au as well. GaiaPMEX excludes all stellar companions with sma in the range 0.3 to 4 au, and all BD in with sma in the range 1.5 to 2 au. Depending on their masses, stellar or BD companions can also be excluded outside these boundaries (see Fig. 5). Additional data are needed to assess the SB status.
- V\*PX Vir (AB Dor) is classified as a SB1 by ZF21, and mentioned as a single line binary characterized by Griffin (2010) with a period of 216 d. Recently, both components were characterized using RV, absolute and relative astrometry, revealing a mass ratio of about 0.5 (Wang et al. 2023). Frac is 3. GaiaPMEX cannot find a solution because the Gaia DR3 archive only reports a 2-parameters fit (`astrometric_params_solved=3`).

In summary, among the 14 SB reported by ZF21 in BPC, THA, OCT, ARG, COL and ABDor which are not found by GaiaPMEX as binaries based on the ruwe or PMA criteria, eight need to be confirmed as spectroscopic binaries. In three cases, GaiaPMEX failed at finding solutions, but two have high Frac, possible indicating a pair, and one has a Frac of 3. One is detected using the AEN excess. For the remaining cases, the non-detection by Gaia indicates that the companions must orbit closer than 0.1-0.3 au.

Globally, we conclude that GaiaPMEX is very efficient at identifying stellar binaries for non-accreting stars members of young and close associations in the range of about 0.1 to 10-20 au. Moreover, it is yet only partly sensitive to very close binaries (sma less than typically 0.1 au), which consequently represents the sweet spot region for spectroscopic detection of binaries in the Gaia context. For separations greater than 10-20 au, high contrast imaging is best suited to the detection of binaries down to BD masses for these young systems. This demonstrates the complementarity of the various detection methods.

#### 4.3. Binary rates

Determining accurate binary rates is beyond the scope of this paper, because the number of targets considered for each association is small and the sample is probably biased due to selection effects (stars suitable for RV measurements), and because, as seen above, there are for a number of sources doubts about their classifications among the different associations. Furthermore, computing binary rates corrected from completeness effects requires taking several assumptions on the distribution of the  $q$ -ratio, from very low values (planets) to 1 (equal-mass binaries) and on the radial distribution of the binaries that are not justified (these are information that we would actually like to know). We note that such assumptions were taken by ZF21 to estimate their corrected binary rates and because of the associated uncertainties, they caution about the obtained corrected rates.

Nonetheless, we provide hereafter very tentative estimates of *observed* binary rates for BPC ( $\approx 24$  Myr, see Table 1), COL ( $\approx 42$  Myr), THA ( $\approx 45$  Myr), and AB Dor (120-200 Myr), which have more than 40 targets in the ZF21 sample. Using the numbers reported in Table 3, we compute the binary rates

as  $N_{\text{det}}/N_{\text{total}}$ , where  $N_{\text{det}}$  is the number of binaries detected with Gaia (either from the ruwe and/or PMA). We do not correct  $N_{\text{det}}$  from any false positive (FP) effect related to the detections with  $N-\sigma_{\text{ruwe}}$  or  $N-\sigma_{\text{PMA}}$  between 2 and 3, because they are very few (see Table 3), because among them, several are known as binaries from other techniques, and also because in a second step, we also consider the spectroscopic detections, for which we do not know the FP. The uncertainties were computed as  $\sqrt{N_{\text{det}}}/N_{\text{total}}$ . We obtained rates of astrometric binaries of  $43 \pm 10$ ,  $28 \pm 8$ ,  $29 \pm 6$  and  $37 \pm 9$  % for BPC, COL, THA, and AB Dor, respectively.

In a second step, we added the number of astrometric binaries found with GaiaPMEX and the number of spectroscopic binaries (SB or SB?) that were not already identified as astrometric binaries. We assume thus that when an SB is reported and a GaiaPMEX companion is found, they correspond to the same companion (which may actually not be always the case, and may reduce the actual number of binaries). We obtained rates of  $52 \pm 11$ ,  $30 \pm 8$ ,  $37 \pm 6$  and  $41 \pm 9$  %. We see that in most cases, the rates are of about 30-40 %, except for BPC, for which the rate is higher. We note, however, that the BPC hosts three planetary mass companions, that are included in the estimation, and contribute to the estimated rate.

Finally, considering the BANYAN classification leads to rates of  $41 \pm 10$ ,  $37 \pm 10$ ,  $28 \pm 8$ , and  $43 \pm 9$  % for BPC, COL, THA, and AB Dor, respectively. When adding the spectroscopic binaries, we get rates of  $51 \pm 10$ ,  $40 \pm 10$ ,  $39 \pm 8$ ,  $43 \pm 9$  %. This highlights the importance of securing the members of these associations.

## 5. Vetting planetary candidate companions

### 5.1. Planetary candidate companions derived from ruwe and from combining ruwe and PMA

Among the binaries identified in all associations but TWA and ECH, GaiaPMEX, based on either ruwe or PMA astrometric signatures, as well as combining ruwe + PMA, identified 13 targets with companions with masses possibly in the planetary regime. Two companions have sma less than  $\approx 1$  au, and the others have sma greater than  $\approx 1$  au. We show their GaiaPMEX solutions in Figure 6, and describe them below.

- HD 3221 (HIP 2729, THA SACY, THA BAN; ? in ZF21) is a K4 star, reported both as a binary with a proj. sep. of 20 mas from high contrast imaging (Bonavita et al. 2022), and an RV binary (Grandjean et al. 2020). The 20 mas separation is consistent with the Frac of 0 and the very low GoF. All GaiaPMEX solutions have sma less than 1 au (short period (SP) solutions). The solutions are degenerate with L-shaped solutions. Only the equal mass binary solutions are compatible with the observed projected separation (1 au), and the flux ratio of about 1 reported by (Bonavita et al. 2022).
- HD 40216 (HIP 28036, COL SACY, COL BAN; ? in ZF21) was classified as a binary by (Bonavita et al. 2022) based on data from the Spectro-Polarimetric High-contrast Exoplanet Research (SPHERE) instrument (Beuzit et al. 2019). It was previously detected by Galicher et al. (2016) and Song et al. (2003). The mass  $0.12 M_{\odot}$  and projected separation (110 au) are compatible with the low Frac and GoF, and with the GaiaPMEX solutions.
- HD 178085 (HIP 94235, AB Dor SACY, AB Dor BAN; ? in ZF21) was classified as binary thanks to NACO data (Chauvin et al. 2015). Interestingly, a short period (7.7 d)

- mini Neptune was recently reported around this star by Zhou et al. (2022), who also further constrained the properties of the stellar companion. With an sma of about 56 au (about 0.9") and mass of about 0.26  $M_{\odot}$ , the companion may explain the observed Frac (68) and almost zero GoF. They are also compatible with characteristics are compatible with the GaiaPMEX solutions.
- HD 222259 (HIP 116748, DS Tuc, THA SACY, THA BAN; ? in ZF21) has a 8.1 d period giant planet detected by TESS (Newton et al. 2019) and a binary companion at 5" i.e. more than 100 au (Torres et al. 2006; Pearce et al. 2020). The sma and mass (about 175 au (3.8") and 0.8  $M_{\odot}$ , Pearce et al. 2020) of the binary companion, are consistent with the low Frac and GoF, since it must be outside Gaia's window aperture. They are also compatible with the GaiaPMEX solutions.
  - CD -561032 (HIP 22738, AB Dor SACY, AB Dor BAN; SB1 in ZF21) is classified as a SB in SIMBAD. It is member of a binary system made of two M-type stars with  $q=0.7$  and separated by about 90 au (8") (Tokovinin & Kiyeva 2016; Winters et al. 2019). These values are consistent with the low Frac and GoF, as the binary is resolved by Gaia. They are also compatible with the GaiaPMEX solutions, even though these results should be taken with care given the angular separation and low contrast between both components (see Section 2).
  - HD 53842 (HIP 32435, THA SACY, THA BAN; ? in ZF21) is reported as a member of a binary system, with a secondary M-dwarf at a projected separation of 82 au (1.3") by (Dahlqvist et al. 2022). These values are marginally compatible with the Frac value (6), given the binary separation and the window size. The GaiaPMEX solutions are in agreement with the properties of the companion.
  - HD 41071 (HIP 28474, RT Pic, COL SACY, COL BAN; ? in ZF21) is an eclipsing binary (Malkov et al. 2006) with a not yet determined period. It has a known low mass stellar companion (Chauvin et al. 2010; Bonavita et al. 2022; Tokovinin et al. 2020) with a 0.7" projected separation and a 4.6 mag contrast (Tokovinin et al. 2020). Such values are consistent with the low Frac and GoF, and compatible with the GaiaPMEX solutions.
  - V\* PZ Tel (HIP 92680, BPC SACY, BPC BAN; SB? in ZF21) is known to host a BD which is well characterized through direct imaging and RV data. The most recent estimates using also the star PMa (Fra 2023) of its mass (27  $M_{\text{Jup}}$ ) and sma (27 au, 0.6") fit well with the GaiaPMEX solutions. Note that the high contrast in magnitude explains the low Frac and GoF despite a separation of 0.6".
  - V\* AF Lep (HIP 25486, BPC SACY, BPC BAN; ? in ZF21) has been recently shown to host a planet whose properties (Mesa et al. 2023b) are compatible with Gaia data. Note that the high contrast in magnitude explains the low Frac and GoF despite a separation of 0.4".
  - HD 23208 (HIP 17338, OCT SACY, OCT BAN; ? in ZF21) is a close (DR3 parallax = 17.6 mas) G8V type star. It was identified to have a PMa by Kervella et al. (2019b) and Brandt (2021b). The low Frac and GoF do not suggest the presence of a close pair, in agreement with the GaiaPMEX results. Palomar observations rule out stellar companion beyond about 1" (56 au) (Metchev & Hillenbrand 2009). This leaves us with solutions most probably in the BD or planet domain. We further characterize the companion in the next section. We note that the smallest sma, down to 1-2 au, would require higher spatial resolution instruments on the ELT, while planetary mass companions at 10 au could be detected with VLT high contrast instruments.
  - G80-21 (HIP 67659, AB Dor SACY, AB Dor BAN; ? in ZF21), HD 44627 (aka AB Pic or HIP 30034, COL SACY, CAR BANYAN, and HD 14082 B (HIP 10679, BPC SACY, BPC BAN) are found to have light companions. We discuss and characterize them in a dedicated section below.
- In summary, among the 13 candidates for planetary-mass companions, 7 are in fact stellar companions, one is a well known and characterized BD, one is a well known and characterized planet. Another one, HD 23208 is known in this paper to have a sub-stellar companion orbiting below typically 60 au, which requires additional data for further characterization. The last three targets, G80-21, AB Pic and HD14082B are shown to have sub-stellar companions that we characterize and discuss in Section 6 thanks to high contrast imaging and RV data in addition to Gaia and PMa data.

## 5.2. Planetary candidate companions derived from ruwe analysis only

GaiaPMEX, based on the ruwe astrometric signature only, finds 19 companions with masses ranging from the stellar regime to the planetary regime in these associations. We wish to vet, whenever possible, between stellar companions and planetary mass companions, using available data.

- HD 217379A (AB Dor, SACY), BD +30397B (BPC, SACY), BD -211074B (BPC, SACY), HD 139084B (BPC, SACY), HD 164249 B (BPC, SACY) are members of known close bound binary systems. Hence, no planets are needed to explain the Gaia results.
- 2MASS J10010873-7913074 (THA SACY, THA BAN) is also classified as a T Tauri, but is classified as a THA member by BANYAN. Its status needs further clarification. We note low values of Frac and GoF.
- HD 319139 (BPC SACY, BPC BAN) is reported as a binary in the WDS and as a SB2 by ZF21, and as a member of a K7+K2 system in SIMBAD. This can explain the Gaia results.
- TYC 8083-45-5 (THA SACY, THA BAN) is reported as a visual binary (sep. 1"; delta K = 1.2 in the near IR) by the WDS. The high Frac (50) and low GoF is consistent with a binary system. The Gaia data are compatible with a bound binary provided the orbit of the secondary is elliptical, but as seen in section 2, the GaiaPMEX results have to be taken with care when the Frac is high.
- CD -29 2531 (COL SACY, COL BAN). It is reported as a member of a visual binary system (0.8") in the WDS. Given the star distance (more than 100 pc), the visual companion, if gravitationally bound to the star, can account for the Gaia results only if orbiting on a very eccentric orbit.
- 2MASS J08500540-7554380 (THA SACY, LCC BAN) is reported as a T Tauri star in SIMBAD, and classified as a LCC member by BANYAN. If its T Tauri status is confirmed, the Gaia results should be taken with caution.
- BD -13 1328 (AB Dor BAN; ? SACY) is reported as a dubious member of a visual binary system with a 2" separation by the WDS, based on the Tycho Double Star catalog (additional DD list). It is also reported as a member of a bound binary system with a separation of 20". This remote companion cannot be responsible for Gaia results, as the maximum sma of the solution is less than 30 au. More observations are needed to further constrain the status of the dubious companion candidate reported in the WDS. Note that the Frac and GoF do not suggest the presence of a close stellar companion.

- EXO 02352-5216 (COL BAN, ? SACY) is not reported as a binary in the literature. The (sma, mass) solutions go well in the planetary mass regime and the maximum sma is 20 au. It is reported as a SB ? by ZF21. More observations are needed to clarify the SB status of this object.
- Barta 16112 (BPC SACY, ? BAN), LP 776-25 (AB Dor SACY, AB Dor BAN), HW Cet (AB Dor SACY, AB Dor BAN), HD 309851 (ARG SACY, ARG BAN), UCAC361-3820 (THA SACY, THA BAN), CD-292360 (ARG, BANYAN, ? SACY) are not reported as members of binary systems or spectroscopic binaries. HD 309851 is not reported as a binary by Gratton et al. (2024). At this stage, these targets are then promising candidates and deserve dedicated observations to further constrain the companions responsible for the Gaia signature. Note that all but CD -29 2360 have low Frac and GoF, while CD -29 2360 has a large Frac (64) and a low GoF, suggesting the possible presence of a stellar companion.
- RXJ 05200+0612 (THOR BAN, ? SACY) is reported to be a member of a bound binary system, with a very remote companion, which cannot account for the ruwe. This target is then also a promising candidate, and more observations are needed to further constrain its companion. Note that Frac and GoF are low.

In summary, among the 19 stars found as hosting a companion with possible mass in the planetary regime using ruwe only, eight are known binaries, and two need to be confirmed as non-accreting stars before further interpretation. Additional data are needed to further constrain the companions of the remaining nine stars.

## 6. Characterization of the low mass companions around G80-21, AB Pic and HD 14082B

### 6.1. G80-21

#### 6.1.1. A close sub-stellar companion to G80-21

G80-21 (HIP 17659, AB Dor SACY, AB Dor BAN; ? in ZF21) is classified as an eruptive variable,  $0.46M_{\odot}$ , M3-type star. Figure 7 shows the (sma, mass) solutions compatible with the ruwe only (Left), the PMA (Middle), and both quantities combined (Right). G80-21 shows a significant  $\alpha_{ruwe}$  with  $N\text{-}\sigma_{ruwe} = 3.5$ , and no significant PMA excess at<sup>10</sup>, indicative, like in the case of HD 3221, of a close (less than 1-3 au) companion. The low Frac and GoF also suggest either a very close pair, as for HD 3221, or a high contrast companion BD/planetary mass companion if below 1".

ZF21 do not report a SB status for G80-21 on the basis of a few UVES data spread over 100 days. The analysis of higher RV accuracy HARPS data (described in Appendix D) spread over about 110 days reveal 0.4 km/s peak to peak variations (compatible with the amplitude of the UVES data). These variations occur over a few days period of time, a timescale compatible with the estimated rotation period of 3.8 days for this young and active ( $\log(R'HK) = -3.98$  Shan et al. 2024) M-star. Hence these high amplitude variations are probably linked with stellar activity. Note that, unlike the case of AU Mic, the bisector velocity spans are not fully correlated to the RVs, which might indicate either a complex spots pattern or a very close companion

in addition to the spot-induced variations. The TESS light curve clearly shows a periodic signal with a  $\approx 4d$  period, compatible with two features. Furthermore, we note that the minimum mass of the companion that would be needed to explain the RV variations would not exceed 2 Jupiter masses, and would therefore not account for the absolute astrometry signal, unless orbiting on a very improbable pole-on orbit. We conclude that most if not all the RV variations are due to stellar activity.

Finally, G80-21 was observed by many teams in high-contrast imaging, but no companion has been found yet (see e.g. Lannier et al. 2016, who got a 7.76 contrast at 0.5" at L'), corresponding to roughly  $10 M_{Jup}$ .

We then constrained the properties of the "astrometric" companion using these HARPS RV in addition to the absolute astrometry. We first computed the detection limits set by the RV data and overplotted the GaiaPMEX solutions. To get a global overview, we considered sma up to 10 au, an eccentricity between 0 and 0.9, and an inclination of the orbital plane between 10 and 90° (10° were chosen instead of 0 to avoid any divergence when, at  $i \approx 0^\circ$ ,  $\sin i \approx 0$ ). The results are showed in Figure 8. We see that the sma solutions are mainly in the range 0.5-2 au, and the mass is lower than 8-10  $M_{Jup}$ . A peak is present at 0.3 au, which corresponds to the gap in the available RV temporal coverage. Additional smaller peaks, correspond to harmonics of this peak. These peaks are probably not physical. We therefore conclude that unless the orbit of the companion is seen pole-on, the companion to G80-21 is a planet orbiting between 0.5 and 2 au. As the RV limits are very sensitive to the inclination of the planet, we then repeated this approach fixing the inclination to 10, 45 and 90 degrees. The results are also showed in Figure 8. As expected, the higher the inclination, the lower the RV detection limits, and hence the lower peaks below 0.5 au.

We then used our MCMC code described in Appendix E to check these results in the general case (no assumptions on the inclination). The priors and resulting corner plot are provided in Appendix E. As expected, given the limited RV data available, most parameters are not well constrained, except the sma and the companion mass. We show in Figure 9 the obtained (sma, mass) solutions. We first note that the peak centered at about 0.33 au is also present, and due to the window function of the RV observations. The companion sma is therefore less in the range 0.5-2 au, with a maximum below 1 au, and its mass in the 2-6  $M_{Jup}$  range, with a maximum probability between 3 and 4  $M_{Jup}$ . Additional RV data are needed to improve the temporal coverage of the data and therefore the window function, and thus further constrain its physical and orbital parameters.

#### 6.1.2. Additional companions to G80-21

Finally, we constrain the properties of any additional companion, using at the same time the RV and absolute astrometry (Gaia and PMA). Figure 10 provides these detection limits. The tool used to do so is described in Appendix E.

#### 6.1.3. Discussion

To our knowledge, G80-21 b is the only young planet among the 11 RV planets with masses in the range 1-20  $M_{Jup}$  orbiting stars with masses in the range 0.2-0.5  $M_{sun}$  (exoplanet.eu) and with a known sma between 0.017 and 5 au. As such, it offers the possibility to study the early stages of planetary systems around low mass stars. Additional RV data are needed to further constrain its actual sma, and to precise its location with respect to

<sup>10</sup> Note that it was flagged as a binary by Kervella et al. (2019a) on the basis of Gaia DR2 PMA, but GaiaPMEX does not confirm this classification.  $N\text{-}\sigma_{PMA} = 0.7$

the snow line. Also, detailed RV monitoring of such a system with an outer giant planet (if its sma is indeed in the range 1-2 au) would be particularly interesting to search for inner terrestrial planets, forming thus a young solar system-like "scaled" to a low mass star, with the possibility to image the outer giant planet in the future with Gravity+ or with the ELT.

## 6.2. AB Pic

With a  $\approx 13 M_{\text{Jup}}$  companion (AB Pic b) imaged at about 260 au in the mid 2000 (Chauvin et al. 2005), the solar-type star AB Pic (K1V) has become an iconic system. This was indeed the first low-mass substellar object (at the boundary between planets and BD mass) imaged around a main sequence star. The star was recently classified as a member of the Carina association (CAR) with therefore an age of about 13 Myr instead of 20 Myr as previously adopted (Booth et al. 2021). Such an age would lead to a planet mass of  $10 \pm 1 M_{\text{Jup}}$ , lower than previously estimated, and well into the planetary mass domain. Due to its large projected distance to the star (about 190 au), its orbital parameters are still rather poorly constrained, though there is evidence of a non-negligible eccentricity and an almost edge-on orbit (Palma-Bifani et al. 2023, hereafter PB23). The formation process of this remote planet is still unclear. In situ formation via core accretion is not an option because of a lack of material and inappropriate timescales, but a formation closer to the star followed by an ejection due to the dynamical interaction with a third body is plausible (a scenario also considered to explain the presence of HD 106906 b orbiting currently at 650 au from the star (Rodet et al. 2017, 2019). Alternatively, the planet could have formed by gravitational instability in an extended disk or by gravo-turbulent fragmentation.

### 6.2.1. AB Pic c properties: previous works

Using the PMa estimated using Gaia DR3 and Hipparcos data, PB23 concluded that an additional, inner planet (AB Pic c) could be present in the system. Comparing the (sma, mass) solutions derived on the one hand from the PMa constraints using Kervella et al. (2019b) approach, and on the other hand, the detection limits obtained using SPHERE data obtained in Dec. 2015, PB23 estimated a sma of 2 to 10 au, and a mass of  $6 M_{\text{Jup}}$  for this companion. These values need further confirmation for three reasons. First, PB23 did not consider the possibility of companions closer than typically 1-2 au, while such companions would have been compatible with the PMa constraints only. Second, the (sma, mass) constraints derived from the PMa based on the approach proposed by Kervella et al. (2019b) are approximate as they take into account the impact of inclination and eccentricity only statistically. Finally, Kervella et al. (2019b) does not take into account any instrumental noise in this approach. These points were left for a more detailed study (the present one).

Recently, Gratton et al. (2024) published a very narrow solution range of solutions for the mass and sma of AB Pic c:  $8.4 \pm 4.2 M_{\text{Jup}}$  and  $3.571 \pm 1.167$  au. However, no detail is provided on the way the sma and masses are computed and how the compatibility of each simulated orbit with the various measurements (Gaia and Hipparcos astrometry, RV, high contrast imaging) is quantified, and which errors are taken into account.

### 6.2.2. AB Pic c properties: more robust estimates

AB Pic shows a clear PMa ( $N\text{-}\sigma_{\text{PMa}} = 4.2$ ) and no significant  $\alpha_{\text{ruwe}}$  at  $N\text{-}\sigma_{\text{ruwe}} = 0.6$ , indicative of a companion beyond a few au. Figure 12 shows the (sma, mass) solutions compatible with the Gaia astrometric signature only (Left), the PMa (Middle), and both quantities combined (Right). We see that the solutions found with the PMa data alone are very degenerate, while the combined Gaia signature + PMa constraints lift a significant part of the degeneracies. A mass of  $0.84 \pm 0.1 M_{\odot}$  was assumed for AB Pic (Stassun et al. 2019). AB Pic b (190 au, 9-11  $M_{\text{Jup}}$ ) is well out of the domain of possible solutions. Hence, an additional companion is necessarily present in the system.

We use in the following SPHERE, GPI (Macintosh et al. 2014) and RV data to robustly constrain the properties of this additional companion. The data, as well as their reduction, are described in Appendix D and E. Noticeably, compared to PB23 and to Gratton et al. (2024), we use, in addition to the Dec. 2015 SPHERE data, a GPI data set, as well as an additional SPHERE data obtained in Oct. 2023 (see Appendix for a description of the data and their reduction). These two additional data sets allow to significantly improve the detection limits in the case of edge-on orbits. This can be seen comparing Figure 11, which provides the detection limits obtained respectively with the Dec 2015 set of data and the limits obtained using in addition both Dec 2015 and Oct. 2023 data (see Appendix for a description of the computation of the detection limits). While companions can be detected (68 % probability) beyond 11 au when using the Dec 2015 data only, they can be detected beyond 5.5 au when using these additional data (case  $i = 90^\circ$ ). This significant improvement is due to the fact that the data sets were obtained several years apart and companions hidden behind the mask in the first data set (and hence not detectable) could be outside the mask during the second observation (and hence detectable). The effect is, expectedly, not as high when considering less inclined orbits.

To estimate the possible (sma, mass) of the companion, we superimpose GaiaPMEX maps with the detection limit maps obtained using all available direct imaging data (that is the two SPHERE epochs and one GPI set of data, see Appendix D) and radial velocity data, assuming different inclinations. We show in Figure 13 the results obtained assuming inclinations of  $90^\circ$ ,  $45^\circ$  and<sup>11</sup>  $10^\circ$ . We see that the (sma, mass) space is wider in case of pole-on orbits, and more reduced in case of edge-on ones. For pole-on orbits, most solutions (68% probability) are between 2.5 and 9  $M_{\text{Jup}}$ , and sma between 2.5 and 6 au. For edge-on orbits, the solutions in terms of mass are much more reduced, between 3 and 5  $M_{\text{Jup}}$ .

Given the sma of AB Pic c, and the distance of the system, a direct detection of AB Pic c is not within the reach of current high-contrast imagers on 10-m class telescopes, but should be easily detected by imagers on the ELTs. Alternatively, it might be within the reach of the VLT/GRAVITY instrument if its mass and sma are on the higher sides of the current possible ranges. This would imply a pole-on orbit, hence a configuration different from the almost edge-on orbit of AB Pic b. Note that, in such a case, the detection would be more demanding in terms of performances than the detection of AF Lep b ( $\sim 3 M_{\text{Jup}}$ ,  $\sim 300$  mas).

<sup>11</sup> We used  $10^\circ$  instead of 0 to avoid any divergence when, at  $i \approx 0^\circ$ ,  $\sin i \approx 0$

### 6.2.3. Additional companions around AB Pic

Finally, we constrain the properties of any additional companion, using at the same time the RV, absolute astrometry (Gaia and PMA), and the direct imaging data from SPHERE and GPI described in Table D.2, and the detection tool described in Appendix E. The results are shown in Fig.14 assuming three inclinations: 90, 45, and 10 degrees. As expected, the detection limits depend on the inclination of the companion, especially in the regions where they are dominated by the RV ( $\sin(i)$  effect) or direct imaging (reduced limits for inclined orbit with respect to pole-on one, as long period planets may happen to be located in projection behind the mask at all observation epochs).

In any case, the data at hand allow, for the first time, a quantitative estimate of the properties of any possible additional planet (planet d) around the star from less than 0.01 au to more than 100 au. We can exclude additional planets more massive than AB Pic b or c in the system.

### 6.2.4. Consequences on the system

This work shows that AB Pic c is definitely lighter than AB Pic b, and that there is no companion more massive than AB Pic b at all separations, up to AB Pic b distance. This severely questions any scenario of ejection of AB Pic b by a third companion close to the star to explain its present location. This is for instance in contrast with the case of the HD 106906 system, for which the binary companion was shown to possibly be responsible for the ejection of HD 106906 b. Here any gravitational interaction between AB Pic b and AB Pic c, whether direct or resonant, would inevitably result in a stronger perturbation of the lighter body's orbit, i.e., AB Pic c.

Among the other possible explanations of AB Pic b's large separation, a fly-by acting on an originally much closer-in AB Pic b cannot be ruled out but is rather improbable as the perturbing star should have come very close to the initial position of AB Pic b. Subsequently, AB Pic c should have been impacted as well by this process. Hence the geometry of this encounter should be able to explain why only AB Pic b was ejected. The suitable parameter space is presumably reduced, but our still poor knowledge of AB Pic b and c's current orbital properties prevents us from initiating any detailed dynamical investigation.

Migration within the protoplanetary disk is not favored because of the high mass of AB Pic b, and because this would require a very massive disk up to 200 au at least. A more complex possible scenario could be that AB Pic was formerly a member of a wide ( $> 1000$  au separation), now disrupted binary system with a low-mass star with a highly inclined orbit with respect to the orbital plane of AB Pic b. Such a configuration would inevitably lead to strong coupled eccentricity and inclination oscillations of AB Pic b due to Kozai-Lidov resonance (Kozai 1962) (hereafter KL). Under this process, the apoastron of AB Pic b could have been increased up to its present position. However such a scenario requires a rapid stabilization of AB Pic b around 200 au by a direct interaction at apoastron. As a matter of fact, a similar extra interaction at apoastron after ejection was also required in the HD 106906 system to freeze the present-day configuration (Rodet et al. 2017). Here again also, KL oscillations triggered by the putative binary companion are also expected to affect AB Pic c as well, and one should explain why only AB Pic b was affected. The answer to this issue could be a matter of timescales. KL cycles in triple systems are characterized by a

oscillation period basically equal to

$$P_{\text{KL}} = \frac{M_{\text{tot}} P_{\text{out}}^2}{M_{\text{in}} P_{\text{in}}} \quad (1)$$

within a factor of order unity (Beust & Dutrey 2006; Krymowski & Mazeh 1999; Ford et al. 2000), where  $M_{\text{tot}}$  is the total mass,  $M_{\text{in}}$  is the inner mass,  $P_{\text{out}}$  is the outer orbital period (here the outer binary companion), and  $P_{\text{in}}$  is the inner orbital period (here AB Pic b or c). Now, if we assume that the ratio  $M_{\text{tot}}/M_{\text{in}}$  is  $\sim 1.5$  (the outer companion should be less massive than AB Pic), that the outer companion's sma is  $\sim 1000$  au, and that the initial sma of AB Pic b is  $\sim 40$  au, then we derive  $P_{\text{KL}} \approx 4$  Myr. Comparing to the estimated age of 13 Myr for AB Pic, this gives enough time to KL to have been able to significantly affect AB Pic b. Redoing the same calculation for AB Pic c assuming now a sma of  $\sim 4$  au leads to  $P_{\text{KL}} > 100$  Myr, which is far above the age of AB Pic. KL resonance should not have had enough time to perturb AB Pic c. This way we may explain why only AB Pic b could have been ejected. However, a stabilization process at large distance is still required.

Other possible scenarios include AB Pic b having been captured from another system or being a captured free-floating planet. Note that a capture from another system necessarily implies a similar ejection at large distance within that other system prior to capture by AB Pic, which drives us back to our previous issue. But that other system could have hold an inner binary like HD 106906 and more easily trigger the ejection.

The last, probably simpler scenarios are either in situ gravitational instability within a disk, or a gravitational collapse. In such a case, AB Pic b would be a so far unique system with two planets definitely formed by different processes. Detailed studies of the planets atmospheric compositions could further help test this hypothesis.

## 6.3. HD 14082 B

HD 14082 B is a close (40 pc) young solar-type star, member of the BPMG. Like many members of this moving group, the star shows IR excess in the mid- and far-infrared (e.g. Riviere-Marichalar et al. 2014), indicative of the presence of a yet unresolved dust disk. Noticeably, it shares a common proper motion with the F-type star HD 14082 A, orbiting 557 au away, i.e. 14" on the plane of the sky (Mamajek & Bell 2014; Elliott & Bayo 2016).

### 6.3.1. A sub-stellar companion close to the ice-line of HD 14082 B

Like AB Pic, HD14082B shows a clear PMA ( $N\text{-}\sigma_{\text{PMA}} = 5.0$  and no significant  $\alpha_{\text{ruwe}}$  at  $N\text{-}\sigma_{\text{ruwe}} = 0.5$ , indicative of a companion beyond a few au. The ruwe, the PMA, and the combined ruwe + PMA maps are shown in Figure 15. They were computed considering inclinations between 0 and 90 degrees. The PMA map reveals the presence of a companion, with a still unconstrained PMA between 0.1 and about 100 au. Adding the ruwe constraints allows us to rule out short-period companions. HD 14082 A is too far to account for the observed GaiaPMEX excess. We note that the GaiaPMEX map is reminiscent of the AF Lep or AB Pic maps, where possible companion masses reach the planetary mass, albeit slightly higher.

At the time of writing this paper, a candidate companion with a mass of  $0.0054 \pm 0.0030 M_{\odot}$  ( $= 5.7 \pm 3.1 M_{\text{Jup}}$ ) and a distance of  $5.74 \pm 2.96$  au was reported by Gratton et al. (2024) around

HD14082B. Yet, as in the case of AB Pic b, detailed information on the way these parameters and their associated uncertainties were derived is lacking. Given the limited amount of data available on this system (no RV data, less imaging data; hence less data than in the case of AB Pic), and given the fact that the PMA used does not take into account the instrumental noises, the robustness of the derived parameters is not assessed.

We used SPHERE data to further constrain the companion characteristics. They are described in Appendix D. The data were both reduced with the Patch Covariance (PACO) tool (Flasseur et al. 2020b), as the AB Pic data, and with the SPEckle CALibration (SPECAL) tool (Galicher et al. 2018). Both clearly (SNR > 40 with PACO) detect a companion close to the edge of the FoV (see Figure 6.3.1). Checking the Gaia DR3 database shows that this companion is a faint, M star, not connected to HD 14082B.

As for AB Pic, we combined the direct imaging detection limits with the GaiaPMEX solutions to find the possible (sma, mass) solutions for the companion. We considered three different inclinations: 0, 45 and 90 degrees. The results are shown in Fig. 17. As expected, the solutions are much more constrained when the inclination is moderate, with a mass ranging between 8 and 20  $M_{\text{Jup}}$  and a sma between 3 and 5 au ( $1\sigma$  values). For highly inclined orbits, the mass ranges between 8 and 40  $M_{\text{Jup}}$ , and the sma between 3 and 7 au ( $1\sigma$  values). Given the distance of the star, the companion is well suited for direct detection with the VLT/Gravity instrument.

### 6.3.2. Additional companions around HD 14082 B

Finally, we combine the ruwe + PMA data with the direct imaging data to compute the upper limits in (sma, mass) of any additional companion to HD 14082B. We consider three inclinations: 0, 45, and 90 degrees. The results are provided in Fig. 18. As we do not have RV data, the (sma, mass) constraints are rather poor below a fraction of an au. At 1 au, we exclude additional companions more massive than 10  $M_{\text{Jup}}$  beyond 1 au and more massive than 2  $M_{\text{Jup}}$  at 10 au, except for edge-on orbits. For edge-on orbits, the corresponding masses are higher: 5  $M_{\text{Jup}}$  (68 % probability) and 30  $M_{\text{Jup}}$  (90 % probability) at 10 au. Adding high-contrast imaging data and RV data would help further constraining the properties of additional companions.

### 6.3.3. Notes on the HD 14082 system

Among the confirmed exoplanets with semi-major axes in the 3–10 au range, only three have been directly detected (HCI and/or interferometry):  $\beta$  Pictoris b and c (parent star A5), and AF Lep b (parent star F8). Given its angular separation, HD 14082B b could be with SPHERE+ and with forthcoming imagers on the ELT. It may also be within the reach of the Gravity interferometer. Gravity data would in addition allow spectroscopic studies of its atmosphere.

Interestingly, HD14082B forms a binary system with HD14082A, located  $\sim 500$  au away, opening up the opportunity to study planetary formation in binary systems. Finally, HD 14082B also hosts a debris disk detected through its Spitzer/MIPS infrared excess (Sierchio et al. 2014), suggesting two belts at respectively 1 and 18 au (Cotten & Song 2016), not detected in scattered light yet. The putative planet may therefore orbit between the two belts, similarly to the giant planets between the asteroid and Kuiper belt in our Solar System, opening also the perspective to study disk/planet interactions.

## 7. Unconfirmed astrometric detections of planets

Recently, a list of 17 candidate planets based on a PMA computed by (Kervella et al. 2019b) has been proposed, together with associated (sma, mass) solutions (Gratton et al. 2024). In addition to AB Pic and HD 14082B that were discussed above, two candidates belong to the present sample: HIP 30314 (HD 45270) and HIP 88399 (HD 164249). The reported sma and masses are  $13.28 \pm 13.93$  au and  $0.0011 \pm 0.0004 M_{\odot}$  ( $= 1.2 \pm 0.4 M_{\text{Jup}}$ ) for HIP 30314b, and  $7.02 \pm 3.39$  au and  $0.0043 \pm 0.0026 M_{\odot}$  ( $= 4.5 \pm 2.7 M_{\text{Jup}}$ ) for HIP 88399b. No quantitative information is available, though, on how these numbers were determined. Based on our estimation of the noise budget in the measured PMA and RUWE, we rule out any evidence of companion in the HIP 30314 system, as the  $N\text{-}\sigma_{\text{ruwe}}$  and  $N\text{-}\sigma_{\text{PMA}}$  are respectively 0.4 and 1.2, hence below  $2\sigma$ . For HIP 88399, we find a  $N\text{-}\sigma_{\text{ruwe}}$  of 1.4 and a  $N\text{-}\sigma_{\text{PMA}}$  of 1.7, hence below  $2\sigma$ , hence again below our detection threshold. Gaia and Hipparcos data do not show sufficient evidence for a companion in this system. We show in Figure 19 the detection limits obtained with GaiaPMEX on these targets. We attribute the discrepancy between our negative detection results and the positive detection of (Gratton et al. 2024) to the fact that unlike in Kervella et al. (2019b), we take into account the instrumental noise when computing the PMA. These examples highlight the importance of estimating and taking into account instrumental noise when dealing with the PMA or the Gaia excess. Note that this need will remain in the context of Gaia DR4.

## 8. Conclusion

We have searched for companions around a sample of more than 300 stars members of young close associations or moving groups (BPC, OCT, ECH, TWA, ARG, ABDor, COL, THA), based on available absolute astrometry data: Gaia alone (ruwe), or Gaia and Hipparcos data (ruwe+ PMA). We showed that large ruwe cannot be straightforwardly attributed to the presence of companions for some members of the two youngest associations, ECH and TWA. These specific targets were not analyzed with GaiaPMEX.

Detection limits in terms of (mass, sma) have been derived for each target. This information will allow for optimizing the target samples in future surveys dedicated to the search for low mass companions, and avoiding spending observing time on targets for which absolute astrometry already tells that no companion is present within the instrument sensitivity domain.

We computed the (sma, mass) solutions for all binaries. For each target with a positive detection, degeneracies are observed, so that the companions may be either stars, or stars or BDs, or stars or BD or planets (referred to as "planetary mass candidates").

The sample was built for a spectroscopic binary search. It allows therefore to compare the respective merits of spectroscopy and absolute astrometry for stellar binary searches. It turns out that absolute astrometry sensitivity outperforms spectroscopy for separations greater than 0.1 au, while below, spectroscopy outperforms absolute astrometry. Such techniques are then very complementary to get full and (almost) unbiased census of stellar binarity below 10 au. We thus derive minimum unbiased binary rates for sma of different values.

Ten of the 13 planetary-mass candidates found using both ruwe and PMA in BPC, OCT, ARG, ABDor, COL, THA, happen to be in fact stellar companions or known BD/planet companions, based on SPHERE imaging data, and/or literature. One

target need additional observations to conclude on the nature of its companion. For the last three systems, G80-21, AB Pic and HD 14082B, we show that the companions are definitely planetary/BD objects. We provide quantitative information on their possible (sma, mass). G80-21 has a 4-8  $M_{\text{Jup}}$  companion with an sma in the range 0.5-1 au. Noticeably, conversely to AB Pic and HD 14082B, which show no significant  $\alpha_{\text{ruwe}}$ , but a significant PMa, G80-21 does not show a significant PMa, but a significant  $\alpha_{\text{ruwe}}$ . AB Pic c has a mass ranging between 2.5 and 9  $M_{\text{Jup}}$ , and a sma between 2.5 and 6 au. The mass range can be refined according to the inclination of the orbital plane with respect to the line of sight. AB Pic c being less massive and the outer AB Pic b tend to favor a gravitational instability or gravitational collapse for the origin of AB Pic b. For HD 14082B, the mass varies between 8 and 20  $M_{\text{Jup}}$ , and the sma between 3 and 5 au in case of moderate inclinations. Higher masses and sma are however possible in case of close-to-edge-on configurations. With separations below 100 mas, the companions to G80-21, AB Pic, and HD 14082B cannot be detected with current high contrast imagers, but they could be within the reach of the future ELT imagers. In addition, AB Pic c and HD 14082B b could be within the reach of the VLTI/Gravity instrument.

From a methodological point of view, this work highlights the impact of the use of Gaia data to precise the (sma, mass) parameters, compared to the sole use of Gaia-Hipparcos PMa, and the need for additional data (RV, imaging), to lift the degeneracies in the absolute astrometry solutions. We anticipate that the need for such additional data will remain even with the DR4 outputs, in case of long-period companions. This work also shows the important impact of the inclination of the orbit of the companion on the (sma, mass) solutions. This has to be taken into account to optimize the direct detection of these companions.

Finally, we do not confirm the presence of a planetary-mass companion recently announced around HD 45270, and show that the companion announced around HD 164249 is below the  $2\sigma$  detection threshold of GaiaPMEX. These examples highlight the importance of the instrumental noise in the analysis of the Gaia-Hipparcos PMa.

*Acknowledgements.* We thank the anonymous referee for her/his comments. This work has made use of data from the European Space Agency (ESA) mission *Gaia* (<https://www.cosmos.esa.int/gaia>), processed by the *Gaia* Data Processing and Analysis Consortium (DPAC, <https://www.cosmos.esa.int/web/gaia/dpac/consortium>). Funding for the DPAC has been provided by national institutions, in particular the institutions participating in the *Gaia* Multilateral Agreement. This project has received funding from the European Research Council (ERC) under the European Union's Horizon 2020 research and innovation programme (COBREX; grant agreement 885593). A.Z. acknowledges support from ANID – Millennium Science Initiative Program – Center Code NCN2021\_080. This work has made use of the High Contrast Data Centre, jointly operated by OSUG/IPAG (Grenoble), PYTHEAS/LAM/CeSAM (Marseille), OCA/Lagrange (Nice), Observatoire de Paris/LESIA (Paris), and Observatoire de Lyon/CRAL, and supported by a grant from Labex OSUG@2020 (Investissements d'avenir – ANR10 LABX56). This work made use of the European Space Agency space mission *Gaia*, and of the SIMBAD and VizieR CDS facilities. Last, AML thanks D. Segransan, C. Mordasini and O. Schid for fruitful discussions.

## References

2023, *AJ*, 165, 246  
 Alcalá, J. M., Gangi, M., Biazzo, K., et al. 2021, *A&A*, 652, A72  
 Bell, C. P. M., Mamajek, E. E., & Naylor, T. 2015, *MNRAS*, 454, 593  
 Berdyugina, S. V. & Järvinen, S. P. 2005, *Astronomische Nachrichten*, 326, 283  
 Beust, H. & Dutrey, A. 2006, *A&A*, 446, 137  
 Beuzit, J. L., Vigan, A., Mouillet, D., et al. 2019, *A&A*, 631, A155  
 Biller, B. A., Liu, M. C., Wahhaj, Z., et al. 2010, *ApJ*, 720, L82  
 Bonavita, M., Gratton, R., Desidera, S., et al. 2022, *A&A*, 663, A144  
 Booth, M., del Burgo, C., & Hambaryan, V. V. 2021, *MNRAS*, 500, 5552

Brandt, T. D. 2021a, *ApJS*, 254, 42  
 Brandt, T. D. 2021b, *ApJS*, 254, 42  
 Chauvin, G., Lagrange, A. M., Bonavita, M., et al. 2010, *A&A*, 509, A52  
 Chauvin, G., Lagrange, A. M., Zuckerman, B., et al. 2005, *A&A*, 438, L29  
 Chauvin, G., Vigan, A., Bonnefoy, M., et al. 2015, *A&A*, 573, A127  
 Chomez, A., Lagrange, A. M., Delorme, P., et al. 2023, *A&A*, 675, A205  
 Cotten, T. H. & Song, I. 2016, *ApJS*, 225, 15  
 Cutispoto, G., Pastori, L., Pasquini, L., et al. 2002, *A&A*, 384, 491  
 Cutri, R. M., Wright, E. L., Conrow, T., et al. 2021, *VizieR Online Data Catalog*, II/328  
 Dahlqvist, C. H., Milli, J., Absil, O., et al. 2022, *A&A*, 666, A33  
 De Rosa, R. J., Nielsen, E. L., Wahhaj, Z., et al. 2023, *A&A*, 672, A94  
 Dickson-Vandervelde, D. A., Wilson, E. C., & Kastner, J. H. 2021, *AJ*, 161, 87  
 Elliott, P. & Bayo, A. 2016, *MNRAS*, 459, 4499  
 Elliott, P., Bayo, A., Melo, C. H. F., et al. 2014, *A&A*, 568, A26  
 Elliott, P., Bayo, A., Melo, C. H. F., et al. 2016, *A&A*, 590, A13  
 Flasseur, O., Denis, L., Thiébaud, É., & Langlois, M. 2020a, *Astronomy & Astrophysics*, 634, A2  
 Flasseur, O., Denis, L., Thiébaud, E., & Langlois, M. 2020b, *Astronomy & Astrophysics*, 637, A9  
 Ford, E. B., Kozinsky, B., & Rasio, F. A. 2000, *ApJ*, 535, 385  
 Franson, K., Bowler, B. P., Zhou, Y., et al. 2023, *arXiv e-prints*, arXiv:2302.05420  
 Gagné, J., Mamajek, E. E., Malo, L., et al. 2018, *ApJ*, 856, 23  
 Gaia Collaboration, Arenou, F., Babusiaux, C., et al. 2023a, *A&A*, 674, A34  
 Gaia Collaboration, Vallenari, A., Brown, A. G. A., et al. 2023b, *A&A*, 674, A1  
 Galicher, R., Boccaletti, A., Mesa, D., et al. 2018, *A&A*, 615, A92  
 Galicher, R., Marois, C., Macintosh, B., et al. 2016, *A&A*, 594, A63  
 Galland, F., Lagrange, A. M., Udry, S., et al. 2005, *A&A*, 443, 337  
 Gangi, M., Antonucci, S., Biazzo, K., et al. 2022, *A&A*, 667, A124  
 Grandjean, A., Lagrange, A. M., Keppler, M., et al. 2020, *A&A*, 633, A44  
 Gratton, R., Bonavita, M., Mesa, D., et al. 2024, *A&A*, 685, A119  
 Griffin, R. F. 2010, *The Observatory*, 130, 125  
 Hagelberg, J., Engler, N., Fontanive, C., et al. 2020, *A&A*, 643, A98  
 Hales, A. S., De Gregorio-Monsalvo, I., Montesinos, B., et al. 2014, *AJ*, 148, 47  
 Hall, J. C., Lockwood, G. W., & Skiff, B. A. 2007, *AJ*, 133, 862  
 Holl, B., Perryman, M., Lindegren, L., Segransan, D., & Raimbault, M. 2022, *A&A*, 661, A151  
 Holl, B., Sozzetti, A., Sahlmann, J., et al. 2023, *A&A*, 674, A10  
 James, D. J., Aarnio, A. N., Richert, A. J. W., et al. 2016, *MNRAS*, 459, 1363  
 James, D. J., Melo, C., Santos, N. C., & Bouvier, J. 2006, *A&A*, 446, 971  
 Kastner, J. H., Hily-Blant, P., Sacco, G. G., Forveille, T., & Zuckerman, B. 2010, *ApJ*, 723, L248  
 Kastner, J. H. & Principe, D. A. 2022, in *Handbook of X-ray and Gamma-ray Astrophysics*, 49  
 Kervella, P., Arenou, F., Mignard, F., & Thévenin, F. 2019a, *A&A*, 623, A72  
 Kervella, P., Arenou, F., Mignard, F., & Thévenin, F. 2019b, *A&A*, 623, A72  
 Kervella, P., Arenou, F., & Thévenin, F. 2022, *A&A*, 657, A7  
 Kiefer, F., Lagrange, A.-M., Rubini, P., & Philipot, F. 2024a, *arXiv e-prints*, *A&A*, in press, arXiv:2409.16992  
 Kiefer, F., Lagrange, A.-M., Rubini, P., & Philipot, F. 2024b, *arXiv e-prints*, *A&A*, in press, arXiv:2409.16993  
 Kozai, Y. 1962, *AJ*, 67, 591  
 Kraus, A. L., Shkolnik, E. L., Allers, K. N., & Liu, M. C. 2014, *AJ*, 147, 146  
 Krymowski, Y. & Mazeh, T. 1999, *MNRAS*, 304, 720  
 Lagrange, A. M., Meunier, N., Desort, M., & Malbet, F. 2011, *A&A*, 528, L9  
 Lannier, J., Delorme, P., Lagrange, A. M., et al. 2016, *A&A*, 596, A83  
 Lannier, J., Lagrange, A. M., Bonavita, M., et al. 2017, *A&A*, 603, A54  
 Lockwood, G. W., Skiff, B. A., Henry, G. W., et al. 2007, *ApJS*, 171, 260  
 Lopez Martí, B., Jimenez Esteban, F., Bayo, A., et al. 2013, *A&A*, 551, A46  
 Luhman, K. L. 2023, *AJ*, 165, 269  
 Macintosh, B., Graham, J. R., Ingraham, P., et al. 2014, *Proceedings of the National Academy of Science*, 111, 12661  
 Malkov, O. Y., Oblak, E., Snegireva, E. A., & Torra, J. 2006, *A&A*, 446, 785  
 Mamajek, E. E. & Bell, C. P. M. 2014, *MNRAS*, 445, 2169  
 Martioli, E., Hébrard, G., Correia, A. C. M., Laskar, J., & Lecavelier des Etangs, A. 2021, *A&A*, 649, A177  
 McGinnis, P. T., Alencar, S. H. P., Guimarães, M. M., et al. 2015, *A&A*, 577, A11  
 Mesa, D., Gratton, R., Kervella, P., et al. 2023a, *A&A*, 672, A93  
 Mesa, D., Gratton, R., Kervella, P., et al. 2023b, *A&A*, 672, A93  
 Metchev, S. A. & Hillenbrand, L. A. 2009, *ApJS*, 181, 62  
 Meunier, N. 2021, *arXiv e-prints*, arXiv:2104.06072  
 Meunier, N. & Lagrange, A. M. 2022, *A&A*, 659, A104  
 Mignon, L., Meunier, N., Delfosse, X., et al. 2023, *A&A*, 675, A168  
 Mugrauer, M., Vogt, N., Neuhäuser, R., & Schmidt, T. O. B. 2010, *A&A*, 523, L1  
 Murphy, S. J. & Lawson, W. A. 2015, *MNRAS*, 447, 1267  
 Newton, E. R., Mann, A. W., Tofflemire, B. M., et al. 2019, *ApJ*, 880, L17  
 Nguyen, C. T., Costa, G., Girardi, L., et al. 2022, *A&A*, 665, A126

- Offner, S. S. R., Moe, M., Kratter, K. M., et al. 2023, in *Astronomical Society of the Pacific Conference Series*, Vol. 534, *Protostars and Planets VII*, ed. S. Inutsuka, Y. Aikawa, T. Muto, K. Tomida, & M. Tamura, 275
- Palma-Bifani, P., Chauvin, G., Bonnefoy, M., et al. 2023, *A&A*, 670, A90
- Pearce, L. A., Kraus, A. L., Dupuy, T. J., et al. 2020, *ApJ*, 894, 115
- Perrin, M. D., Ingraham, P., Follette, K. B., et al. 2016, in , Edinburgh, United Kingdom, 990837
- Perrin, M. D., Maire, J., Ingraham, P., et al. 2014, in , 91473J, arXiv:1407.2301 [astro-ph]
- Perryman, M., Hartman, J., Bakos, G. Á., & Lindegren, L. 2014, *ApJ*, 797, 14
- Riviere-Marichalar, P., Barrado, D., Montesinos, B., et al. 2014, *A&A*, 565, A68
- Rodet, L., Beust, H., Bonnefoy, M., et al. 2019, *A&A*, 631, A139
- Rodet, L., Beust, H., Bonnefoy, M., et al. 2017, *A&A*, 602, A12
- Sacco, G. G., Kastner, J. H., Forveille, T., et al. 2014, *A&A*, 561, A42
- Sahlmann, J., TriAUD, A. H. M. J., & Martin, D. V. 2015, *MNRAS*, 447, 287
- Shan, Y., Revilla, D., Skrzypinski, S. L., et al. 2024, *A&A*, 684, A9
- Shkolnik, E. L., Allers, K. N., Kraus, A. L., Liu, M. C., & Flagg, L. 2017, *AJ*, 154, 69
- Sierchio, J. M., Rieke, G. H., Su, K. Y. L., & Gáspár, A. 2014, *ApJ*, 785, 33
- Skrutskie, M. F., Cutri, R. M., Stiening, R., et al. 2006, *AJ*, 131, 1163
- Song, I., Zuckerman, B., & Bessell, M. S. 2003, *ApJ*, 599, 342
- Squicciarini, V. & Bonavita, M. 2022, *A&A*, 666, A15
- Stassun, K. G., Oelkers, R. J., Paegert, M., et al. 2019, *AJ*, 158, 138
- Thomas, A. D., Nielsen, E. L., De Rosa, R. J., et al. 2023, *AJ*, 166, 246
- Tokovinin, A. 2016, *AJ*, 152, 11
- Tokovinin, A. & Horch, E. P. 2016, *AJ*, 152, 116
- Tokovinin, A. & Kiyaeva, O. 2016, *VizieR Online Data Catalog*, J/MNRAS/456/2070
- Tokovinin, A., Mason, B. D., Mendez, R. A., Costa, E., & Horch, E. P. 2020, *AJ*, 160, 7
- Torres, C. A. O., Quast, G. R., da Silva, L., et al. 2006, *A&A*, 460, 695
- Torres, C. A. O., Quast, G. R., Melo, C. H. F., & Sterzik, M. F. 2008, in *Handbook of Star Forming Regions*, Volume II, ed. B. Reipurth, Vol. 5, 757
- Trifonov, T., Tal-Or, L., Zechmeister, M., et al. 2020, *A&A*, 636, A74
- van Leeuwen, F. 2007, *A&A*, 474, 653
- Venuti, L., Stelzer, B., Alcalá, J. M., et al. 2019, *A&A*, 632, A46
- Vogt, N., Mugrauer, M., Neuhäuser, R., et al. 2015, *Astronomische Nachrichten*, 336, 97
- Wahhaj, Z., Cieza, L., Koerner, D. W., et al. 2010, *ApJ*, 724, 835
- Wang, J. J., Ruffio, J.-B., De Rosa, R. J., et al. 2015, *Astrophysics Source Code Library*, ascl:1506.001, aDS Bibcode: 2015ascl.soft06001W
- Wang, X., Xia, F., & Fu, Y. 2023, *PASJ*, 75, 368
- Winters, J. G., Henry, T. J., Jao, W.-C., et al. 2019, *AJ*, 157, 216
- Zhou, G., Wirth, C. P., Huang, C. X., et al. 2022, *AJ*, 163, 289
- Zicher, N., Barragán, O., Klein, B., et al. 2022, *MNRAS*, 512, 3060
- Zúñiga-Fernández, S., Bayo, A., Elliott, P., et al. 2021, *A&A*, 645, A30
- Zuckerman, B. 2019, *ApJ*, 870, 27

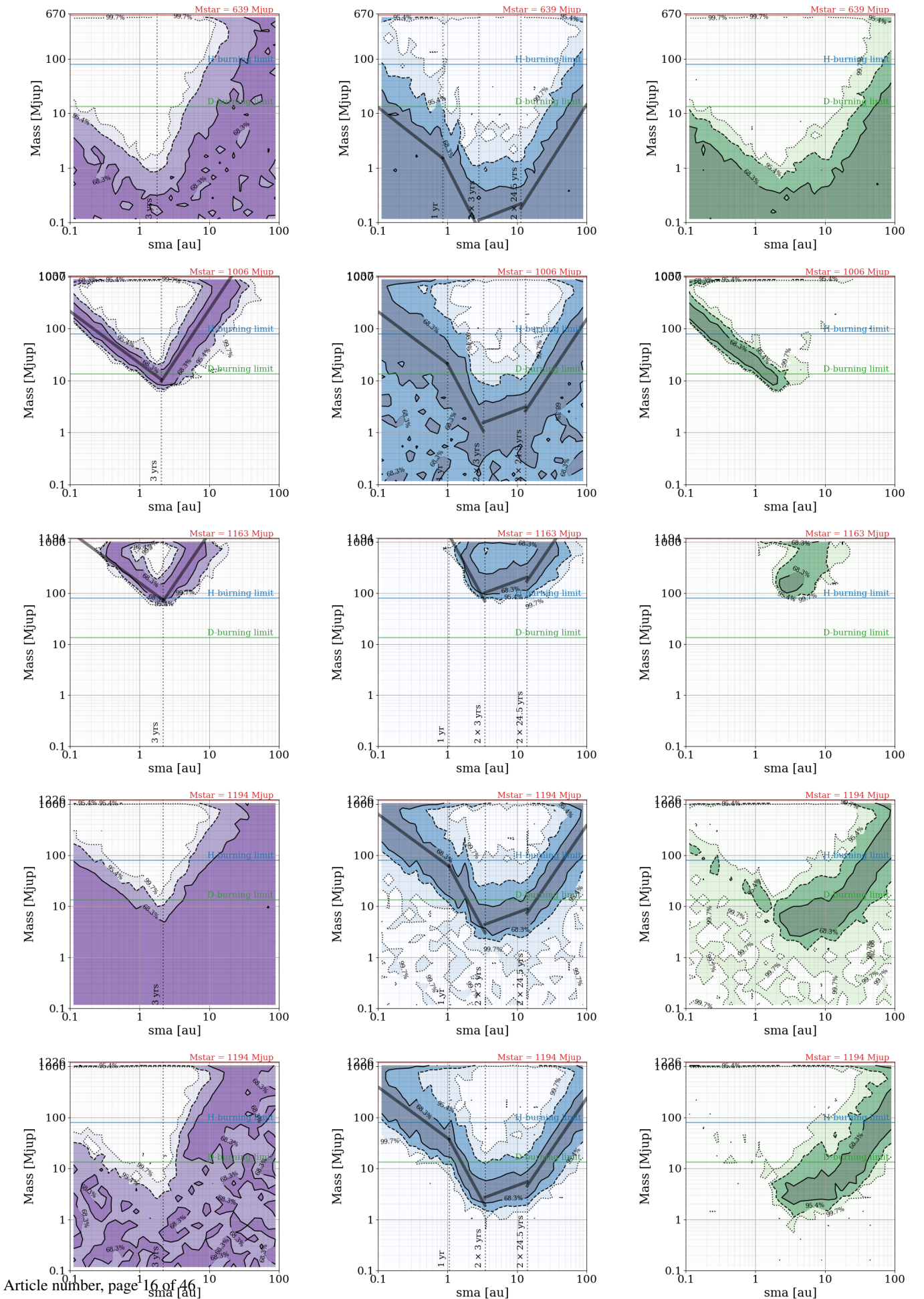


**Fig. 2.** GaiaPMEX (sma, mass) solutions for potential companions. Constraints from ruwe only (Left), constraints from PMA only (Middle), and constraints from ruwe + PMA (Right). Each row, from Top to Bottom: 1/ No detection: AU Mic. 2/ Star with a "small" sma or BD companion: HD 3221. 3/ Star with a well constrained sma companion: HD 139084. 4/ Star with a "large" sma or BD companion: PZ Tel. 5/ Star with a "large" sma or BD or Planet companion: AF Lep. The contours show the 68%, 95%, and 99.7% confidence intervals. The black lines show the model relationships developed in K24

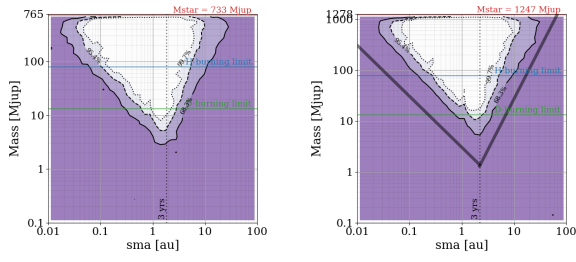


**Fig. 3.** Impact of the star masses on the Gaia alone sensitivity domain. Left: CD-351167 ( $0.7 M_{\odot}$ ) and Right: HD 13246 ( $1.2 M_{\odot}$ ). Both stars have parallaxes of  $\approx 22$  mas. Note that the y-axes cover different mass ranges.

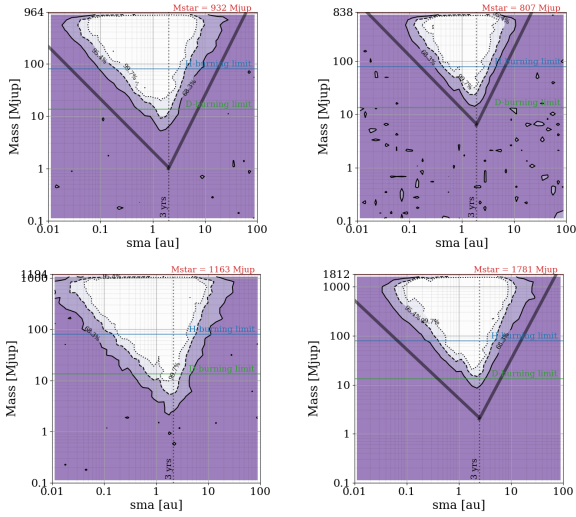


**Fig. 4.** Impact of the distance on the Gaia alone sensitivity domain. Top, Left: HD 23208 ( $0.9 M_{\odot}$ ,  $\pi = 17.6$  mas) and Right: TYC 7066-1037-1 ( $0.8 M_{\odot}$ ,  $\pi = 7.4$  mas). Bottom, Left: HD 105 ( $1.1 M_{\odot}$ ,  $\pi = 25$  mas) and Right: HD 47875 ( $1.1 M_{\odot}$ ,  $\pi = 14$  mas). Note that the y-axes cover different mass ranges.

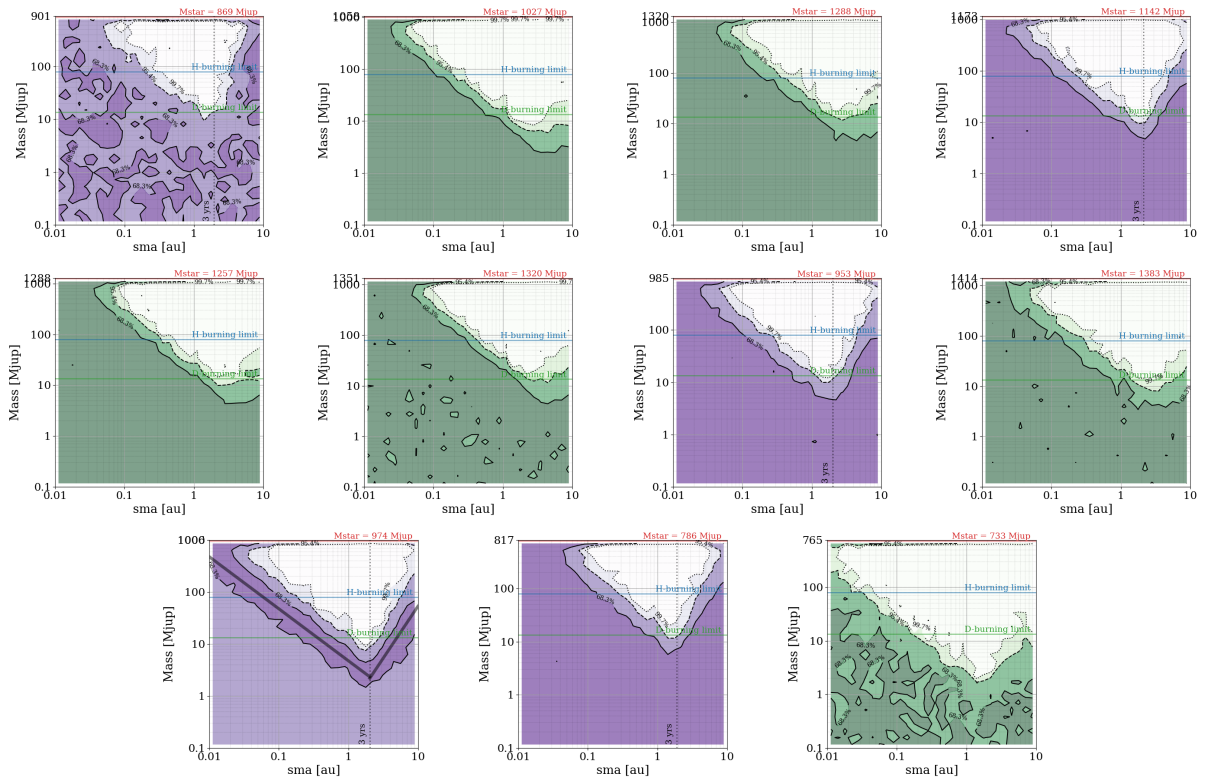


**Fig. 5.** GaiaPMEX maps for stars listed as SB by ZF21 and not classified as binaries according to GaiaPMEX results (see text).

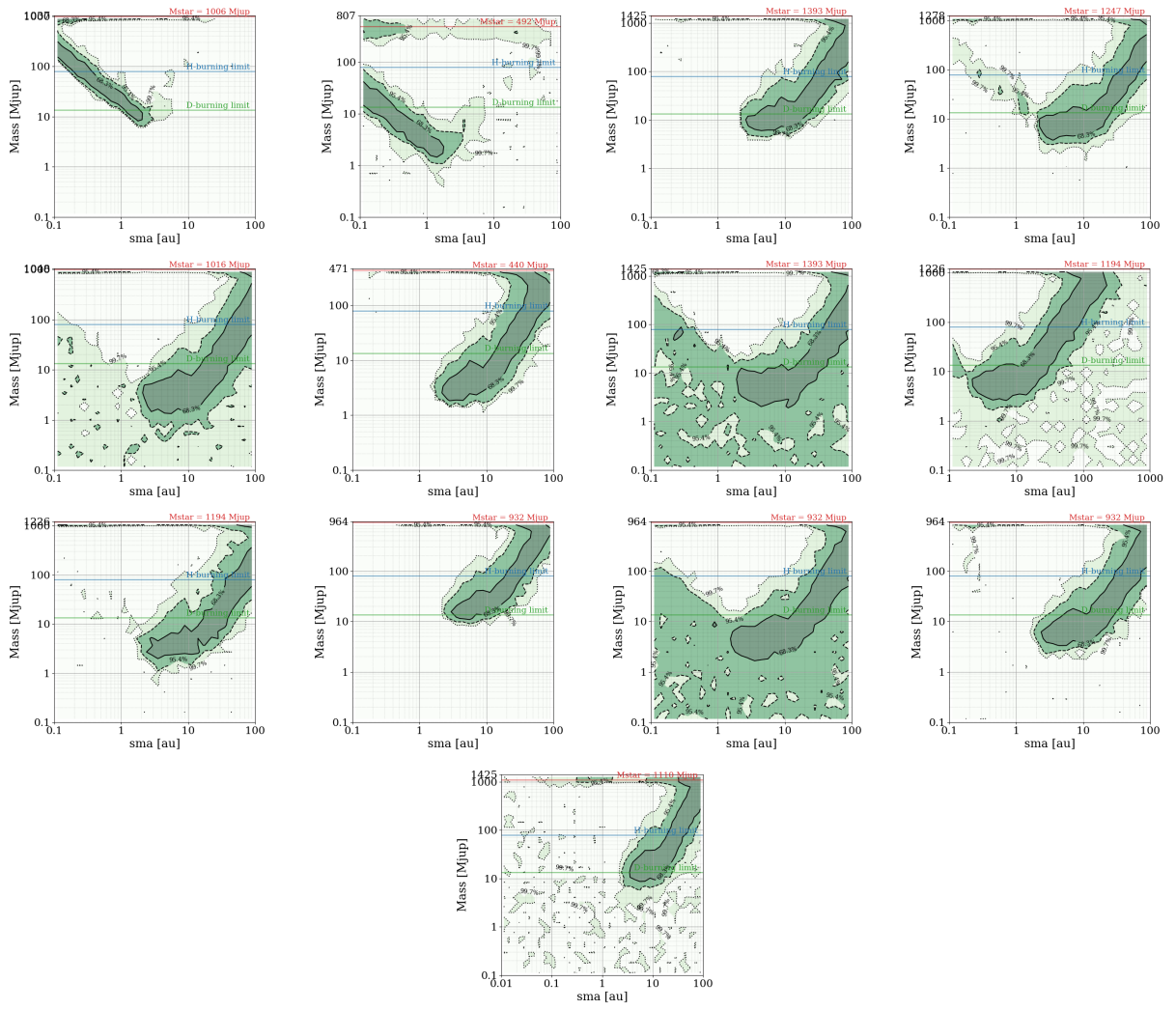


**Fig. 6.** Targets having companions with masses possibly in the planetary regimes (see text). From top to bottom and left to right: HD3221, G80-21, HD40216, HD 178085, HD 222259, CD-561032, HD 53842, PZ Tel, AF Lep, HD 41071, HD 23208, AB Pic, and HD 14082B.

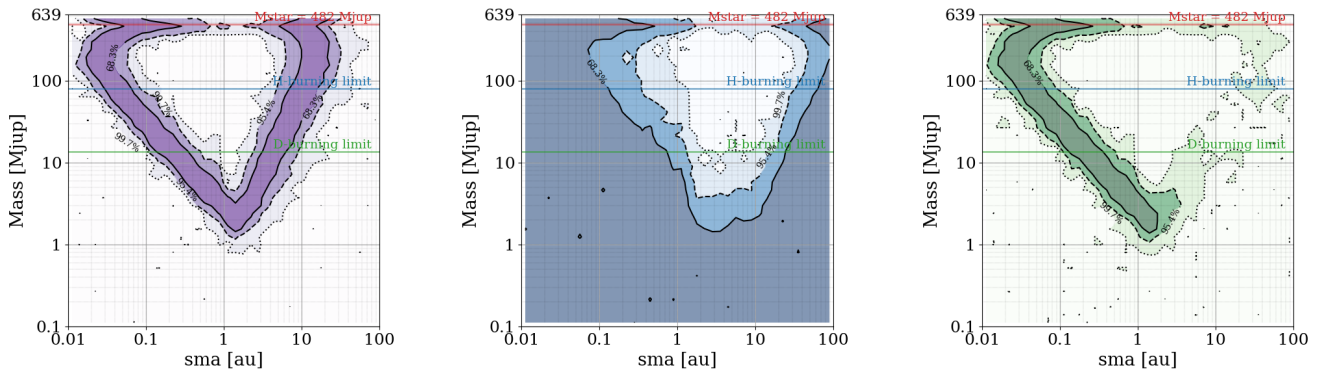


**Fig. 7.** From Left to Right: Gaia excess, PMa and combined maps for G80-21.

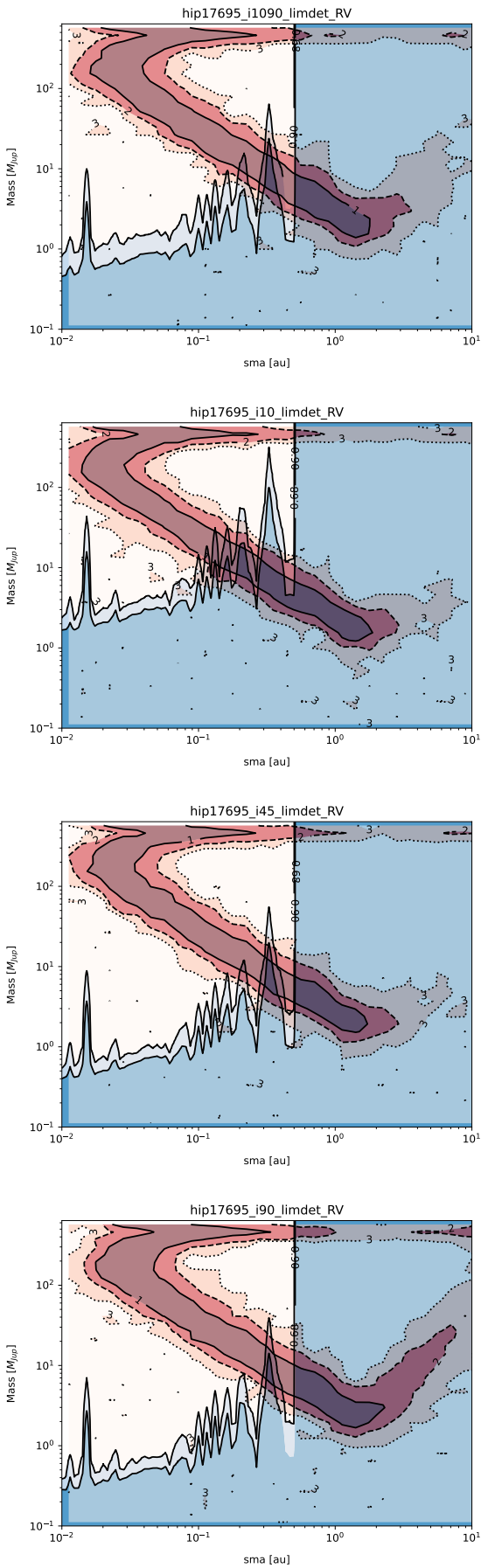


**Fig. 8.** Possible sma and mass of G80-21 b. Superimposition of the RV detection limits and the GaiaPMEX (sma,mass) solutions. The black-lines limiting the blue regions correspond to the RV detection limits (90 and 98 % probabilities). From Top to Bottom: an inclination between 10 and 90 deg is assumed, then inclinations of 10, 45, and 90 degrees.

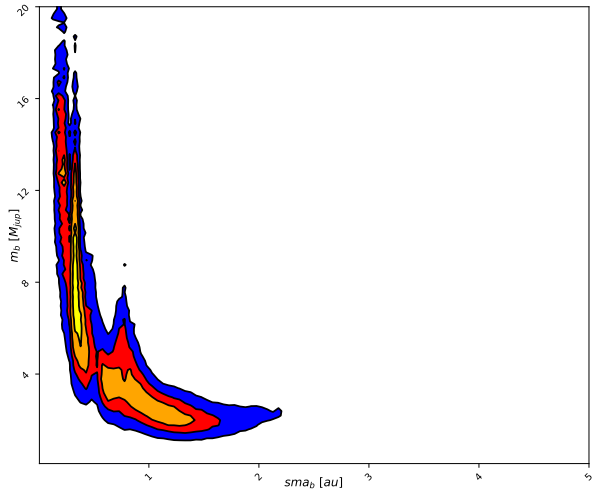


**Fig. 9.** (sma,mass) solutions for G80-21 b, derived from the MCMC analysis, and taking into account the available RV data, and the Gaia and PMA data.

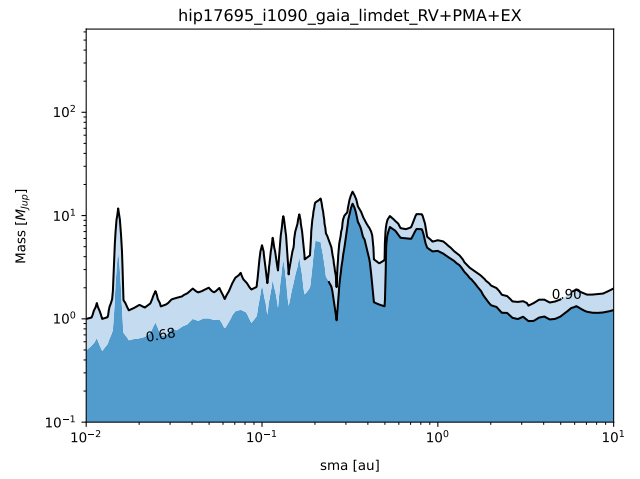


**Fig. 10.** Limits on the masses of the potential planets around G80-21, using RV and GAIPMEX.

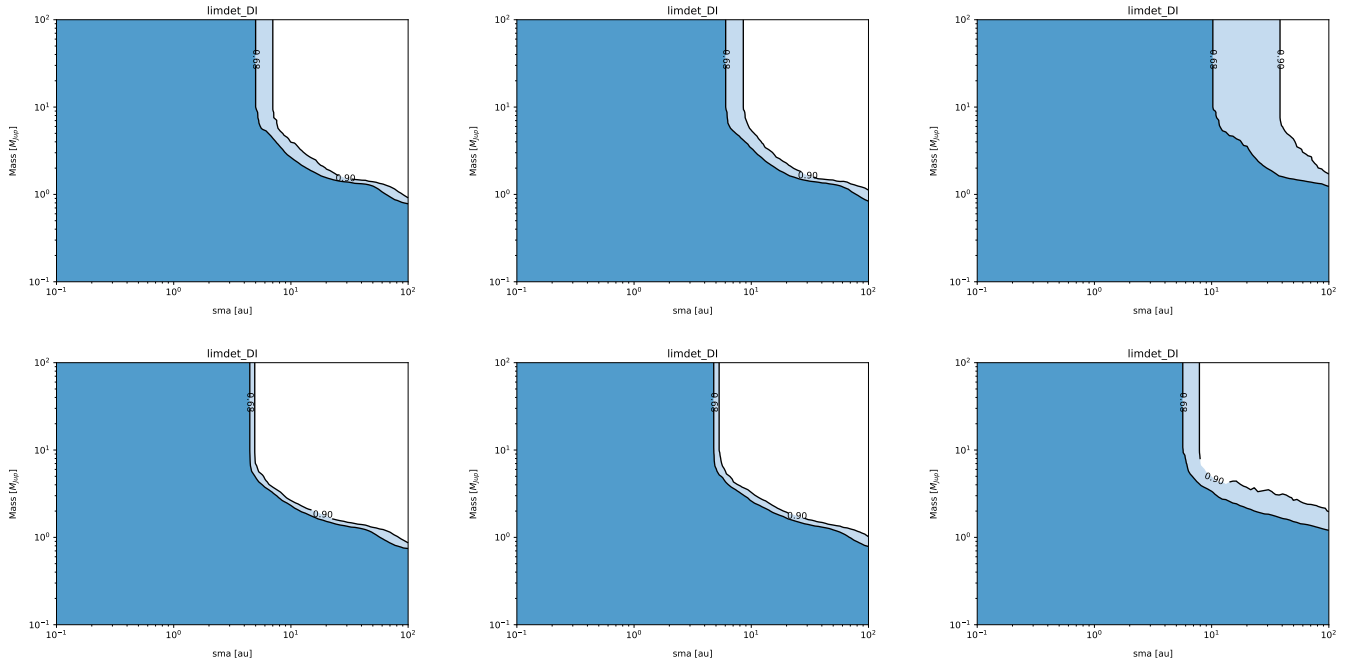


**Fig. 11.** Detection limits for AB Pic obtained using SPHERE high contrast imaging data obtained in Dec. 2015 (First row) and the same data plus SPHERE data obtained in Oct. 2023, as well as GPI high contrast imaging data obtained in 2018 (see Appendix). We assume, from Left to Right, inclinations of  $0^\circ$ ,  $45^\circ$  and  $90^\circ$ . The iso-contours correspond to 90 and 68 % detection probabilities.

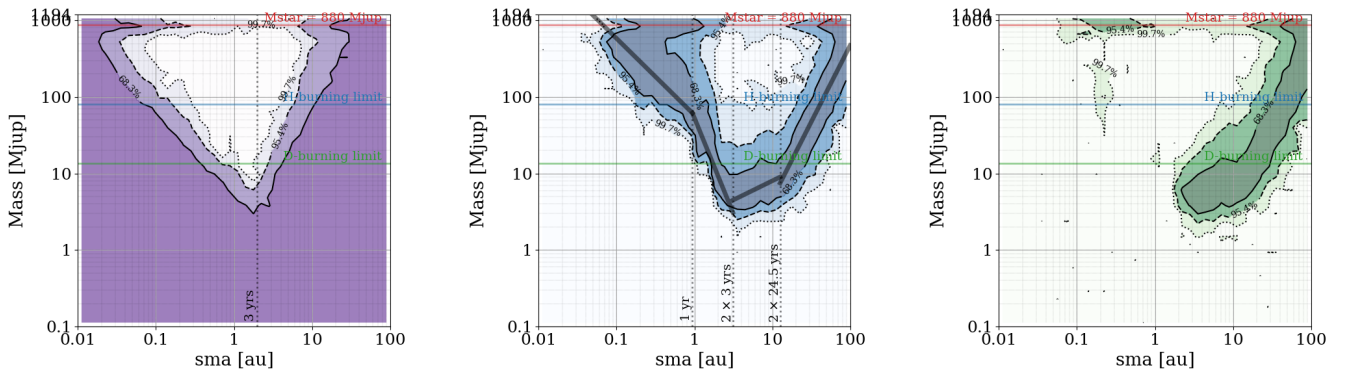


**Fig. 12.** From Left to Right: Gaia excess, PMA and combined maps for AB Pic. No constraint on the inclination of the orbital plane of companions.

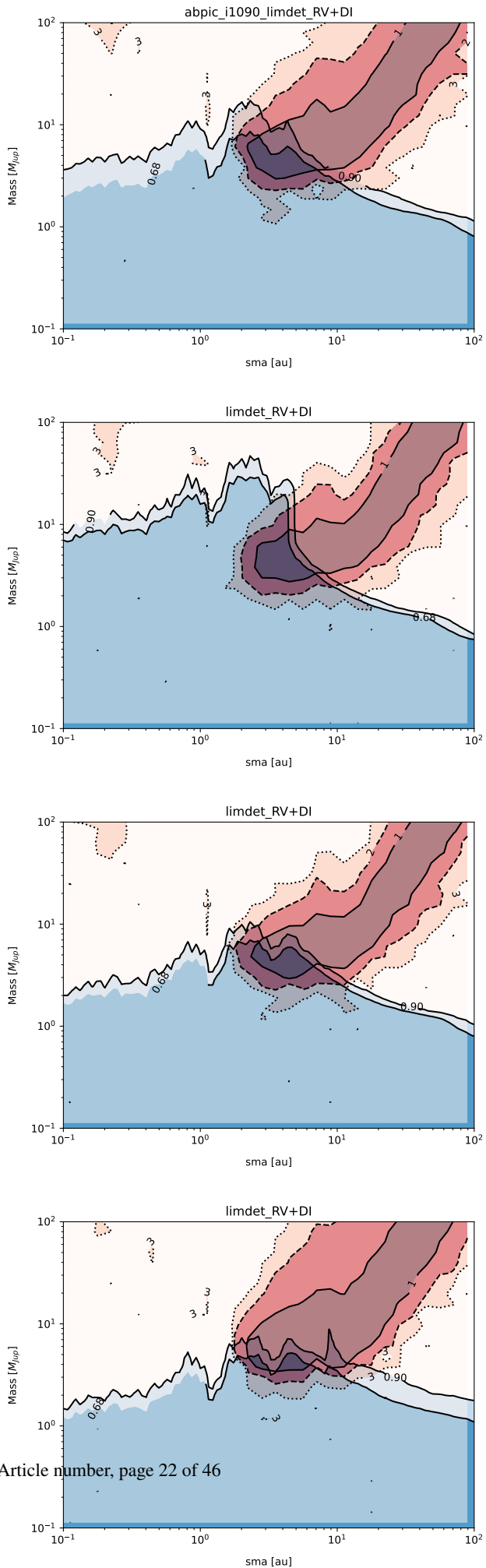


**Fig. 13.** AB Pic. Superimposition of the (sma, mass) solutions from

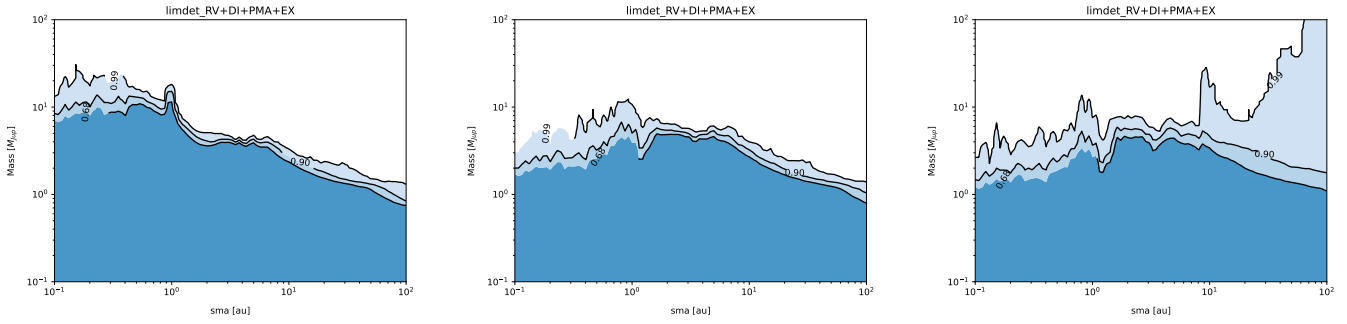


**Fig. 14.** From Left to Right: Detection limits for AB Pic combining RV, GaiaPMEX, and HCI data. From Left to Right:  $i = 0, 45,$  and  $90$  degrees.

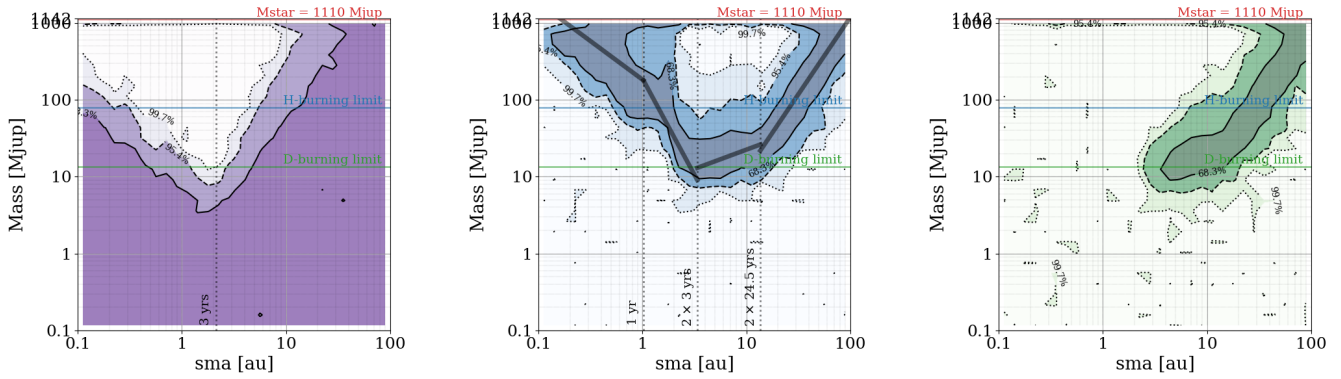


**Fig. 15.** From Left to Right: Gaia excess, PMA, and combined maps for HD 14082 B. No constraints on the orbital plane inclination.

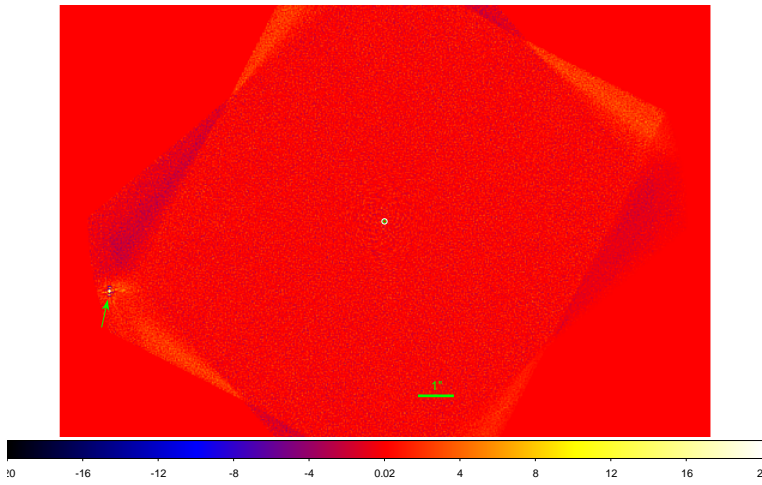


**Fig. 16.** SPHERE image of HD 14082B as reduced with PACO. A faint source (indicated by an arrow) is observed at  $7.7''$  from the star (indicated by a yellow circle, at the center of the image).

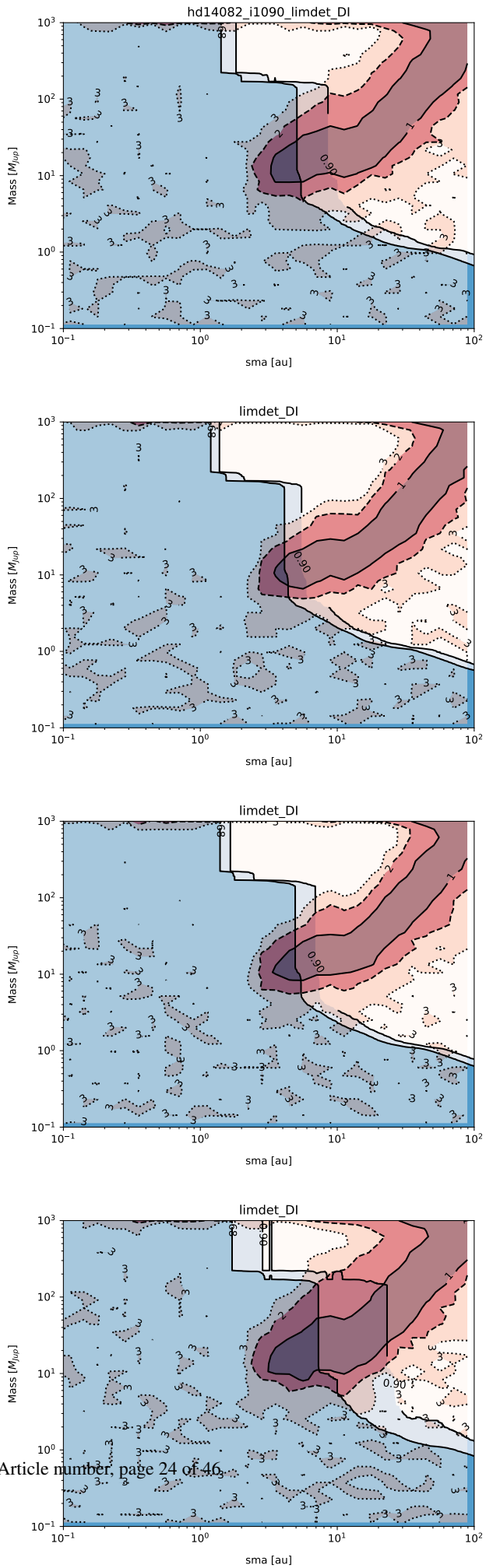


**Fig. 17.** HD 14082B. Superimposition of the GaiaPMEX (sma,mass)

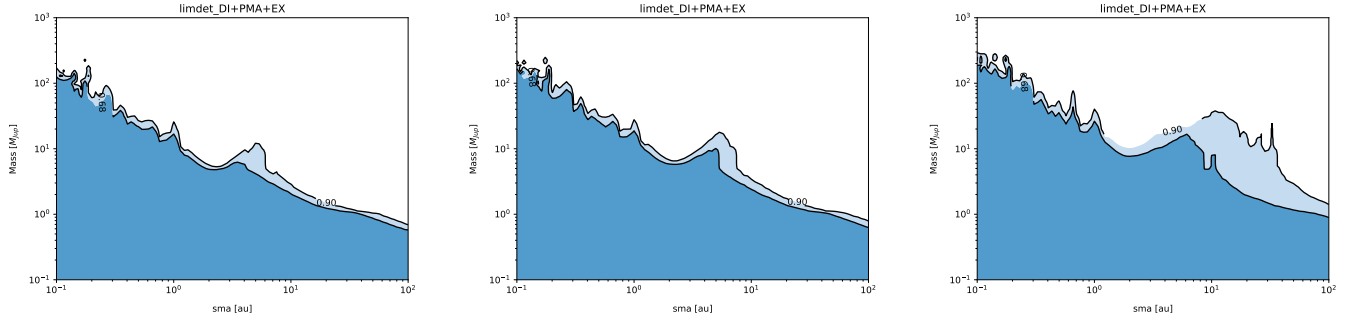


**Fig. 18.** From Left to Right: Detection limits for HD14082B combining GaiaPMEX and HCI data. From Left to Right:  $i = 0, 45,$  and  $90$  degrees.

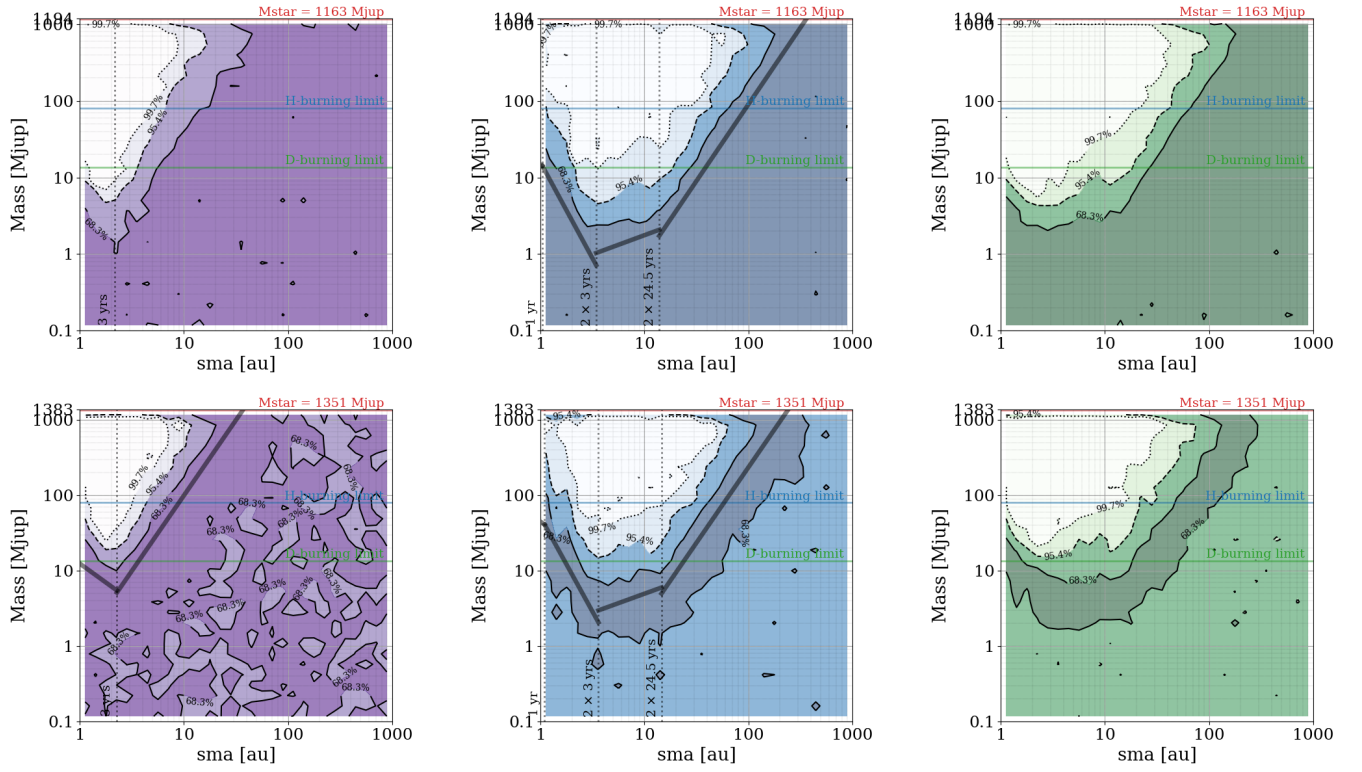


**Fig. 19.** GaiaPMEX results on HD 45270 (top), and HD 164249 (bottom). From left to right: Gaia, PMA, and Gaia+PMA.

## Appendix A: Acronyms and symbols

**Table A.1.** List and definition of relevant, non-trivial, acronyms and symbols used in the text.

| Acronyms or Symbols                         | Definition   |
|---|--|
| <i>Young associations and moving groups</i> |  |
| MG  | Moving Group   |
| YMG   | Young Moving Groups  |
| BPC   | $\beta$ Pictoris   |
| BPMG  | $\beta$ Pictoris moving group  |
| OCT   | Octans   |
| ECH   | $\epsilon$ Chamaeleontis   |
| TWA   | TW Hydrae or TW Hya  |
| ARG   | Argus  |
| ABDor                                       | AB Doradus   |
| COL   | Columba  |
| THA   | Tucana-Horologium  |
| LCC   | Lower Centaurus-Crux   |
| CAR   | Carina association   |
| THOR  | 32 Ori MG  |
| <i>Bibliographic References</i>             |  |
| ZF21  | Zúñiga-Fernández et al. (2021)   |
| K24   | Kiefer et al. (2024a)  |
| WDS   | Washington Double Star Catalog   |
| PB23  | Palma-Bifani et al. (2023)   |
| <i>Methods</i>                              |  |
| GaiaPMEX                                    | Gaia DR3 Proper Motion anomaly and astrometric noise EXcess                            |
| GaiaExplore                                 | Gaia DR3 Exploring and characterisation of PMA, AEN and ruwe                           |
| SACY  | Search for associations containing young stars (Torres et al. 2008)                    |
| BANYAN or BAN                               | Bayesian Analysis for Nearby Young AssociatioNs (?)                                    |
| MCMC  | Markov-Chain Monte-Carlo algorithm   |
| <i>Other Data, Symbols and Names</i>        |  |
| PMa   | Proper Motion anomaly  |
| ruwe  | Renormalised Unit Weight Error   |
| AEN   | Astrometric Excess Noise   |
| $\alpha_{\text{ruwe}}$                      | Astrometric Signature Based on ruwe  |
| $\alpha_{\text{PMA}}$                       | Astrometric Signature Based on PMA   |
| $\alpha_{\text{AEN}}$                       | Astrometric Signature Based on AEN   |
| $N-\sigma_{\text{ruwe}}$                    | Significance as $p$ -value of ruwe compared to noise converted to a number of $\sigma$ |
| $N-\sigma_{\text{PMA}}$                     | Significance as $p$ -value of PMA compared to noise converted to a number of $\sigma$  |
| $N-\sigma_{\text{AEN}}$                     | Significance as $p$ -value of AEN compared to noise converted to a number of $\sigma$  |
| PSF   | Point Spread Function  |
| GoF   | <code>ipd_gof_harmonic_amplitude</code>  |
| Frac  | <code>ipd_frac_multi_peak</code>   |
| IPD   | Image Parameter Determination  |
| AL  | Along-scan Direction on Gaia's Detector  |
| RVSA  | Radial Velocity Semi-Amplitude   |
| BD  | Brown Dwarf  |
| SB  | Spectroscopic Binary   |
| SB1   | 1-spectral-component SB  |
| SB2   | 2-spectral-component SB  |
| KL  | Kozai-Lidov resonance  |

## Appendix B: Target sample

**Table B.1.** Targets sample. The star masses are from ZF21.

| Star name       | Gaia DR3 ID         | $RA_{JCRS}$   | $DEC_{JCRS}$  | SACYMG | SACYprob | BANMG | BANprob | star mass | plx(mas) | plx err |
|-----------------|---------------------|---------------|---------------|--------|----------|-------|---------|-----------|----------|---------|
| HD 105          | 4995853014646189696 | 00:05:52.6847 | -41:45:12.269 | THA    | 0.997    | THA   | 1.000   | 1.11      | 25.75    | 0.02    |
| HD 987          | 468829253688494536  | 00:13:53.3451 | -74:41:18.636 | THA    | 0.996    | THA   | 1.000   | 0.9       | 21.8     | 0.01    |
| HD 984          | 2431157720981843200 | 00:14:10.3654 | -07:11:57.900 | COL    | 0.843    | COL   | 1.000   | 1.26      | 21.88    | 0.02    |
| HD 1466         | 4901229043960053248 | 00:18:26.3386 | -63:28:39.928 | THA    | 0.997    | THA   | 1.000   | 1.15      | 23.36    | 0.02    |
| Smethells 165   | 4901926409210453760 | 00:24:09.1823 | -62:11:05.115 | THA    | 0.950    | THA   | 1.000   | 0.74      | 22.8     | 0.06    |
| V* CT Tuc       | 4902014095262270336 | 00:25:14.8587 | -61:30:49.151 | THA    | 0.996    | THA   | 1.000   | 0.7       | 22.65    | 0.01    |
| HD 3221         | 4901802507993393664 | 00:34:51.4029 | -61:54:58.972 | THA    | 0.801    | THA   | 1.000   | 0.96      | 22.51    | 0.02    |
| CD-78 24        | 4635593356881798912 | 00:42:20.7179 | -77:47:40.215 | THA    | 0.998    | THA   | 1.000   | 0.82      | 20.08    | 0.01    |
| HD 6569         | 2371914419569515136 | 01:06:26.2633 | -14:17:48.620 | ABD    | 0.930    | ABD   | 1.000   | 0.88      | 21.99    | 0.02    |
| BD-12 243       | 2470272812780609280 | 01:20:32.3893 | -11:28:05.918 | ABD    | 0.976    | ABD   | 1.000   | 0.91      | 28.33    | 0.03    |
| HD 8558         | 4909846500703006976 | 01:23:21.4390 | -57:28:51.267 | THA    | 0.999    | THA   | 1.000   | 0.97      | 22.09    | 0.02    |
| HD 8813         | 4637584916037247488 | 01:23:26.3274 | -76:36:42.740 | THA    | 0.932    | THA   | 1.000   | 1.04      | 21.62    | 0.01    |
| V* CC Phe       | 4916062039935185792 | 01:28:08.8475 | -52:38:19.835 | THA    | 0.999    | THA   | 1.000   | 0.82      | 25.11    | 0.01    |
| Barta 16112     | 2477870708709917568 | 01:35:14.0286 | -07:12:52.240 | BPC    | 0.567    | ?     | 1.000   | 0.4       | 26.82    | 0.05    |
| V* EX Cet       | 2477815222028038272 | 01:37:35.6513 | -06:45:39.100 | ?      | 0.987    | BPC   | 1.000   | 0.89      | 41.56    | 0.02    |
| CD-52 381       | 4913138232358905216 | 01:52:14.7130 | -52:19:33.352 | COL    | 0.995    | COL   | 1.000   | 0.86      | 11.54    | 0.01    |
| UCAC3 61-3820   | 471755979772987520  | 01:52:18.5247 | -59:50:17.210 | THA    | 0.995    | THA   | 1.000   | 0.5       | 25.26    | 0.02    |
| V* DK Cet       | 5135093346121603712 | 01:57:49.0967 | -21:54:06.148 | THA    | 0.841    | THA   | 1.000   | 0.97      | 24.21    | 0.02    |
| BD-16 351       | 5147904718169224704 | 02:01:35.6428 | -16:10:01.345 | ?      | 0.999    | COL   | 0.999   | 1.0       | 13.8     | 0.06    |
| CD-53 386       | 4936385034903884288 | 02:01:53.7824 | -52:34:53.351 | COL    | 0.765    | COL   | 1.000   | 1.0       | 8.51     | 0.03    |
| HD 13183        | 4743944043046490240 | 02:07:18.2141 | -53:11:56.895 | THA    | 0.998    | THA   | 1.000   | 0.98      | 20.16    | 0.02    |
| HD 13246        | 4714764481913306496 | 02:07:26.3208 | -59:40:46.236 | THA    | 1.000    | THA   | 1.000   | 1.19      | 22.03    | 0.02    |
| CD-60 416       | 4714764447553568640 | 02:07:32.4055 | -59:40:21.419 | THA    | 0.997    | THA   | 1.000   | 0.73      | 22.0     | 0.01    |
| CD-46 644       | 4943150845347891840 | 02:10:55.4777 | -46:03:59.082 | ?      | 0.902    | ABD   | 1.000   | 0.79      | 12.34    | 0.06    |
| HD 14082B       | 107774198474602368  | 02:17:24.8414 | +28:44:29.272 | BPC    | 0.902    | BPC   | 1.000   | 1.06      | 25.23    | 0.02    |
| HD 14082        | 107774202769886848  | 02:17:25.3926 | +28:44:40.958 | BPC    | 0.911    | BPC   | 1.000   | 1.15      | 25.28    | 0.02    |
| BD+30 397B      | 132363027978672000  | 02:27:28.1581 | +30:58:39.184 | BPC    | 0.900    | BPC   | 1.000   | 0.54      | 24.43    | 0.03    |
| BD+30 397       | 132362959259196032  | 02:27:29.3532 | +30:58:23.442 | BPC    | 0.880    | BPC   | 1.000   | 0.83      | 24.42    | 0.02    |
| CD-44 753       | 4946633857666189952 | 02:30:32.5254 | -43:42:23.505 | ?      | 0.998    | COL   | 0.998   | 0.87      | 18.53    | 0.21    |
| EXO 02352-5216  | 4745195905754074496 | 02:36:51.8800 | -52:03:03.606 | ?      | 0.993    | COL   | 0.993   | 0.39      | 25.75    | 0.02    |
| CD-53 544       | 4742040410461492096 | 02:41:47.0072 | -52:59:52.621 | THA    | 0.912    | THA   | 1.000   | 0.89      | 22.94    | 0.05    |
| V* AF Hor       | 4742040513540707072 | 02:41:47.4711 | -52:59:30.830 | THA    | 0.747    | THA   | 1.000   | 0.69      | 23.08    | 0.04    |
| CD-58 553       | 4726518501732727936 | 02:42:33.1923 | -57:39:36.958 | THA    | 1.000    | THA   | 1.000   | 0.74      | 20.11    | 0.01    |
| HD 17250        | 6478258087046528    | 02:46:14.6896 | +05:35:32.616 | THA    | 0.868    | THA   | 0.987   | 1.23      | 17.53    | 0.02    |
| HD 17332B       | 84625630419434496   | 02:47:27.3490 | +19:22:18.229 | ABD    | 0.975    | ABD   | 1.000   | 1.17      | 30.24    | 0.03    |
| HD 17332A       | 84625634714435968   | 02:47:27.5540 | +19:22:16.027 | ABD    | 0.989    | ABD   | 1.000   | 1.2       | 30.19    | 0.02    |
| GSC 08057-00342 | 4748158986511426688 | 02:54:33.3239 | -51:08:31.580 | ?      | 0.985    | THA   | 0.999   | 0.67      | 22.84    | 0.08    |
| TYC 8862-19-1   | 4721546166554166528 | 02:58:04.0973 | -62:41:13.476 | COL    | 0.985    | COL   | 1.000   | 0.8       | 9.71     | 0.01    |
| V* IS Eri       | 5166951386298774144 | 03:09:42.3848 | -09:34:48.384 | ?      | 0.892    | ABD   | 1.000   | 0.92      | 25.82    | 0.02    |
| HD 20121A       | 4850405974392619648 | 03:12:25.8918 | -44:25:10.947 | THA    | 0.892    | ?     | 1.000   | 1.32      | 17.42    | 0.03    |
| V* HW Cet       | 14457169156045440   | 03:12:34.3466 | +09:44:55.660 | ABD    | 0.893    | ABD   | 1.000   | 0.82      | 17.42    | 0.03    |
| HD 20385        | 3261733202649972992 | 03:16:40.7557 | -03:31:49.711 | THA    | 0.605    | COL   | 0.981   | 1.29      | 20.37    | 0.03    |
| CD-35 1167      | 5047124994197379456 | 03:19:08.7812 | -35:07:00.616 | THA    | 0.999    | THA   | 1.000   | 0.7       | 22.02    | 0.02    |
| BD-11 648       | 5163141131831884544 | 03:21:49.6986 | -10:52:18.207 | COL    | 0.794    | FIELD | 1.000   | 0.88      | 7.67     | 0.02    |

Table B.1 continued from previous page

| Star name            | Gaia DR3 ID         | $RA_{ICRS}$   | $DEC_{ICRS}$  | SACYMG | SACYprob | BANMG | BANprob | star mass | plx(mas) | plx err |
|----------------------|---------------------|---------------|---------------|--------|----------|-------|---------|-----------|----------|---------|
| GSC 08499-00304      | 4723899224517492992 | 03:24:15.1374 | -59:01:12.560 | COL    | 0.973    | COL   | 1.000   | 0.82      | 11.94    | 0.04    |
| BD+03 480            | 3275301176136626432 | 03:28:15.0062 | +04:09:47.760 | THA    | 0.658    | THA   | 1.000   | 1.18      | 12.2     | 0.03    |
| CD-46 1064           | 4846466733467661184 | 03:30:49.2369 | -45:55:57.444 | THA    | 1.000    | THA   | 1.000   | 0.83      | 22.78    | 0.01    |
| HD 21997             | 5084963312478488960 | 03:31:53.7108 | -25:36:51.179 | COL    | 0.998    | COL   | 1.000   | 1.27      | 14.35    | 0.03    |
| CD-44 1173           | 4848412525451859328 | 03:31:55.7725 | -43:59:13.615 | THA    | 0.999    | THA   | 1.000   | 0.76      | 22.17    | 0.03    |
| HD 22213             | 5115334331896590208 | 03:34:16.4336 | -12:04:07.846 | THA    | 0.993    | THA   | 0.998   | 1.09      | 19.46    | 0.02    |
| HD 22705             | 4832672020067562624 | 03:36:53.5519 | -49:57:28.842 | THA    | 0.997    | THA   | 1.000   | 1.19      | 23.66    | 0.18    |
| HD 23208             | 5088895681454956672 | 03:42:39.8085 | -20:32:43.224 | OCT    | 0.806    | OCT   | 0.995   | 0.89      | 17.57    | 0.02    |
| G80-21               | 3250328209054347264 | 03:47:23.5340 | -01:58:24.332 | ABD    | 0.981    | ABD   | 1.000   | 0.47      | 59.43    | 0.03    |
| HD 24636             | 4629074455519836032 | 03:48:11.7279 | -74:41:38.427 | THA    | 0.996    | THA   | 1.000   | 1.36      | 17.51    | 0.02    |
| HD 24681             | 3256189465023650048 | 03:55:20.4501 | -01:43:46.666 | ABD    | 0.939    | ABD   | 1.000   | 0.98      | 17.94    | 0.02    |
| BD-15 705            | 5109911781067864064 | 04:02:16.5581 | -15:21:30.236 | THA    | 0.993    | THA   | 1.000   | 0.83      | 18.28    | 0.01    |
| HD 25457             | 3256786534197166208 | 04:02:36.9043 | -00:16:12.145 | ABD    | 0.993    | ABD   | 1.000   | 1.2       | 53.46    | 0.07    |
| HD 25953             | 3258856089957102720 | 04:06:41.5722 | +01:41:00.563 | ABD    | 0.871    | ABD   | 1.000   | 1.2       | 17.52    | 0.03    |
| CD-58 860            | 4682151077248467456 | 04:11:55.6645 | -58:01:46.892 | OCT    | 0.988    | OCT   | 1.000   | 0.91      | 10.43    | 0.01    |
| HD 26980             | 4844618213903654784 | 04:14:22.6258 | -38:19:01.537 | COL    | 1.000    | COL   | 1.000   | 1.15      | 12.61    | 0.01    |
| HD 27679             | 4896343707641120384 | 04:21:10.3715 | -24:32:21.097 | COL    | 0.993    | COL   | 1.000   | 1.07      | 11.82    | 0.01    |
| CD-43 1395           | 4839354748662015488 | 04:21:48.7175 | -43:17:32.527 | COL    | 0.643    | ?     | ?       | 1.25      |          |         |
| CD-44 1533           | 4839139553621190784 | 04:22:45.7030 | -44:32:51.760 | THA    | 0.757    | COL   | 1.000   | 1.01      | 9.98     | 0.06    |
| 2M J04240094-5512223 | 4778915109878774912 | 04:24:01.0269 | -55:12:22.128 | COL    | 0.989    | ?     | ?       | 0.63      | 13.25    | 0.02    |
| CD-441568            | 4791203492348511232 | 04:27:20.5630 | -44:20:39.219 | COL    | 0.950    | COL   | 1.000   | 0.84      | 11.28    | 0.02    |
| CD-43 1451           | 4791763208191226624 | 04:30:27.3194 | -42:48:45.811 | OCT    | 0.783    | ?     | ?       | 1.07      | 7.73     | 0.51    |
| CD-36 1785           | 4867591989673394944 | 04:34:50.8225 | -35:47:21.132 | COL    | 0.996    | COL   | 1.000   | 0.79      | 11.43    | 0.01    |
| BD-12 943            | 3178069026432500992 | 04:36:47.1580 | -12:09:21.016 | THA    | 0.979    | THA   | 1.000   | 0.88      | 14.59    | 0.01    |
| * c Eri              | 3205095125321700480 | 04:37:36.1796 | -02:28:25.800 | BPC    | 0.792    | BPC   | 1.000   | 1.512     | 33.44    | 0.08    |
| GJ 3305              | 3205094369407459456 | 04:37:37.5138 | -02:29:29.707 | ?      |          | BPC   | 1.000   | 0.78      | 36.01    | 0.48    |
| TYC 91-82-1          | 3282264001022709248 | 04:37:51.4944 | +05:03:07.544 | ?      |          | ABD   | 1.000   | 0.88      | 10.37    | 0.04    |
| HD 29615             | 4891725758804030208 | 04:38:44.0094 | -27:02:01.978 | THA    | 0.999    | THA   | 1.000   | 1.11      | 18.4     | 0.01    |
| HD 30447             | 4881312593414911616 | 04:46:49.5687 | -26:18:08.932 | THA    | 0.895    | FIELD | 1.000   | 0.9       | 12.45    | 0.02    |
| TYC 8083-45-5        | 4784584668571800960 | 04:48:00.7634 | -50:41:25.387 | THA    | 0.973    | THA   | 1.000   | 0.77      | 17.19    | 0.02    |
| HD 32195             | 4622453093418397952 | 04:48:05.4948 | -80:46:44.618 | THA    | 0.913    | THA   | 1.000   | 1.2       | 16.01    | 0.02    |
| GSC 08077-01788      | 4786900240059859968 | 04:51:53.0778 | -46:47:30.730 | THA    | 0.947    | COL   | 1.000   | 0.7       | 11.96    | 0.03    |
| HD 31242             | 4786900244356750976 | 04:51:53.5864 | -46:47:13.102 | COL    | 0.998    | COL   | 1.000   | 0.83      | 11.88    | 0.01    |
| LP 776-25            | 2980822034888930176 | 04:52:24.5508 | -16:49:25.296 | ABD    | 0.969    | ABD   | 1.000   | 0.47      | 63.13    | 0.03    |
| BD-20 951            | 2974596325173490816 | 04:52:49.5637 | -19:55:01.939 | THA    | 0.930    | FIELD | 1.000   | 1.12      | 16.09    | 0.02    |
| HD 272836            | 4786264859778429824 | 04:53:05.2471 | -48:44:38.484 | COL    | 0.996    | COL   | 1.000   | 0.86      | 11.9     | 0.01    |
| CD-561032B           | 4776266798684508928 | 04:53:30.8232 | -55:51:30.551 | ABD    | 1.000    | ABD   | 1.000   | 0.31      | 90.15    | 0.02    |
| CD-561032            | 4776266794388393472 | 04:53:31.4640 | -55:51:35.954 | ?      |          | ABD   | 1.000   | 0.42      | 90.17    | 0.02    |
| HD 31652             | 3183414542727824896 | 04:57:22.3391 | -09:08:00.388 | ?      |          | ABD   | 1.000   | 0.95      | 10.99    | 0.01    |
| BD-08 995            | 3183457561120188672 | 04:58:48.5657 | -08:43:40.067 | COL    | 0.884    | COL   | 1.000   | 0.92      | 11.47    | 0.02    |
| BD-19 1062           | 2975997549665260416 | 04:59:32.0864 | -19:17:41.924 | THA    | 0.993    | THA   | 1.000   | 0.81      | 15.04    | 0.01    |
| V* V1005 Ori         | 3231945508509506176 | 04:59:34.8760 | +01:46:59.151 | BPC    | 0.993    | BPC   | 1.000   | 0.7       | 40.99    | 0.01    |
| CD-57 1054           | 4764027962957023104 | 05:00:47.1994 | -57:15:24.267 | BPC    | 0.992    | BPC   | 1.000   | 0.78      | 37.21    | 0.01    |
| HD 32372             | 4813691219557127808 | 05:00:51.9118 | -41:01:06.558 | COL    | 0.998    | COL   | 1.000   | 1.07      | 12.88    | 0.01    |
| LP 476-207           | 3291643148740384128 | 05:01:58.8072 | +09:58:58.095 | BPC    | 0.975    | BPC   | 1.000   | 0.95      | 42.04    | 0.03    |

Table B.1 continued from previous page

| Star name       | Gaia DR3 ID         | $RA_{J2000}$  | $DEC_{J2000}$ | SACYMG | SACYprob | BANMG | BANprob | star mass | plx(mas) | plx err |
|-----------------|---------------------|---------------|---------------|--------|----------|-------|---------|-----------|----------|---------|
| CD-40 1701      | 4814134872498801408 | 05:02:30.4750 | -39:59:13.404 | ?      |          | ABD   | 1.000   | 0.63      | 18.11    | 0.01    |
| HD 32981        | 2986060653741078784 | 05:06:27.7083 | -15:49:31.119 | ?      |          | ABD   | 1.000   | 1.1       | 11.76    | 0.01    |
| BD-21 1074B     | 2962658549474035712 | 05:06:49.4823 | -21:35:04.301 | BPC    | 0.978    | BPC   | 1.000   | 0.6       | 50.52    | 0.06    |
| BD-21 1074A     | 2962658549474035584 | 05:06:49.9703 | -21:35:09.374 | BPC    | 0.956    | BPC   | 1.000   | 0.46      | 50.43    | 0.02    |
| HD 271037       | 4651456423469407744 | 05:06:50.5557 | -72:21:11.245 | OCT    | 0.797    | OCT   | 1.000   | 1.2       | 7.04     | 0.05    |
| HD 33999        | 4825917101662188928 | 05:12:35.8493 | -34:28:48.587 | ?      |          | ABD   | 1.000   | 1.24      | 10.79    | 0.05    |
| BD-09 1108      | 3014411427921646080 | 05:15:36.5557 | -09:30:51.663 | THA    | 0.953    | THA   | 1.000   | 0.92      | 12.2     | 0.01    |
| CD-30 2310      | 2906284045696794880 | 05:18:29.0938 | -30:01:32.162 | THA    | 0.998    | THA   | 1.000   | 0.77      | 14.91    | 0.03    |
| HD 35650        | 4819591920506512768 | 05:24:30.2287 | -38:58:11.663 | ABD    | 0.998    | ABD   | 1.000   | 0.7       | 57.27    | 0.01    |
| HD 35841        | 2958833623399371392 | 05:26:36.6091 | -22:29:23.798 | THA    | 0.844    | COL   | 1.000   | 1.21      | 9.7      | 0.01    |
| V* AF Lep       | 3009908378049913216 | 05:27:04.7817 | -11:54:04.255 | BPC    | 0.963    | BPC   | 1.000   | 1.14      | 37.25    | 0.02    |
| HD 36705        | 4660766641264343680 | 05:28:44.9676 | -65:26:52.662 | ?      |          | BPC   | 1.000   | 0.92      | 67.33    | 0.44    |
| HD 274576       | 4799008375640297344 | 05:28:51.3555 | -46:28:19.026 | OCT    | 0.998    | OCT   | 1.000   | 1.02      | 7.69     | 0.01    |
| HD 274561       | 4799433474323211776 | 05:28:55.1266 | -45:34:58.213 | COL    | 0.970    | COL   | 1.000   | 0.76      | 9.78     | 0.01    |
| V* UX Col       | 2901725882804010368 | 05:28:56.5317 | -33:28:15.985 | ABD    | 0.924    | ABD   | 1.000   | 0.84      | 15.84    | 0.03    |
| HD 36329        | 4822948351549058304 | 05:29:24.1334 | -34:30:55.425 | COL    | 1.000    | COL   | 1.000   | 1.26      | 13.87    | 0.02    |
| HD 269620       | 4658442922197295232 | 05:29:27.1575 | -68:52:04.324 | THA    | 0.916    | ?     | 1.000   | 1.1       | 11.23    | 0.01    |
| V* AG Lep       | 2968785096982770304 | 05:30:19.0995 | -19:16:31.924 | COL    | 0.876    | COL   | 1.000   | 1.28      | 8.84     | 0.02    |
| BD-20 1111      | 2965432033197734016 | 05:32:29.3251 | -20:43:33.088 | OCT    | 0.958    | OCT   | 1.000   | 1.14      | 6.92     | 0.03    |
| TYC 8098-414-1  | 4793327233418050176 | 05:33:25.6490 | -51:17:12.759 | THA    | 1.000    | THA   | 1.000   | 0.67      | 18.56    | 0.01    |
| V* AH Lep       | 2972231722338351360 | 05:34:09.1896 | -15:17:03.551 | COL    | 0.971    | COL   | 1.000   | 1.19      | 17.35    | 0.02    |
| CD-29 2360      | 2905633272252337920 | 05:34:59.2533 | -29:54:03.444 | ?      |          | ARG   | 0.996   | 0.9       | 17.42    | 0.02    |
| CD-34 2331      | 2900656848263249920 | 05:35:04.1199 | -34:17:52.337 | ABD    | 0.775    | ABD   | 1.000   | 0.72      | 11.62    | 0.01    |
| CD-48 1893      | 4795596831576255488 | 05:36:55.1418 | -47:57:47.897 | ABD    | 0.997    | ABD   | 1.000   | 0.7       | 40.76    | 0.04    |
| V* UY Pic       | 4795598309045006208 | 05:36:56.8896 | -47:57:52.902 | ABD    | 0.998    | ABD   | 1.000   | 0.92      | 40.66    | 0.01    |
| V* AT Col       | 4808094705371742464 | 05:37:05.3557 | -39:32:26.290 | ?      |          | THA   | 1.000   | 1.09      | 13.19    | 0.44    |
| HD 37551        | 4802947444765743104 | 05:37:12.9359 | -42:42:55.937 | ABD    | 0.913    | ABD   | 1.000   | 1.09      | 12.43    | 0.01    |
| HD 37551B       | 4802947444765742848 | 05:37:13.2591 | -42:42:57.507 | ABD    | 0.911    | ABD   | 1.000   | 1.04      | 12.43    | 0.01    |
| HD 37484        | 2907308172059100544 | 05:37:39.6563 | -28:37:34.705 | ?      |          | COL   | 1.000   | 1.36      | 17.0     | 0.02    |
| TYC 119-1242-1  | 3224016964521247616 | 05:37:45.3664 | +02:30:56.894 | COL    | 0.942    | COL   | 0.992   | 0.8       | 14.75    | 0.01    |
| TYC 119-497-1   | 3224017823514705920 | 05:37:46.5219 | +02:31:25.833 | COL    | 0.931    | COL   | 0.999   | 0.79      | 14.74    | 0.01    |
| HD 269921       | 4657783116463742336 | 05:38:34.5749 | -68:53:06.151 | THA    | 0.791    | CARN  | 1.000   | 0.97      | 10.8     | 0.04    |
| BD-08 1195      | 3015216991987620096 | 05:38:35.0254 | -08:56:40.790 | COL    | 0.989    | COL   | 1.000   | 1.04      | 12.21    | 0.02    |
| Parénaço 2752   | 3016917008762062336 | 05:38:56.6423 | -06:24:41.477 | ?      |          | ABD   | 0.999   | 0.92      | 8.08     | 0.01    |
| TYC 7605-1429-1 | 4804618114028288896 | 05:41:14.3307 | -41:17:58.675 | ?      |          | ABD   | 0.995   | 0.96      | 8.17     | 0.06    |
| HD 38207        | 2966779995793890560 | 05:43:20.9734 | -20:11:21.513 | ?      |          | COL   | 1.000   | 1.25      | 9.09     | 0.02    |
| CD-47 1999      | 4795466883045648768 | 05:43:32.1181 | -47:41:10.675 | OCT    | 0.868    | OCT   | 1.000   | 1.31      | 7.19     | 0.01    |
| HD 38397        | 4808165830030420352 | 05:43:35.8442 | -39:55:24.494 | COL    | 1.000    | COL   | 0.997   | 1.17      | 18.66    | 0.02    |
| HD 38497        | 2996181112816572160 | 05:45:41.2531 | -14:46:31.144 | ?      |          | ABD   | 1.000   | 1.27      | 13.09    | 0.06    |
| CD-41 2076      | 4804797819756106112 | 05:48:30.4226 | -41:27:30.252 | ABD    | 0.850    | ABD   | 1.000   | 0.78      | 17.85    | 0.1     |
| CD-27 2520      | 2904801835303287808 | 05:49:06.5957 | -27:33:55.614 | THA    | 0.959    | THA   | 1.000   | 0.86      | 12.86    | 0.01    |
| CD-29 2531      | 2904320936405427072 | 05:50:21.4507 | -29:15:20.563 | COL    | 0.924    | COL   | 1.000   | 0.83      | 8.8      | 0.01    |
| CD-52 1363      | 4792175838585883904 | 05:51:01.1779 | -52:38:12.432 | COL    | 0.808    | COL   | 1.000   | 1.05      | 7.54     | 0.01    |
| V* TZ Col       | 2904454389629265536 | 05:52:15.9890 | -28:39:25.414 | ?      |          | ABD   | 1.000   | 1.18      | 10.86    | 0.16    |
| HD 42270        | 4621305817457618176 | 05:53:29.5095 | -81:56:52.170 | COL    | 0.964    | CAR   | 1.000   | 1.07      | 17.0     | 0.01    |

Table B.1 continued from previous page

| Star name       | Gaia DR3 ID          | $RA_{ICRS}$   | $DEC_{ICRS}$  | SACYMG | SACYprob | BANMG | BANprob | star mass | plx(mas) | plx err |
|-----------------|----------------------|---------------|---------------|--------|----------|-------|---------|-----------|----------|---------|
| HD 40216        | 2883892182159616256  | 05:55:43.1902 | -38:06:16.098 | COL    | 0.996    | COL   | 1.000   | 1.33      | 18.95    | 0.02    |
| V* TY Col       | 2884080885842578176  | 05:57:50.8042 | -38:04:03.449 | ABD    | 0.918    | ABD   | 1.000   | 0.84      | 13.75    | 0.04    |
| TYC 7066-1037-1 | 2889149393928673664  | 05:58:11.7871 | -35:00:48.996 | OCT    | 0.986    | OCT   | 1.000   | 0.77      | 7.39     | 0.01    |
| HD 41071        | 5570953464908732928  | 06:00:41.3260 | -44:53:49.733 | COL    | 0.979    | COL   | 0.986   | 0.89      | 18.48    | 0.01    |
| BD-13 1328      | 2997190322755484032  | 06:02:21.8915 | -13:55:34.074 | ?      |          | ABD   | 1.000   | 0.68      | 22.13    | 0.02    |
| CD-49 2037      | 5554101009671475584  | 06:03:35.4318 | -49:11:25.353 | ?      |          | OCT   | 1.000   | 1.18      | 6.02     | 0.07    |
| CD-34 2676      | 2886635051355088640  | 06:08:33.8714 | -34:02:55.215 | ABD    | 0.884    | ABD   | 1.000   | 0.94      | 11.48    | 0.03    |
| CD-35 2722      | 2885863400349980288  | 06:09:19.2033 | -35:49:31.962 | ABD    | 0.994    | ABD   | 1.000   | 0.6       | 44.72    | 0.01    |
| V* AO Men       | 5266270443442455040  | 06:18:28.1811 | -72:02:40.257 | BPC    | 0.955    | BPC   | 1.000   | 0.85      | 25.57    | 0.01    |
| V* V1358 Ori    | 31116883781327753216 | 06:19:08.0689 | -03:26:21.035 | COL    | 0.872    | ?     |         | 1.16      | 19.35    | 0.02    |
| HD 44627        | 5495052596695570816  | 06:19:12.9419 | -58:03:14.803 | COL    | 0.998    | CAR   | 0.997   | 0.89      | 19.95    | 0.01    |
| HD 45270        | 5481848424118748672  | 06:22:30.9163 | -60:13:06.112 | ABD    | 0.998    | ABD   | 1.000   | 1.11      | 41.89    | 0.01    |
| CD-66 395       | 5283645647739198464  | 06:25:12.3918 | -66:29:09.980 | OCT    | 0.998    | OCT   | 1.000   | 1.0       | 7.47     | 0.01    |
| GSC 08894-00426 | 5481843025342799104  | 06:25:56.0383 | -60:03:25.266 | ABD    | 0.999    | ABD   | 1.000   | 0.29      | 74.42    | 0.02    |
| CD-40 2458      | 5570338906629079936  | 06:26:06.9183 | -41:02:53.587 | COL    | 0.949    | COL   | 1.000   | 1.11      | 10.12    | 0.01    |
| CD-48 2324      | 5552120961029170944  | 06:28:06.0891 | -48:26:52.351 | THA    | 0.655    | COL   | 0.994   | 1.08      | 7.76     | 0.01    |
| HD 47875        | 5278895306528592000  | 06:34:41.0462 | -69:53:05.551 | THA    | 0.974    | THA   | 1.000   | 1.07      | 13.86    | 0.01    |
| HD 48189        | 547978765278589568   | 06:38:00.2597 | -61:31:58.991 | ABD    | 0.891    | ABD   | 1.000   | 1.16      | 45.71    | 0.44    |
| CD-61 1439      | 5479782647926975360  | 06:39:49.9631 | -61:28:40.329 | ABD    | 0.997    | ABD   | 1.000   | 0.68      | 45.03    | 0.01    |
| CD-30 3394      | 2894187150051042560  | 06:40:04.8608 | -30:33:03.210 | OCT    | 0.851    | OCT   | 1.000   | 1.22      | 5.37     | 0.09    |
| CD-30 3394B     | 2894187150052094080  | 06:40:05.7116 | -30:33:08.778 | OCT    | 0.727    | OCT   | 1.000   | 1.15      | 5.21     | 0.15    |
| HD 48370        | 3105749748629384576  | 06:43:01.0393 | -02:53:20.455 | COL    | 0.971    | COL   | 1.000   | 0.94      | 27.81    | 0.02    |
| HD 49855        | 5265670762922792960  | 06:43:46.2712 | -71:58:34.422 | COL    | 0.970    | CAR   | 1.000   | 1.03      | 18.05    | 0.01    |
| HD 53842        | 5194203331750283392  | 06:46:13.7255 | -83:59:28.515 | THA    | 0.960    | THA   | 1.000   | 1.33      | 17.34    | 0.02    |
| CD-36 3202      | 5578127400323942016  | 06:52:46.7417 | -36:36:16.824 | COL    | 0.980    | COL   | 1.000   | 0.87      | 11.03    | 0.01    |
| TYC 9178-284-1  | 5280793308412118656  | 06:55:25.2000 | -68:06:20.505 | COL    | 0.965    | LCC   | 0.997   | 0.86      | 9.02     | 0.01    |
| HD 51797        | 5557658685702796544  | 06:56:23.5440 | -46:46:54.776 | ?      |          | COL   | 1.000   | 1.05      | 10.59    | 0.01    |
| HD 55279        | 5208216951043609216  | 07:00:30.5017 | -79:41:45.026 | COL    | 0.995    | CAR   | 1.000   | 0.85      | 15.76    | 0.01    |
| CD-39 3026      | 5565429312334118272  | 07:01:51.7792 | -39:22:04.202 | ?      |          | ARG   | 0.984   | 0.84      | 6.82     | 0.03    |
| CD-42 2906      | 5562571883473697152  | 07:01:53.3887 | -42:27:55.601 | ?      |          | ARG   | 1.000   | 0.91      | 11.37    | 0.01    |
| CD-57 1709      | 5486699125824396928  | 07:21:23.7018 | -57:20:36.612 | THA    | 0.843    | ?     |         | 0.89      | 9.32     | 0.01    |
| BD+20 1790      | 3363049071685181056  | 07:23:43.5146 | +20:24:54.959 | ?      |          | ABD   | 1.000   | 0.66      | 36.09    | 0.02    |
| CD-48 2972      | 5506101790904438656  | 07:28:21.9862 | -49:08:36.941 | ?      |          | ARG   | 1.000   | 1.03      | 11.47    | 0.01    |
| CD-29 4446      | 5605469402661155968  | 07:28:51.2160 | -30:14:51.885 | ABD    | 0.881    | ?     |         | 0.66      | 64.14    | 0.47    |
| CD-84 80        | 5193207655251945088  | 07:30:59.2321 | -84:19:26.760 | ABD    | 0.907    | ABD   | 1.000   | 0.94      | 14.54    | 0.02    |
| CD-42 3328      | 5536071767758647808  | 07:33:21.1715 | -42:55:42.143 | THA    | 0.838    | FIELD | 1.000   | 0.83      | 7.2      | 0.01    |
| HD 61005        | 5592237639209047424  | 07:35:47.3929 | -32:12:12.855 | ARG    | 0.733    | ARG   | 1.000   | 0.89      | 27.43    | 0.02    |
| CD-60 1850      | 5289434954410657280  | 07:43:42.8646 | -61:07:16.892 | THA    | 0.977    | ?     |         | 0.87      | 10.22    | 0.03    |
| HD 64982        | 5208790376420706432  | 07:45:35.4456 | -79:40:07.500 | ABD    | 0.820    | ABD   | 0.992   | 1.15      | 11.52    | 0.12    |
| CD-48 3199      | 5518068330006200192  | 07:47:25.9364 | -49:02:50.630 | ARG    | 0.993    | ARG   | 1.000   | 0.87      | 8.75     | 0.01    |
| CD-43 3604      | 5532434308418963072  | 07:48:49.7856 | -43:27:05.058 | ?      |          | ARG   | 1.000   | 0.97      | 10.62    | 0.08    |
| TYC 8561-970-1  | 5295688117557736448  | 07:53:55.4413 | -57:10:06.926 | ARG    | 0.568    | ARG   | 1.000   | 0.85      | 6.52     | 0.01    |
| TYC 8557-1251-1 | 5488367737800067072  | 07:55:31.6313 | -54:36:50.464 | THA    | 0.979    | ?     |         | 0.87      | 7.87     | 0.01    |
| TYC 8570-1980-1 | 5319076203049591808  | 08:11:09.3268 | -55:55:56.098 | THA    | 0.952    | CARN  | 0.992   | 0.85      | 7.06     | 0.01    |
| BD-07 2388      | 3062970156370624512  | 08:13:50.9664 | -07:38:25.381 | COL    | 0.885    | FIELD | 1.000   | 0.86      | 19.97    | 0.2     |

Table B.1 continued from previous page

| Star name            | Gaia DR3 ID         | $RA_{ICRS}$   | $DEC_{ICRS}$  | SACYMG | SACYprob | BANMG  | BANprob | star mass | plx(mas) | plx err |
|----------------------|---------------------|---------------|---------------|--------|----------|--------|---------|-----------|----------|---------|
| TYC 8162-1020-1      | 5321517672922567040 | 08:28:45.5936 | -52:05:26.393 | ARG    | 0.974    | ARG    | 1.000   | 1.12      | 6.5      | 0.01    |
| UCAC4 192-018437     | 5322281008869471488 | 08:29:51.8809 | -51:40:39.261 | ARG    | 0.817    | ARG    | 1.000   | 1.07      | 5.73     | 0.02    |
| GSC08162-01222       | 5321275295028390912 | 08:34:18.1087 | -52:15:57.377 | ARG    | 0.998    | ARG    | 0.971   | 0.8       | 6.5      | 0.01    |
| UCAC4 189-019053     | 5321280728169745536 | 08:35:01.1496 | -52:14:01.039 | ARG    | 1.000    | ?      |         | 0.84      | 6.83     | 0.01    |
| CJ* IC 2391 PMM 3359 | 5318176875565072768 | 08:36:54.9475 | -53:08:33.890 | ARG    | 0.997    | IC2391 | 1.000   | 0.86      | 6.74     | 0.01    |
| V* EG Cha            | 5209082129256747008 | 08:36:56.0495 | -78:56:45.203 | ECH    | 0.869    | ETAC   | 1.000   | 1.22      | 10.11    | 0.09    |
| CPD-54 1712          | 5317655157295238656 | 08:37:10.9445 | -55:18:10.334 | THA    | 0.927    | CARN   | 0.999   | 1.14      | 6.69     | 0.01    |
| HD 73777             | 5321190155898133248 | 08:37:47.0084 | -52:52:11.893 | ARG    | 0.943    | IC2391 | 1.000   | 1.3       | 6.58     | 0.01    |
| CJ* IC 2391 D 41     | 5318077507199948672 | 08:37:51.5236 | -53:45:45.404 | ARG    | 0.999    | IC2391 | 1.000   | 0.9       | 6.66     | 0.01    |
| VXR PSPC 2a          | 5318185671658160768 | 08:37:55.5257 | -52:57:10.477 | ?      |          | ARG    | 1.000   | 0.95      | 6.71     | 0.06    |
| CD-52 2467           | 5318186221414047104 | 08:38:22.8647 | -52:56:47.650 | ARG    | 0.996    | IC2391 | 0.999   | 1.02      | 6.69     | 0.01    |
| CD-58 2194           | 5302826215770873088 | 08:39:11.4815 | -58:34:27.597 | ?      |          | ARG    | 1.000   | 1.06      | 8.73     | 0.03    |
| CJ* IC 2391 PMM 686  | 5318059532750974720 | 08:39:22.5213 | -53:55:05.326 | ARG    | 0.990    | ?      |         | 0.83      | 6.51     | 0.04    |
| V* V364 Vel          | 5318545521198976000 | 08:39:53.0064 | -52:57:56.463 | ARG    | 0.988    | IC2391 | 1.000   | 0.89      | 6.62     | 0.01    |
| VXR PSPC 16a         | 5318546822567826944 | 08:40:16.2070 | -52:56:28.801 | ARG    | 0.984    | IC2391 | 1.000   | 0.82      | 6.66     | 0.02    |
| CJ* IC 2391 SMY 23   | 5318093243960659456 | 08:40:49.0574 | -53:37:44.981 | ARG    | 1.000    | IC2391 | 1.000   | 1.09      | 6.72     | 0.01    |
| CD-61 2010           | 5300857711997333120 | 08:42:00.4641 | -62:18:26.094 | THA    | 0.748    | PL8    | 0.994   | 1.02      | 7.93     | 0.01    |
| CJ* IC 2391 PMM 756  | 5317884439832479872 | 08:43:00.3609 | -53:54:07.268 | ARG    | 0.933    | IC2391 | 1.000   | 1.07      | 6.46     | 0.01    |
| V* V376 Vel          | 5318512260971706496 | 08:44:05.1821 | -52:53:16.839 | ARG    | 0.988    | IC2391 | 1.000   | 1.15      | 6.5      | 0.02    |
| V* EO Cha            | 5209135352491538432 | 08:44:31.7278 | -78:46:30.712 | ECH    | 0.907    | ETAC   | 1.000   | 0.58      | 10.19    | 0.01    |
| V* V379 Vel          | 5318328676892604800 | 08:45:26.8863 | -52:52:01.728 | ARG    | 0.999    | IC2391 | 1.000   | 0.75      | 6.7      | 0.01    |
| 2M J08500540-7554380 | 5216440061069982592 | 08:50:05.3754 | -75:54:37.562 | THA    | 0.817    | LCC    | 1.000   | 0.84      | 9.75     | 0.02    |
| CD-57 2315           | 5304243658062322176 | 08:50:08.0323 | -57:45:58.677 | ARG    | 0.848    | ARG    | 1.000   | 1.2       | 10.27    | 0.12    |
| TYC 8927-2035-1      | 5301732820175622912 | 08:52:19.2044 | -60:04:43.960 | THA    | 0.947    | ?      |         | 1.06      | 7.24     | 0.01    |
| TYC 8590-1193-1      | 5304374843544543104 | 08:56:31.4803 | -57:00:40.436 | THA    | 0.867    | CARN   | 0.994   | 0.857     | 6.35     | 0.01    |
| TYC 8582-3040-1      | 5317269950278675072 | 08:57:45.5879 | -54:08:36.462 | THA    | 0.660    | PL8    | 1.000   | 0.94      | 7.28     | 0.01    |
| CD-49 4008           | 5325281335588219008 | 08:57:52.1249 | -49:41:50.379 | COL    | 0.907    | PL8    | 0.998   | 0.96      | 7.93     | 0.01    |
| TYC 8594-58-1        | 5303472350654243712 | 09:02:03.8820 | -58:08:49.456 | ARG    | 0.979    | ARG    | 1.000   | 0.88      | 6.73     | 0.01    |
| CD-55 2543           | 5310127660192135552 | 09:09:29.3222 | -55:38:26.970 | THA    | 0.729    | PL8    | 1.000   | 1.14      | 7.88     | 0.04    |
| TYC 8174-1586-1      | 5325609711604226048 | 09:11:15.7842 | -50:14:14.701 | THA    | 0.539    | PL8    | 0.999   | 0.77      | 8.2      | 0.01    |
| CD-621197            | 6630890508110702208 | 18:16:36.9899 | -62:44:59.178 | ARG    | 0.805    | FIELD  | 1.000   | 1.15      | 2.26     | 0.02    |
| V* V479 Car          | 5299141546145254528 | 09:23:34.9192 | -61:11:35.604 | COL    | 0.885    | CAR    | 0.999   | 1.08      | 10.37    | 0.01    |
| TYC 7695-335-1       | 5426190217812767360 | 09:28:54.0755 | -41:01:18.926 | ARG    | 0.706    | FIELD  | 1.000   | 1.08      | 7.03     | 0.07    |
| HD 309751            | 5247811842236238592 | 09:31:44.7109 | -65:14:52.283 | THA    | 0.714    | FIELD  | 1.000   | 1.28      | 7.22     | 0.02    |
| CPD-52 2481          | 5312245422658960768 | 09:32:26.0514 | -52:37:39.449 | THA    | 0.564    | ?      |         | 0.86      | 7.63     | 0.01    |
| [K2001c] 17          | 5203033750152434176 | 09:34:55.7518 | -78:04:18.938 | ECH    | 0.841    | ?      |         | 0.65      |          |         |
| BD-20 2977           | 5664853853864480768 | 09:39:51.3711 | -21:34:17.328 | ?      |          | ARG    | 1.000   | 1.01      | 11.27    | 0.02    |
| TYC 9217-641-1       | 5218300499165464320 | 09:42:47.3161 | -72:39:49.621 | ARG    | 0.678    | ARG    | 1.000   | 0.8       | 6.42     | 0.01    |
| CD-39 5833           | 5431592977432228992 | 09:47:19.7918 | -40:03:09.579 | ARG    | 0.570    | ARG    | 1.000   | 0.93      | 9.71     | 0.01    |
| HD 85151A            | 5412014832876362624 | 09:48:43.1193 | -44:54:07.376 | ARG    | 0.642    | ARG    | 1.000   | 1.02      | 9.42     | 0.01    |
| CD-65817             | 5249086141843932544 | 09:49:08.9888 | -65:40:20.784 | ARG    | 0.937    | ARG    | 1.000   | 1.17      | 6.82     | 0.01    |
| HD 86356             | 5202135964549093248 | 09:51:50.5349 | -79:01:37.210 | THA    | 0.995    | THA    | 0.975   | 0.91      | 12.67    | 0.01    |
| HD 309851            | 5245641784241253760 | 09:55:58.1881 | -67:21:21.446 | ARG    | 0.981    | ARG    | 1.000   | 1.12      | 9.28     | 0.01    |
| TYC 9217-417-1       | 5242190004920798592 | 09:59:57.5510 | -72:21:46.770 | THA    | 0.992    | LCC    | 0.994   | 0.79      | 11.98    | 0.01    |
| 2M J10010873-7913074 | 5201932413160136064 | 10:01:08.5794 | -79:13:07.097 | THA    | 0.993    | THA    | 1.000   | 0.61      | 12.32    | 0.01    |

Table B.1 continued from previous page

| Star name            | Gaia DR3 ID         | $RA_{ICRS}$   | $DEC_{ICRS}$  | SACYMG | SACYprob | BANMG | BANprob | star mass | plx(mas) | plx err |
|----------------------|---------------------|---------------|---------------|--------|----------|-------|---------|-----------|----------|---------|
| RXJ 10053-7749       | 5202670052321415040 | 10:05:19.8405 | -77:48:42.008 | ECH    | 0.998    | LCC   | 1.000   | 0.43      | 10.03    | 0.01    |
| HD 298936            | 5356713413789090632 | 10:13:14.6621 | -52:30:53.848 | COL    | 0.915    | CAR   | 1.000   | 0.88      | 18.84    | 0.01    |
| TWA 22               | 5355751581627180288 | 10:17:26.5848 | -53:54:26.538 | BPC    | 0.925    | BPC   | 1.000   | 0.17      | 50.52    | 0.2     |
| BD+01 2447           | 3855208897392952192 | 10:28:54.9080 | +00:50:15.889 | ABD    | 0.985    | ABD   | 1.000   | 0.41      | 142.1    | 0.02    |
| CD-69 783            | 5232233789697993728 | 10:41:22.9171 | -69:40:42.733 | THA    | 0.957    | ?     |         | 0.88      | 10.62    | 0.01    |
| V* CE Ant            | 5444751795151480320 | 10:42:29.9496 | -33:40:16.544 | TWA    | 0.646    | TWA   | 0.999   | 0.56      | 29.33    | 0.03    |
| CPD-691432           | 5231590094359089024 | 10:53:51.3740 | -70:02:15.899 | ?      |          | ARG   | 1.000   | 1.12      | 6.35     | 0.03    |
| V* TW Hya            | 5401795662560500352 | 11:01:51.8166 | -34:42:17.255 | TWA    | 0.999    | TWA   | 1.000   | 0.74      | 16.63    | 0.02    |
| TYC 8962-1747-1      | 5240822208157707648 | 11:08:07.7976 | -63:41:46.821 | COL    | 0.879    | LCC   | 0.975   | 0.92      | 11.23    | 0.09    |
| CD-29 8887           | 5452498541764280832 | 11:09:13.6871 | -30:01:40.223 | TWA    | 0.774    | CARN  | 0.985   | 0.93      | 21.77    | 0.2     |
| TWA 3A               | 5396978667759696000 | 11:10:27.7567 | -37:31:51.805 | TWA    | 0.841    | ?     |         | 0.66      | 26.99    | 0.04    |
| V* V1215 Cen         | 5375025440645600000 | 11:13:26.1529 | -45:23:42.826 | TWA    | 0.676    | ?     |         | 0.83      | 10.87    | 0.02    |
| V* V1217 Cen         | 5396105586807802880 | 11:21:05.3951 | -38:45:16.756 | TWA    | 1.000    | TWA   | 1.000   | 0.62      | 15.29    | 0.02    |
| CD-34 7390A          | 5399220743767211776 | 11:21:17.1295 | -34:46:45.790 | TWA    | 1.000    | TWA   | 1.000   | 0.74      | 16.71    | 0.02    |
| CD-34 7390B          | 5399220743767211264 | 11:21:17.3533 | -34:46:50.044 | TWA    | 1.000    | TWA   | 1.000   | 0.82      | 16.71    | 0.02    |
| HD 98800             | 3534414590303807232 | 11:22:05.1894 | -24:46:40.286 | TWA    | 0.979    | TWA   | 0.993   | 1.34      | 23.75    | 0.39    |
| CD-337795            | 5398663566249861120 | 11:31:55.1510 | -34:36:27.564 | TWA    | 0.932    | TWA   | 1.000   | 0.99      | 20.13    | 0.06    |
| CD-26 8623           | 3485098646237003392 | 11:32:41.1575 | -26:51:56.400 | TWA    | 0.976    | TWA   | 1.000   | 0.54      | 21.76    | 0.03    |
| CD-26 8623B          | 3485098646237003136 | 11:32:41.0644 | -26:52:09.494 | TWA    | 0.985    | TWA   | 1.000   | 0.16      | 21.63    | 0.03    |
| 2M J11401658-8321003 | 5197213279191665920 | 11:40:16.2131 | -83:20:59.927 | THA    | 0.985    | THA   | 1.000   | 0.77      | 12.72    | 0.01    |
| CD-36 7429B          | 3463395519358168064 | 11:48:23.6581 | -37:28:48.774 | TWA    | 0.926    | TWA   | 1.000   | 0.39      | 13.14    | 0.03    |
| CD-36 7429A          | 3463395523652894336 | 11:48:24.1514 | -37:28:49.407 | TWA    | 0.980    | TWA   | 1.000   | 0.84      | 13.07    | 0.01    |
| V* DZ Cha            | 5200035927402217088 | 11:49:31.6210 | -78:51:01.126 | ECH    | 0.999    | ECH   | 1.000   | 0.66      | 9.94     | 0.02    |
| V* T Cha             | 5199981334076455680 | 11:57:13.2842 | -79:21:31.668 | ?      |          | ECH   | 1.000   | 0.75      | 9.74     | 0.03    |
| RX J11597-7601       | 5224879500011370496 | 11:59:42.0899 | -76:01:26.274 | ECH    | 0.994    | ECH   | 1.000   | 0.76      | 10.09    | 0.01    |
| V* DX Cha            | 5836666564476158336 | 12:00:04.8820 | -78:11:34.658 | ECH    | 0.959    | ECH   | 1.000   | 1.61      | 9.38     | 0.04    |
| [FLG2003] eps Cha 6  | 5836666560185012352 | 12:00:08.0589 | -78:11:39.416 | ECH    | 0.981    | ECH   | 1.000   | 0.84      | 9.77     | 0.02    |
| [FLG2003] eps Cha 7  | 5836666564480769280 | 12:00:09.0895 | -78:11:42.387 | ECH    | 0.987    | ECH   | 1.000   | 0.93      | 9.98     | 0.03    |
| HD 104467            | 5788345708499360256 | 12:01:38.8817 | -78:59:16.996 | ECH    | 0.977    | ECH   | 1.000   | 0.85      | 10.18    | 0.12    |
| 2M J12020369-7853012 | 578853485859490432  | 12:02:03.4702 | -78:53:01.394 | ECH    | 0.900    | ECH   | 1.000   | 0.86      | 10.18    | 0.06    |
| TWA 23               | 3466308095597260032 | 12:07:27.2829 | -32:47:00.668 | TWA    | 0.596    | TWA   | 1.000   | 0.6       | 17.6     | 0.09    |
| HD 105923            | 5854812388999707008 | 12:11:38.0188 | -71:10:36.144 | ECH    | 0.921    | ?     |         | 0.71      | 9.47     | 0.01    |
| V* V1249 Cen         | 6150861598484393856 | 12:15:30.6136 | -39:48:43.057 | TWA    | 0.996    | TWA   | 1.000   | 0.82      | 18.66    | 0.03    |
| 2M J12164593-7753333 | 5788664871812309376 | 12:16:45.7320 | -77:53:33.607 | ECH    | 0.997    | ECH   | 1.000   | 0.49      | 9.82     | 0.02    |
| 2M J12194369-7403572 | 5841382846589454080 | 12:19:43.5462 | -74:03:57.400 | ECH    | 0.992    | ECH   | 1.000   | 0.57      | 9.92     | 0.01    |
| RX J12204-7407       | 5841334609821849472 | 12:20:21.6304 | -74:07:39.645 | ?      |          | ECH   | 0.998   | 0.86      | 8.42     | 0.35    |
| TWA 16               | 6132134299824086144 | 12:34:56.2301 | -45:38:07.956 | TWA    | 0.953    | ?     |         | 0.81      | 12.22    | 0.16    |
| CD-74 712            | 5838361599097855104 | 12:39:21.1178 | -75:02:39.381 | ECH    | 0.996    | ECH   | 0.999   | 1.23      | 9.7      | 0.01    |
| CD-69 1055           | 5844573358774024320 | 12:58:25.4527 | -70:28:49.412 | ECH    | 0.814    | LCC   | 0.999   | 1.37      | 10.51    | 0.01    |
| V* PX Vir            | 3677911582262521728 | 13:03:49.4499 | -05:09:46.016 | ABD    | 0.714    | ?     |         | 0.91      |          |         |
| CPD-68 1894          | 5844296281847839232 | 13:22:07.4246 | -69:38:12.539 | ECH    | 0.817    | LCC   | 0.999   | 1.52      | 10.22    | 0.01    |
| 2M J13491293-7549475 | 5789867600093615360 | 13:49:12.6739 | -75:49:47.933 | ARG    | 0.860    | ARG   | 1.000   | 1.01      | 12.09    | 0.01    |
| HD 129496            | 5848129213744138880 | 14:46:21.2691 | -67:46:16.263 | ARG    | 0.605    | ARG   | 1.000   | 1.24      | 12.13    | 0.01    |
| V* NY Aps            | 5792536565791371776 | 15:12:23.1264 | -75:15:16.834 | ARG    | 0.771    | ARG   | 1.000   | 0.85      | 19.09    | 0.01    |
| HD 139084B           | 5882581895192805632 | 15:38:56.6791 | -57:42:20.554 | BPC    | 0.898    | BPC   | 1.000   | 0.2       | 25.44    | 0.02    |

Table B.1 continued from previous page

| Star name            | Gaia DR3 ID         | $RA_{ICRS}$   | $DEC_{ICRS}$  | SACYMG | SACYprob | BANMG | BANprob | star mass | plx(mas) | plx err |
|----------------------|---------------------|---------------|---------------|--------|----------|-------|---------|-----------|----------|---------|
| HD 139084            | 5882581895219921024 | 15:38:57.4476 | -57:42:28.830 | BPC    | 0.775    | BPC   | 1.000   | 1.11      | 25.83    | 0.2     |
| HD 139751            | 6254299662396908288 | 15:40:28.3225 | -18:41:48.648 | ABD    | 0.785    | ABD   | 1.000   | 0.81      | 25.96    | 0.04    |
| LP 745-70            | 4338433743723131648 | 16:33:41.5395 | -09:33:14.782 | ABD    | 0.963    | ABD   | 1.000   | 0.58      | 32.17    | 0.02    |
| HD 152555            | 4377537462448122112 | 16:54:08.1026 | -04:20:26.487 | ABD    | 0.903    | ABD   | 1.000   | 1.16      | 22.13    | 0.02    |
| CD-2711535           | 4107812485571331328 | 17:15:03.6033 | -27:49:40.470 | BPC    | 0.649    | BPC   | 0.996   | 1.14      |          |         |
| GSC 08350-01924      | 5949369736173100544 | 17:29:20.66   | -50:14:53.9   | BPC    | 0.964    | ?     |         | 0.84      | 15.96    | 0.08    |
| CD-54 7336           | 5924485966955008896 | 17:29:55.0675 | -54:15:49.664 | BPC    | 0.962    | BPC   | 1.000   | 1.06      | 14.79    | 0.01    |
| HD 155177            | 5767017686883156864 | 17:42:09.1975 | -86:08:05.596 | OCT    | 0.939    | OCT   | 1.000   | 0.59      | 7.83     | 0.05    |
| HD 161460            | 5945104490030338432 | 17:48:33.7368 | -53:06:44.288 | BPC    | 0.670    | BPC   | 0.993   | 1.22      |          |         |
| HD 164249            | 6702775135228913280 | 18:03:03.4137 | -51:38:57.811 | BPC    | 0.993    | BPC   | 1.000   | 1.29      | 20.29    | 0.02    |
| HD 164249B           | 6702775508886369408 | 18:03:04.1114 | -51:38:57.712 | BPC    | 0.825    | BPC   | 1.000   | 0.54      | 20.33    | 0.02    |
| HD 319139            | 4045698423617983488 | 18:14:10.4863 | -32:47:35.360 | BPC    | 0.980    | BPC   | 0.973   | 1.11      | 13.99    | 0.02    |
| GSC 07396-00759      | 4045698732855626624 | 18:14:22.0777 | -32:46:10.976 | BPC    | 0.975    | BPC   | 1.000   | 0.9       | 13.92    | 0.02    |
| CD-64 1208           | 6438274728259539072 | 18:45:37.0992 | -64:51:48.359 | BPC    | 0.818    | ARG   | 1.000   | 0.86      | 35.16    | 0.18    |
| Smethells 20         | 6631685008336771072 | 18:46:52.5824 | -62:10:37.896 | BPC    | 0.986    | BPC   | 1.000   | 0.72      | 19.72    | 0.02    |
| UCAC2 1331888        | 6418631162754209920 | 18:49:45.1858 | -71:56:58.178 | OCT    | 0.900    | OCT   | 1.000   | 0.89      | 6.8      | 0.01    |
| CD-31 16041          | 6736232346363422336 | 18:50:44.5047 | -31:47:48.539 | BPC    | 0.952    | BPC   | 1.000   | 0.86      | 20.22    | 0.01    |
| V* PZ Tel            | 6655168686921108864 | 18:53:05.9006 | -50:10:51.265 | BPC    | 0.840    | BPC   | 1.000   | 1.14      | 21.16    | 0.02    |
| TYC 6872-1011-1      | 6760846563417053056 | 18:58:04.1696 | -29:53:05.439 | BPC    | 0.919    | BPC   | 1.000   | 0.98      | 13.45    | 0.04    |
| HD 178085            | 6632318361397624960 | 19:10:57.8753 | -60:16:21.539 | ABD    | 0.902    | ABD   | 1.000   | 1.19      | 17.08    | 0.02    |
| CD-26 13904          | 6764026419748892160 | 19:11:44.6913 | -26:04:09.301 | ?      |          | BPC   | 1.000   | 1.11      | 14.77    | 0.21    |
| * eta Tel            | 6643602576214115584 | 19:22:51.2534 | -54:25:27.473 | BPC    | 0.991    | BPC   | 1.000   | 1.19      | 20.6     | 0.1     |
| HD 181327            | 6643589352010758400 | 19:22:58.9885 | -54:32:18.290 | BPC    | 0.966    | BPC   | 1.000   | 1.19      | 20.93    | 0.03    |
| TYC 486-4943-1       | 4289366113217575424 | 19:33:03.7686 | +03:45:38.654 | ABD    | 0.893    | ABD   | 1.000   | 0.78      | 14.23    | 0.01    |
| CPD-79 1037          | 6362543597150911616 | 19:47:03.9241 | -78:57:43.429 | OCT    | 0.914    | ?     |         | 1.04      | 6.92     | 0.01    |
| CPD-82 784           | 6347492932234149120 | 19:53:57.0553 | -82:40:42.057 | OCT    | 0.880    | ?     |         | 1.14      | 8.28     | 0.02    |
| UCAC3 116-474938     | 6747467431032539008 | 19:56:02.9824 | -32:07:19.826 | BPC    | 0.685    | BPC   | 0.998   | 0.72      | 19.54    | 0.73    |
| TYC 7443-1102-1      | 6747467224874108288 | 19:56:04.4141 | -32:07:38.769 | BPC    | 0.989    | BPC   | 1.000   | 0.78      | 19.49    | 0.02    |
| 2M J20013718-3313139 | 6747106443324127488 | 20:01:37.2100 | -33:13:14.993 | BPC    | 0.987    | BPC   | 1.000   | 0.73      | 16.68    | 0.02    |
| BD-03 4778           | 4222102218052861440 | 20:04:49.3880 | -02:39:21.547 | ABD    | 0.916    | ABD   | 1.000   | 0.96      | 14.88    | 0.01    |
| CD-52 9381           | 6666178680963755008 | 20:07:23.9230 | -51:47:29.558 | ?      |          | ARG   | 1.000   | 0.59      | 29.36    | 0.01    |
| HD 191089            | 6847146784384459648 | 20:09:05.2635 | -26:13:27.598 | BPC    | 0.990    | BPC   | 1.000   | 1.32      | 19.96    | 0.02    |
| V* AT Mic            | 6792436799475128960 | 20:41:51.5010 | -32:26:12.677 | BPC    | 0.985    | FIELD | 1.000   | 0.442*    | 100.79   | 0.07    |
| V* AU Mic            | 6794047652729201024 | 20:45:09.8838 | -31:20:33.000 | BPC    | 0.992    | BPC   | 1.000   | 0.61      | 102.94   | 0.02    |
| HD 199058            | 1750317374916618752 | 20:54:21.1180 | +09:02:22.855 | ABD    | 0.845    | ABD   | 1.000   | 1.31      | 13.06    | 0.06    |
| IRXS J2054280+090615 | 1750318749306157824 | 20:54:28.0340 | +09:06:05.803 | ABD    | 0.887    | ABD   | 1.000   | 0.77      | 13.34    | 0.02    |
| HD 358623            | 6882838031333427456 | 20:56:02.8029 | -17:10:54.762 | BPC    | 0.940    | ?     |         | 0.92      | 21.7     | 0.02    |
| HD 201919            | 6834123756346400768 | 21:13:05.3650 | -17:29:15.030 | ABD    | 0.999    | ABD   | 1.000   | 0.72      | 26.02    | 0.02    |
| HD 202917            | 6463782435948431616 | 21:20:50.0133 | -53:02:04.685 | THA    | 0.975    | THA   | 1.000   | 0.9       | 21.41    | 0.02    |
| BD+22 4409           | 1797276382668029440 | 21:31:01.8704 | +23:20:05.055 | ABD    | 0.998    | FIELD | 1.000   | 0.76      | 41.29    | 0.02    |
| Smethells 86         | 6409848126430574592 | 21:44:30.2139 | -60:58:40.391 | THA    | 0.990    | THA   | 1.000   | 0.68      | 21.55    | 0.01    |
| HD 207575            | 6408937971321777152 | 21:52:09.8251 | -62:03:09.965 | THA    | 0.976    | THA   | 1.000   | 1.26      | 21.39    | 0.01    |
| BPS CS 22881-0003    | 6571446820698811904 | 22:02:16.3330 | -42:10:34.777 | THA    | 0.950    | ?     |         | 0.62      | 22.49    | 0.02    |
| CPD-72 2713          | 6382640367603744128 | 22:42:49.2563 | -71:42:22.037 | BPC    | 0.991    | BPC   | 1.000   | 0.79      | 27.23    | 0.01    |
| V* WW Psa            | 6603693881832177792 | 22:44:58.1923 | -33:15:03.715 | BPC    | 0.998    | BPC   | 1.000   | 0.35      | 47.92    | 0.03    |

Table B.1 continued from previous page

| Star name      | Gaia DR3 ID         | $RA_{ICRS}$   | $DEC_{ICRS}$  | SACYMG | SACYprob | BANMG | BANprob | star mass | plx(mas) | plx err |
|----------------|---------------------|---------------|---------------|--------|----------|-------|---------|-----------|----------|---------|
| V* TX PsA      | 6603693808817829760 | 22:45:00.2897 | -33:15:28.025 | BPC    | 0.993    | BPC   | 1.000   | 0.19      | 48.0     | 0.03    |
| HD 217343      | 2382711653818308224 | 23:00:19.4167 | -26:09:16.082 | ?      |          | ABD   | 1.000   | 1.02      | 31.47    | 0.02    |
| HD 217379A     | 2382705816958084224 | 23:00:28.0956 | -26:18:45.332 | ABD    | 0.923    | FIELD | 1.000   | 0.93      | 31.48    | 0.02    |
| BD-03 5579     | 2638216857371313664 | 23:09:37.1951 | -02:25:55.981 | THA    | 0.945    | THA   | 1.000   | 0.84      | 19.22    | 0.02    |
| HD 218860      | 6527965258988306304 | 23:11:52.1858 | -45:08:12.130 | ABD    | 0.979    | ABD   | 1.000   | 1.0       | 20.93    | 0.02    |
| CD-45 14955B   | 6527965293348044288 | 23:11:53.7516 | -45:08:01.943 | ?      |          | ABD   | 1.000   | 0.55      | 21.04    | 0.05    |
| TYC 9344-293-1 | 6380514358792367232 | 23:26:10.9662 | -73:23:50.915 | THA    | 0.997    | THA   | 1.000   | 0.63      | 21.61    | 0.01    |
| BD-13 6424     | 2433191886212246784 | 23:32:31.0135 | -12:15:52.776 | BPC    | 0.992    | BPC   | 1.000   | 0.7       | 36.43    | 0.02    |
| HD 22259B      | 6387058411482257280 | 23:39:39.5042 | -69:11:40.547 | THA    | 0.982    | THA   | 1.000   | 0.89      | 22.65    | 0.01    |
| HD 22259       | 6387058411482257536 | 23:39:39.7196 | -69:11:45.788 | THA    | 0.993    | THA   | 1.000   | 0.97      | 22.64    | 0.02    |
| HD 222575      | 2311789825227125632 | 23:41:54.3862 | -35:58:40.867 | ABD    | 0.899    | ABD   | 1.000   | 0.98      | 15.44    | 0.02    |
| HD 223340      | 2328250334633289856 | 23:48:50.6117 | -28:07:17.347 | ABD    | 0.985    | ABD   | 1.000   | 0.87      | 22.68    | 0.02    |
| HD 224228      | 2307132568850133376 | 23:56:10.9564 | -39:03:11.382 | ABD    | 1.000    | ABD   | 1.000   | 0.82      | 45.55    | 0.02    |
| CD-87 121      | 6343364815827362688 | 23:58:18.0852 | -86:26:23.802 | OCT    | 0.937    | OCT   | 1.000   | 1.21      | 8.92     | 0.05    |

## Appendix C: Results

This table provides the results on the stars not known to be accreting and found to be have a companion in the present study.

The column labeled ZF21 indicates the binary status reported by ZF21. WDS stands for Washington visual Double Stars catalogue (?). SB9 stands for the 9th Catalogue of Spectroscopic Binary Orbits (?). NSS refers to the Gaia DR3 Part 3 Non-single stars (Gaia Collaboration, 2022). FMP refers to *IPD\_frac\_multi\_peak*.  $\sigma_{\text{ruwe}}$  refers to the  $N\text{-}\sigma_{\text{ruwe}}$ , and  $\sigma_{\text{PMa}}$  refers to the  $N\text{-}\sigma_{\text{PMa}}$  (see Text). Note that values of 10.0 indicate actual values equal or larger than 10. Max sma indicates the maximum sma of the (sma, Mass) solutions for each identified binary, and Min mass gives the minimum mass in terms of class (Stellar, BD, or Planet) of the (sma, Mass) solutions.

**Table C.1.** Binary status from GaiaPMEX. For a description on the columns, see text.

| Star name            | Gaia DR3 ID         | ZF21              | Nfov | Npts | Dup. | Par.<br>solved | RUWE   | WDS<br>flag | SB9<br>flag | NSS<br>flag | FMP<br>flag | Phot Var. | $\sigma_{PMa}$ | Max sma | Min sma<br>(au) | mass |
|----------------------|---------------------|-------------------|------|------|------|----------------|--------|-------------|-------------|-------------|-------------|-----------|----------------|---------|-----------------|------|
| CD-29 2360           | 2905633272252337920 | ?                 | 56   | 491  | 0    | 31             | 1913.0 | 0           | 0           | 0           | 12.0        | NAV       | 8.2            | 20      | BD              |      |
| CD-44 1173           | 4848412525451859328 | ?                 | 41   | 357  | 0    | 95             | 1811.0 | 1           | 0           | 0           | 36.0        | NAV       | 8.0            | 20      | BD              |      |
| BD-20 951            | 2974596325173490816 | SB2               | 68   | 602  | 0    | 31             | 1806.0 | 0           | 0           | 2           | 1.0         | NAV       | 7.8            | 20      | BD              |      |
| V* V376 Vel          | 5318512260971706496 | ?                 | 40   | 352  | 0    | 31             | 1919.0 | 0           | 0           | 0           | 1.0         | NAV       | 7.7            | 15      | BD              |      |
| V* DX Cha            | 5836666564476158336 | ?                 | 33   | 293  | 1    | 31             | 2071.0 | 1           | 0           | 0           | 2.0         | NAV       | 7.7            | 3       | S               |      |
| V* V1215 Cen         | 5375025440645600000 | SB2               | 80   | 693  | 0    | 31             | 1727.0 | 1           | 0           | 0           | 0.0         | NAV       | 6.9            | 20      | BD              |      |
| [FLG2003] eps Cha 7  | 5836666564480769280 | ?                 | 39   | 344  | 0    | 95             | 1554.0 | 1           | 0           | 0           | 0.0         | NAV       | 6.5            | 10      | BD              |      |
| BD-21 1074B          | 2962658549474035712 | ?                 | 52   | 454  | 0    | 95             | 1948.0 | 1           | 0           | 0           | 59.0        | NAV       | 6.1            | 20      | P               |      |
| CPD-82 784           | 6347492932234149120 | ?                 | 39   | 342  | 0    | 31             | 1.72   | 0           | 0           | 0           | 0.0         | NAV       | 6.1            | 20      | BD              |      |
| CD-84 80             | 5193207655251945088 | ?                 | 31   | 273  | 0    | 31             | 1.63   | 1           | 0           | 0           | 47.0        | NAV       | 5.7            | 20      | BD              |      |
| BD+03 480            | 3275301176136626432 | SB2               | 18   | 159  | 0    | 31             | 1862.0 | 1           | 0           | 0           | 50.0        | NAV       | 5.3            | 20      | BD              |      |
| V* AG Lep            | 2968785096982770304 | ?                 | 47   | 412  | 0    | 31             | 1575.0 | 0           | 0           | 0           | 0.0         | VAR       | 5.2            | 20      | BD              |      |
| HD 38497             | 2996181112816572160 | ?                 | 29   | 235  | 0    | 95             | 1885.0 | 1           | 0           | 0           | 44.0        | NAV       | 4.8            | 20      | P               |      |
| Barta 16112          | 2477870708709917568 | ?                 | 37   | 313  | 0    | 31             | 1.488  | 0           | 0           | 0           | 2.0         | NAV       | 4.4            | 15      | P               |      |
| HD 139751            | 6254299662396908288 | ?                 | 23   | 199  | 0    | 95             | 1807.0 | 1           | 0           | 0           | 49.0        | NAV       | 4.2            | 20      | P               |      |
| V* DZ Cha            | 5200035927402217088 | ?                 | 35   | 306  | 0    | 31             | 1508.0 | 0           | 0           | 0           | 0.0         | NAV       | 4.0            | 15      | BD              |      |
| [FLG2003] eps Cha 6  | 5836666560185012352 | ?                 | 40   | 354  | 0    | 31             | 1.4    | 1           | 0           | 0           | 0.0         | NAV       | 4.0            | 20      | BD              |      |
| G80-21               | 3250328209054347264 | ?                 | 33   | 294  | 0    | 31             | 1.52   | 0           | 0           | 0           | 1.0         | NAV       | 3.9            | 3       | P               |      |
| TYC 8083-45-5        | 4784584668571800960 | ?                 | 27   | 231  | 0    | 31             | 1541.0 | 1           | 0           | 0           | 50.0        | NAV       | 3.9            | 20      | P               |      |
| LP 776-25            | 2980822034888930176 | ?                 | 53   | 460  | 0    | 31             | 1.38   | 0           | 0           | 0           | 1.0         | NAV       | 3.3            | 30      | P               |      |
| CD-26 8623B          | 3485098646237003136 | ?                 | 47   | 409  | 0    | 31             | 1.3    | 1           | 0           | 0           | 0.0         | NAV       | 3.3            | 10      | P               |      |
| V* HW Cet            | 14457169156045440   | ?                 | 21   | 187  | 0    | 31             | 1.45   | 0           | 0           | 0           | 0.0         | NAV       | 3.2            | 25      | P               |      |
| V* T Cha             | 5199981334076455680 | ?                 | 34   | 291  | 0    | 95             | 1.38   | 1           | 0           | 0           | 0.0         | NAV       | 3.1            | 2       | BD              |      |
| CD-36 7429B          | 3463395519358168064 | ?                 | 44   | 385  | 0    | 31             | 1.34   | 1           | 0           | 0           | 0.0         | NAV       | 3.0            | 10      | P               |      |
| HD 20385             | 3261733202649972992 | SB? not stable RV | 23   | 203  | 0    | 31             | 1332.0 | 1           | 0           | 0           | 13.0        | NAV       | 2.9            | 40      | BD              |      |
| EXO 02352-5216       | 4745195905754074496 | SB?               | 46   | 404  | 0    | 31             | 1265.0 | 0           | 0           | 0           | 1.0         | NAV       | 2.7            | 20      | P               |      |
| BD-21 1074A          | 2962658549474035584 | ?                 | 53   | 465  | 0    | 31             | 1278.0 | 1           | 0           | 0           | 0.0         | NAV       | 2.6            | 30      | P               |      |
| RXJ 10053-7749       | 5202670052321415040 | ?                 | 41   | 359  | 0    | 31             | 1274.0 | 0           | 0           | 0           | 0.0         | NAV       | 2.6            | 15      | P               |      |
| CD-34 7390B          | 5399220743767211264 | ?                 | 49   | 425  | 0    | 31             | 1267.0 | 1           | 0           | 0           | 2.0         | NAV       | 2.6            | 30      | P               |      |
| HD 309851            | 5245641784241253760 | ?                 | 39   | 339  | 0    | 31             | 1.17   | 0           | 0           | 0           | 0.0         | NAV       | 2.5            | 30      | BD              |      |
| HD 309751            | 5247811842236238592 | SB2               | 43   | 379  | 0    | 95             | 1334.0 | 0           | 0           | 0           | 0.0         | NAV       | 2.5            | 20      | BD              |      |
| 2M J08500540-7554380 | 5216440061069982592 | ?                 | 32   | 278  | 0    | 31             | 1164.0 | 0           | 0           | 0           | 0.0         | NAV       | 2.4            | 20      | P               |      |
| CD-34 7390A          | 5399220743767211776 | ?                 | 51   | 440  | 0    | 31             | 1.25   | 1           | 0           | 0           | 0.0         | NAV       | 2.4            | 30      | P               |      |
| HD 139084B           | 5882581895192805632 | ?                 | 60   | 523  | 0    | 31             | 1226.0 | 1           | 0           | 0           | 0.0         | NAV       | 2.4            | 20      | P               |      |
| CD-29 2531           | 2904320936405427072 | ?                 | 48   | 416  | 0    | 31             | 1243.0 | 1           | 0           | 0           | 15.0        | VAR       | 2.2            | 20      | P               |      |
| BD+30 397B           | 132363027978672000  | ?                 | 23   | 196  | 0    | 31             | 1332.0 | 1           | 0           | 0           | 0.0         | NAV       | 2.1            | 20      | P               |      |
| UCAC4 192-018437     | 5322281008869471488 | ?                 | 34   | 292  | 0    | 31             | 1148.0 | 0           | 0           | 0           | 0.0         | NAV       | 2.1            | 20      | BD              |      |
| BD-13 1328           | 2997190322755484032 | ?                 | 42   | 368  | 0    | 31             | 1233.0 | 1           | 0           | 0           | 0.0         | NAV       | 2.0            | 30      | P               |      |
| HD 319139            | 4045698423617983488 | SB2               | 23   | 201  | 0    | 31             | 862.0  | 1           | 0           | 0           | 0.0         | VAR       | 2.0            | 30      | P               |      |
| UCAC3 61-3820        | 471755977972987520  | ?                 | 42   | 369  | 0    | 31             | 1.19   | 0           | 0           | 0           | 0.0         | NAV       | 2.0            | 30      | P               |      |
| CD-561032B           | 4776266798684508928 | ?                 | 36   | 317  | 0    | 31             | 1215.0 | 1           | 0           | 0           | 4.0         | NAV       | 2.0            | 30      | P               |      |
| 2M J10010873-7913074 | 5201932413160136064 | ?                 | 39   | 342  | 0    | 31             | 1.2    | 0           | 0           | 0           | 0.0         | NAV       | 2.0            | 30      | P               |      |

**Table C.1.** Binary status from GaiaPMEX. For a description on the columns, see text.

| Star name            | Gaia DR3 ID         | ZF21 | Nfov | Npts | Dup. | Par.<br>solved | RUWE    | WDS<br>flag | SB9<br>flag | NSS<br>flag | FMP<br>flag | Phot Var. | $\sigma_{\text{ruwe}}$ | $\sigma_{\text{PMa}}$ | Max sma | Min sma<br>(au) | mass |
|----------------------|---------------------|------|------|------|------|----------------|---------|-------------|-------------|-------------|-------------|-----------|------------------------|-----------------------|---------|-----------------|------|
| TWA 3A               | 5396978667759696000 | ?    | 40   | 348  | 0    | 31             | 1286.0  | 1           | 0           | 0           | 14.0        | NAV       | 2.0                    |                       | 20      | P               |      |
| HD 164249B           | 6702775508886369408 | ?    | 35   | 299  | 0    | 31             | 1226.0  | 1           | 0           | 0           | 0.0         | NAV       | 2.0                    |                       | 25      | P               |      |
| HD 199058            | 1750317374916618752 | SB2  | 36   | 318  | 0    | 31             | 3188.0  | 1           | 0           | 0           | 20.0        | NAV       | 10.0                   |                       | 15      | BD              |      |
| V* TY Col            | 288408085842578176  | ?    | 42   | 370  | 0    | 31             | 2662.0  | 0           | 0           | 0           | 0.0         | VAR       | 10.0                   |                       | 15      | BD              |      |
| CD-34 2676           | 2886635051355088640 | ?    | 46   | 406  | 0    | 95             | 2317.0  | 1           | 0           | 0           | 57.0        | VAR       | 10.0                   |                       | 15      | BD              |      |
| CD-30 3394           | 2894187150051042560 | ?    | 46   | 400  | 0    | 31             | 7096.0  | 1           | 0           | 0           | 0.0         | NAV       | 10.0                   |                       | 7       | S               |      |
| CD-30 3394B          | 2894187150052094080 | ?    | 46   | 388  | 0    | 95             | 10.9    | 1           | 0           | 0           | 0.0         | NAV       | 10.0                   |                       | 7       | S               |      |
| V* UX Col            | 2901725882804010368 | ?    | 49   | 415  | 0    | 95             | 3.01    | 1           | 0           | 0           | 40.0        | NAV       | 10.0                   |                       | 20      | BD              |      |
| V* TZ Col            | 2904454389629265536 | ?    | 52   | 456  | 0    | 31             | 14481.0 | 0           | 0           | 0           | 0.0         | NAV       | 10.0                   | 10.0                  | 7       | S               |      |
| CD-30 2310           | 2906284045696794880 | ?    | 55   | 479  | 0    | 31             | 2.98    | 1           | 0           | 0           | 35.0        | NAV       | 10.0                   |                       | 10      | BD              |      |
| BD-20 1111           | 2965432033197734016 | SB?  | 95   | 816  | 1    | 31             | 1862.0  | 1           | 0           | 0           | 0.0         | VAR       | 10.0                   |                       | 15      | BD              |      |
| BD-07 2388           | 3062970156370624512 | ?    | 59   | 519  | 0    | 31             | 13796.0 | 1           | 0           | 0           | 0.0         | NAV       | 10.0                   |                       | 10      | S               |      |
| GJ 3305              | 3205094369407459456 | ?    | 49   | 417  | 0    | 31             | 22864.0 | 1           | 0           | 0           | 38.0        | NAV       | 10.0                   |                       | 10      | S               |      |
| TYC 91-82-1          | 3282264001022709248 | ?    | 49   | 427  | 0    | 31             | 2817.0  | 1           | 0           | 0           | 60.0        | NAV       | 10.0                   |                       | 10      | BD              |      |
| TWA 23               | 3466308095597260032 | SB   | 66   | 580  | 0    | 31             | 4327.0  | 0           | 0           | 0           | 0.0         | NAV       | 10.0                   |                       | 8       | BD              |      |
| HD 98800             | 3534414590303807232 | SB2  | 22   | 186  | 0    | 95             | 9354.0  | 1           | 1           | 0           | 97.0        | NAV       | 10.0                   | 10.0                  | 10      | S               |      |
| HD 98800             | 3534414590303807232 | SB2  | 22   | 186  | 0    | 95             | 9354.0  | 1           | 1           | 0           | 97.0        | NAV       | 10.0                   | 10.0                  | 10      | S               |      |
| HD 271037            | 4651456423469407744 | ?    | 38   | 336  | 0    | 31             | 4928.0  | 0           | 0           | 0           | 0.0         | NAV       | 10.0                   |                       | 9       | S               |      |
| HD 269921            | 4657783116463742336 | ?    | 35   | 309  | 0    | 31             | 2847.0  | 0           | 0           | 1           | 0.0         | NAV       | 10.0                   |                       | 10      | BD              |      |
| HD 36705             | 4660766641264343680 | ?    | 30   | 267  | 0    | 31             | 25.13   | 1           | 0           | 0           | 0.0         | NAV       | 10.0                   | 10.0                  | 8       | S               |      |
| GSC 08499-00304      | 4723899224517492992 | ?    | 34   | 291  | 1    | 31             | 2863.0  | 1           | 0           | 0           | 78.0        | NAV       | 10.0                   |                       | 1       | BD              |      |
| CD-53 544            | 4742040410461492096 | ?    | 46   | 404  | 0    | 31             | 4115.0  | 1           | 0           | 0           | 0.0         | NAV       | 10.0                   |                       | 20      | BD              |      |
| V* AF Hor            | 4742040513540707072 | ?    | 47   | 403  | 0    | 31             | 3327.0  | 1           | 0           | 0           | 0.0         | NAV       | 10.0                   |                       | 10      | BD              |      |
| GSC 08057-00342      | 4748158986511426688 | SB1  | 48   | 424  | 0    | 31             | 5267.0  | 0           | 0           | 0           | 0.0         | NAV       | 10.0                   |                       | 10      | BD              |      |
| 2M J04240094-5512223 | 4778915109878774912 | ?    | 42   | 362  | 0    | 31             | 2017.0  | 0           | 0           | 0           | 0.0         | NAV       | 10.0                   |                       | 10      | BD              |      |
| GSC 08077-01788      | 4786900240059859968 | SB2  | 38   | 334  | 0    | 31             | 2529.0  | 1           | 0           | 1           | 0.0         | NAV       | 10.0                   |                       | 15      | BD              |      |
| CD-441568            | 4791203492348511232 | ?    | 40   | 355  | 0    | 31             | 2085.0  | 1           | 0           | 0           | 25.0        | NAV       | 10.0                   |                       | 15      | BD              |      |
| CD-43 1451           | 4791763208191226624 | ?    | 32   | 260  | 0    | 31             | 41935.0 | 1           | 0           | 0           | 91.0        | NAV       | 10.0                   |                       | 7       | S               |      |
| CD-48 1893           | 4795596831576255488 | ?    | 43   | 380  | 0    | 31             | 3799.0  | 1           | 0           | 1           | 1.0         | NAV       | 10.0                   | 10.0                  | 20      | P               |      |
| TYC 7605-1429-1      | 4804618114028288896 | ?    | 49   | 433  | 0    | 31             | 6402.0  | 1           | 0           | 0           | 0.0         | VAR       | 10.0                   |                       | 9       | S               |      |
| CD-41 2076           | 4804797819756106112 | ?    | 44   | 389  | 0    | 31             | 8.22    | 0           | 0           | 0           | 2.0         | NAV       | 10.0                   |                       | 10      | BD              |      |
| V* AT Col            | 4808094705371742464 | ?    | 35   | 292  | 0    | 31             | 34589.0 | 1           | 0           | 0           | 12.0        | NAV       | 10.0                   |                       | 5       | S               |      |
| HD 33999             | 4825917101662188928 | SB3  | 32   | 272  | 0    | 31             | 2567.0  | 1           | 0           | 0           | 72.0        | NAV       | 10.0                   |                       | 15      | BD              |      |
| HD 22705             | 4832672020067562624 | SB?  | 34   | 301  | 0    | 31             | 9442.0  | 1           | 0           | 3           | 0.0         | NAV       | 10.0                   | 10.0                  | 10      | BD              |      |
| CD-44 1533           | 4839139553621190784 | ?    | 41   | 350  | 0    | 95             | 5718.0  | 0           | 0           | 0           | 0.0         | NAV       | 10.0                   |                       | 10      | S               |      |
| HD 3221              | 4901802507993393664 | ?    | 48   | 419  | 0    | 31             | 2081.0  | 1           | 0           | 1           | 0.0         | NAV       | 10.0                   | 1.4                   | 20      | P               |      |
| Smethells 165        | 4901926409210453760 | SB?  | 40   | 347  | 0    | 95             | 3264.0  | 1           | 0           | 0           | 78.0        | NAV       | 10.0                   | 10.0                  | 10      | BD              |      |
| CD-53 386            | 4936385034903884288 | ?    | 47   | 406  | 0    | 95             | 2693.0  | 1           | 0           | 0           | 28.0        | NAV       | 10.0                   |                       | 10      | BD              |      |
| CD-46 644            | 4943150845347891840 | ?    | 52   | 461  | 0    | 31             | 4448.0  | 1           | 0           | 0           | 0.0         | NAV       | 10.0                   |                       | 10      | BD              |      |
| CD-44 753            | 4946633857666189952 | ?    | 55   | 483  | 0    | 31             | 19741.0 | 1           | 0           | 0           | 0.0         | NAV       | 10.0                   |                       | 15      | BD              |      |
| BD-16 351            | 5147904718169224704 | ?    | 37   | 322  | 0    | 31             | 2844.0  | 1           | 0           | 0           | 62.0        | NAV       | 10.0                   |                       | 15      | BD              |      |
| HD 64982             | 5208790376420706432 | ?    | 31   | 274  | 0    | 31             | 7.6     | 1           | 0           | 1           | 0.0         | NAV       | 10.0                   | 3.5                   | 3       | S               |      |

**Table C.1.** Binary status from GaiaPMEX. For a description on the columns, see text.

| Star name            | Gaia DR3 ID         | ZF21 | Nfov | Npts | Dup. | Par.<br>solved | RUWE    | WDS<br>flag | SB9<br>flag | NSS<br>flag | FMP<br>flag | Phot Var. | $\sigma_{\text{PMa}}$ | Max sma | Min sma | mass |
|----------------------|---------------------|------|------|------|------|----------------|---------|-------------|-------------|-------------|-------------|-----------|-----------------------|---------|---------|------|
|                      |                     |      |      |      |      |                |         |             |             |             |             |           |                       |         | (au)    |      |
| V* EG Cha            | 5209082129256747008 | ?    | 37   | 326  | 0    | 31             | 9226.0  | 1           | 0           | 0           | 0.0         | NAV       | 10.0                  | 9       | S       |      |
| CPD-691432           | 5231590094359089024 | ?    | 39   | 344  | 0    | 31             | 2.15    | 0           | 0           | 0           | 8.0         | NAV       | 10.0                  | 10      | BD      |      |
| TYC 8962-1747-1      | 5240822208157707648 | ?    | 47   | 413  | 0    | 31             | 7.0     | 1           | 0           | 0           | 0.0         | NAV       | 10.0                  | 10      | S       |      |
| CD-60 1850           | 5289434954410657280 | ?    | 33   | 286  | 0    | 31             | 2661.0  | 1           | 0           | 0           | 0.0         | NAV       | 10.0                  | 15      | BD      |      |
| CD-58 2194           | 5302826215770873088 | ?    | 41   | 361  | 0    | 31             | 2527.0  | 0           | 0           | 1           | 0.0         | NAV       | 10.0                  | 15      | BD      |      |
| CD-57 2315           | 5304243658062322176 | ?    | 32   | 275  | 0    | 95             | 6.46    | 1           | 0           | 0           | 0.0         | NAV       | 10.0                  | 10      | S       |      |
| CD-55 2543           | 5310127660192135552 | ?    | 37   | 315  | 0    | 95             | 2999.0  | 1           | 0           | 0           | 0.0         | NAV       | 10.0                  | 10      | BD      |      |
| CI* IC 2391 PMM 686  | 5318059532750974720 | ?    | 44   | 385  | 0    | 31             | 4126.0  | 0           | 0           | 0           | 25.0        | NAV       | 10.0                  | 10      | S       |      |
| VXR PSPC 2a          | 5318185671658160768 | ?    | 42   | 364  | 0    | 31             | 4577.0  | 0           | 0           | 0           | 0.0         | NAV       | 10.0                  | 7       | S       |      |
| TWA 22               | 5355751581627180288 | ?    | 43   | 374  | 0    | 31             | 8878.0  | 0           | 0           | 0           | 0.0         | NAV       | 10.0                  | 5       | S       |      |
| CD-337795            | 5398663566249861120 | VB   | 60   | 531  | 0    | 31             | 3327.0  | 1           | 0           | 0           | 2.0         | NAV       | 10.0                  | 15      | BD      |      |
| TYC 7695-335-1       | 5426190217812767360 | ?    | 60   | 527  | 0    | 31             | 5073.0  | 0           | 0           | 0           | 0.0         | NAV       | 10.0                  | 7       | S       |      |
| CD-29 8887           | 5452498541764280832 | ?    | 39   | 319  | 0    | 95             | 8792.0  | 1           | 0           | 0           | 99.0        | NAV       | 10.0                  | 10      | S       |      |
| HD 48189             | 547977876278589568  | ?    | 20   | 176  | 0    | 31             | 24094.0 | 1           | 0           | 0           | 64.0        | NAV       | 10.0                  | 8       | S       |      |
| CD-43 3604           | 5532434308418963072 | SB1  | 44   | 390  | 0    | 31             | 9325.0  | 1           | 0           | 0           | 0.0         | NAV       | 10.0                  | 10      | BD      |      |
| CD-49 2037           | 5554101009671475584 | ?    | 27   | 220  | 0    | 95             | 3.45    | 1           | 0           | 0           | 73.0        | NAV       | 10.0                  | 8       | S       |      |
| CD-39 3026           | 5565429312334118272 | ?    | 37   | 324  | 0    | 31             | 2129.0  | 1           | 0           | 0           | 0.0         | NAV       | 10.0                  | 10      | BD      |      |
| CD-29 4446           | 560546940266115968  | SB   | 45   | 392  | 0    | 95             | 10317.0 | 1           | 0           | 0           | 76.0        | NAV       | 10.0                  | 8       | S       |      |
| HD 155177            | 5767017686883156864 | SB2  | 35   | 306  | 0    | 31             | 3483.0  | 0           | 0           | 0           | 25.0        | NAV       | 10.0                  | 7       | BD      |      |
| HD 104467            | 5788345708499360256 | SB1  | 41   | 362  | 0    | 31             | 7.68    | 0           | 0           | 3           | 0.0         | NAV       | 10.0                  | 7       | S       |      |
| 2M J12020369-7853012 | 5788534858859490432 | SB1  | 41   | 362  | 0    | 31             | 4.49    | 1           | 0           | 0           | 0.0         | NAV       | 10.0                  | 10      | S       |      |
| RX J12204-7407       | 5841334609821849472 | ?    | 45   | 386  | 0    | 95             | 11496.0 | 1           | 0           | 0           | 23.0        | NAV       | 10.0                  | 10      | S       |      |
| HD 139084            | 5882581895219921024 | SB1  | 55   | 485  | 1    | 31             | 8.6     | 1           | 0           | 1           | 0.0         | NAV       | 10.0                  | 6       | S       |      |
| GSC 08350-01924      | 5949369736173100544 | ?    | 66   | 551  | 0    | 95             | 1605.0  | 1           | 0           | 0           | 99.0        | NAV       | 10.0                  | 10      | BD      |      |
| TWA 16               | 6132134299824086144 | ?    | 44   | 375  | 0    | 31             | 10459.0 | 1           | 0           | 0           | 99.0        | NAV       | 10.0                  | 7       | S       |      |
| CD-87 121            | 6343364815827362688 | ?    | 37   | 317  | 0    | 31             | 4.95    | 0           | 0           | 0           | 0.0         | NAV       | 10.0                  | 10      | S       |      |
| CD-64 1208           | 6438274728259539072 | SB2  | 52   | 451  | 0    | 31             | 10937.0 | 1           | 0           | 0           | 6.0         | VAR       | 10.0                  | 10      | BD      |      |
| CD-45 14955B         | 652796529334804288  | ?    | 85   | 743  | 0    | 31             | 3425.0  | 1           | 0           | 0           | 0.0         | VAR       | 10.0                  | 10      | BD      |      |
| UCAC3 116-474938     | 6747467431032539008 | SB3  | 32   | 281  | 0    | 31             | 29.71   | 1           | 0           | 0           | 7.0         | NAV       | 10.0                  | 3       | S       |      |
| TYC 6872-1011-1      | 6760846563417053056 | SB2  | 25   | 218  | 0    | 31             | 2372.0  | 1           | 0           | 0           | 0.0         | NAV       | 10.0                  | 15      | BD      |      |
| CD-26 13904          | 6764026419748892160 | ?    | 26   | 231  | 0    | 31             | 11992.0 | 1           | 0           | 0           | 0.0         | NAV       | 10.0                  | 8       | S       |      |
| V* AT Mic            | 6792436799475128960 | ?    | 48   | 427  | 1    | 31             | 2331.0  | 1           | 0           | 0           | 2.0         | NAV       | 10.0                  | 10.0    | NB      |      |
| HD 17332A            | 84625634714435968   | ?    | 21   | 184  | 0    | 31             | 1011.0  | 1           | 0           | 0           | 0.0         | NAV       | 1.0                   | 7.2     |         |      |
| HD 40216             | 2883892182159616256 | ?    | 39   | 344  | 0    | 31             | 967.0   | 1           | 0           | 0           | 1.0         | NAV       | 0.5                   | 5.3     | 100     | P    |
| HD 14082B            | 107774198474602368  | ?    | 21   | 186  | 0    | 31             | 919.0   | 1           | 0           | 0           | 0.0         | NAV       | 0.5                   | 5.0     | 100     | NB   |
| HD 44627             | 5495052596695570816 | ?    | 30   | 257  | 0    | 31             | 923.0   | 1           | 0           | 0           | 0.0         | NAV       | 0.6                   | 4.2     | 100     | P    |
| V* AF Lep            | 3009908378049913216 | ?    | 72   | 627  | 1    | 31             | 918.0   | 0           | 0           | 0           | 0.0         | VAR       | 0.0                   | 4.0     | 200     | P    |
| HD 178085            | 6632318361397624960 | ?    | 55   | 480  | 0    | 31             | 1.07    | 1           | 0           | 0           | 0.0         | NAV       | 1.3                   | 3.9     | 200     | P    |
| V* PZ Tel            | 6655168686921108864 | SB?  | 35   | 308  | 0    | 31             | 949.0   | 1           | 0           | 0           | 0.0         | NAV       | 0.6                   | 3.0     | 200     | P    |
| HD 222259            | 6387058411482257536 | ?    | 44   | 383  | 0    | 31             | 913.0   | 1           | 0           | 0           | 1.0         | NAV       | 0.3                   | 2.6     | 200     | P    |
| HD 53842             | 5194203331750283392 | ?    | 36   | 313  | 0    | 31             | 1032.0  | 1           | 0           | 0           | 6.0         | NAV       | 1.1                   | 2.2     | 20      | P    |
| HD 23208             | 5088895681454956672 | ?    | 49   | 431  | 0    | 31             | 993.0   | 0           | 0           | 0           | 0.0         | VAR       | 0.8                   | 2.2     | 200     | P    |

**Table C.1.** Binary status from GaiaPMEX. For a description on the columns, see text.

| Star name      | Gaia DR3 ID         | ZF21 | Nfov | Npts | Dup. | Par.<br>solved | RUWE   | WDS<br>flag | SB9<br>flag | NSS<br>flag | FMP<br>flag | Phot Var. | $\sigma_{\text{PMa}}$ | Max sma | Min sma<br>(au) | mass |
|----------------|---------------------|------|------|------|------|----------------|--------|-------------|-------------|-------------|-------------|-----------|-----------------------|---------|-----------------|------|
| LP 476-207     | 3291643148740384128 | SB2  | 29   | 256  | 0    | 31             | 1254.0 | 1           | 0           | 0           | 41.0        | NAV       | 1.8                   | 10.0    | 50              | S    |
| CD-561032      | 4776266794388393472 | SB1  | 38   | 333  | 0    | 31             | 1107.0 | 1           | 0           | 0           | 1.0         | NAV       | 1.5                   | 10.0    | 100             | P    |
| HD 41071       | 5570953464908732928 | ?    | 37   | 319  | 0    | 31             | 1012.0 | 1           | 0           | 0           | 0.0         | NAV       | 1.1                   | 10.0    | 100             | BD   |
| HD 984         | 2431157720981843200 | ?    | 27   | 231  | 0    | 31             | 976.0  | 1           | 0           | 0           | 0.0         | NAV       | 0.9                   | 10.0    | 80              | BD   |
| HD 217379A     | 2382705816958084224 | SB3  | 27   | 238  | 0    | 31             | 1.16   | 1           | 1           | 0           | 0.0         | NAV       | 1.7                   | 1.8     |                 |      |
| HD 164249      | 6702775135228913280 | ?    | 36   | 316  | 0    | 31             | 1093.0 | 1           | 0           | 0           | 0.0         | NAV       | 1.4                   | 1.7     |                 |      |
| HD 1466        | 4901229043960053248 | ?    | 45   | 396  | 0    | 31             | 994.0  | 1           | 0           | 0           | 0.0         | NAV       | 0.7                   | 1.6     |                 |      |
| HD 202917      | 6463782435948431616 | ?    | 44   | 382  | 0    | 31             | 0.9    | 1           | 0           | 0           | 0.0         | NAV       | 0.3                   | 1.3     |                 |      |
| HD 21997       | 508496331247848960  | ?    | 72   | 638  | 1    | 31             | 1079.0 | 1           | 0           | 0           | 0.0         | NAV       | 0.6                   | 1.2     |                 |      |
| HD 152555      | 4377537462448122112 | ?    | 47   | 411  | 0    | 31             | 878.0  | 1           | 0           | 0           | 0.0         | VAR       | 0.1                   | 1.2     |                 |      |
| V* DK Cet      | 5135093346121603712 | ?    | 39   | 340  | 0    | 31             | 967.0  | 1           | 0           | 0           | 0.0         | NAV       | 0.9                   | 1.1     |                 |      |
| V* UY Pic      | 4795598309045006208 | ?    | 42   | 371  | 0    | 31             | 956.0  | 1           | 0           | 0           | 0.0         | VAR       | 0.7                   | 1.1     |                 |      |
| HD 45270       | 5481848424118748672 | ?    | 24   | 211  | 0    | 31             | 0.87   | 1           | 0           | 0           | 0.0         | NAV       | 0.4                   | 1.1     |                 |      |
| HD 49855       | 5265670762922792960 | ?    | 31   | 267  | 0    | 31             | 1.02   | 1           | 0           | 0           | 0.0         | NAV       | 1.4                   | 1.0     | Limite 0        |      |
| HD 14082       | 107774202769886848  | ?    | 22   | 193  | 1    | 31             | 1008.0 | 1           | 0           | 0           | 0.0         | NAV       | 0.8                   | 1.0     |                 |      |
| HD 105         | 4995853014646189696 | ?    | 41   | 360  | 0    | 31             | 913.0  | 0           | 0           | 0           | 0.0         | NAV       | 0.3                   | 1.0     |                 |      |
| HD 207575      | 6408937971321777152 | ?    | 78   | 683  | 1    | 31             | 853.0  | 1           | 0           | 0           | 0.0         | NAV       | 0.0                   | 1.0     | 30              | BD   |
| HD 8558        | 4909846500703006976 | ?    | 49   | 428  | 0    | 31             | 1.07   | 1           | 0           | 0           | 0.0         | NAV       | 1.7                   | 0.9     |                 |      |
| BD-12 243      | 2470272812780609280 | ?    | 52   | 454  | 1    | 31             | 984.0  | 0           | 0           | 0           | 0.0         | VAR       | 1.1                   | 0.9     |                 |      |
| HD 30447       | 4881312593414911616 | ?    | 51   | 451  | 1    | 31             | 1043.0 | 1           | 0           | 0           | 0.0         | NAV       | 1.1                   | 0.9     |                 |      |
| V* EX Cet      | 2477815222028038272 | ?    | 39   | 340  | 0    | 31             | 968.0  | 1           | 0           | 0           | 0.0         | VAR       | 0.9                   | 0.9     |                 |      |
| HD 217343      | 2382711653818308224 | ?    | 31   | 275  | 0    | 31             | 935.0  | 1           | 0           | 0           | 0.0         | NAV       | 0.5                   | 0.9     |                 |      |
| HD 26980       | 4844618213903654784 | ?    | 53   | 458  | 0    | 31             | 948.0  | 0           | 0           | 0           | 0.0         | NAV       | 0.5                   | 0.9     |                 |      |
| RX J11597-7601 | 5224879500011370496 | ?    | 45   | 389  | 0    | 31             | 944.0  | 0           | 0           | 0           | 0.0         | VAR       | 0.5                   | 0.9     |                 |      |
| HD 181327      | 6643589352010758400 | ?    | 30   | 266  | 0    | 31             | 961.0  | 1           | 0           | 0           | 0.0         | NAV       | 0.5                   | 0.9     |                 |      |
| BD+01 2447     | 3855208897392952192 | ?    | 23   | 197  | 0    | 31             | 884.0  | 0           | 0           | 0           | 0.0         | NAV       | 0.4                   | 0.9     |                 |      |
| HD 191089      | 6847146784384459648 | SB1? | 32   | 275  | 0    | 31             | 878.0  | 1           | 0           | 0           | 0.0         | NAV       | 0.3                   | 0.9     |                 |      |
| HD 36329       | 4822948351549058304 | SB2  | 45   | 391  | 0    | 31             | 1.05   | 0           | 0           | 2           | 0.0         | VAR       | 1.3                   | 0.8     |                 |      |
| V* NY Aps      | 5792536565791371776 | ?    | 45   | 394  | 0    | 31             | 1008.0 | 0           | 0           | 0           | 1.0         | VAR       | 0.8                   | 0.8     |                 |      |
| V* CT Tuc      | 4902014095262270336 | ?    | 48   | 421  | 0    | 31             | 1.02   | 0           | 0           | 0           | 2.0         | NAV       | 0.7                   | 0.8     |                 |      |
| HD 24636       | 4629074455519836032 | ?    | 36   | 316  | 0    | 31             | 0.93   | 0           | 0           | 0           | 0.0         | NAV       | 0.6                   | 0.8     |                 |      |
| V* IS Eri      | 5166951386298774144 | ?    | 28   | 248  | 0    | 31             | 951.0  | 1           | 0           | 0           | 0.0         | NAV       | 0.6                   | 0.8     |                 |      |
| V* AO Men      | 5266270443442455040 | ?    | 27   | 238  | 0    | 31             | 843.0  | 0           | 0           | 0           | 0.0         | VAR       | 0.4                   | 0.8     |                 |      |
| HD 32372       | 4813691219557127808 | ?    | 40   | 355  | 0    | 31             | 877.0  | 0           | 0           | 0           | 0.0         | NAV       | 0.2                   | 0.8     |                 |      |
| HD 55279       | 5208216951043609216 | ?    | 33   | 293  | 0    | 31             | 1.12   | 0           | 0           | 0           | 0.0         | NAV       | 1.8                   | 0.7     | Lim. 0          |      |
| HD 38397       | 4808165830030420352 | ?    | 43   | 374  | 0    | 31             | 1062.0 | 0           | 0           | 0           | 0.0         | NAV       | 1.5                   | 0.7     | Lim. 0          |      |
| HD 25953       | 3258856089957102720 | ?    | 33   | 287  | 0    | 31             | 1017.0 | 1           | 0           | 0           | 0.0         | NAV       | 0.9                   | 0.7     |                 |      |
| HD 13246       | 4714764481913306496 | ?    | 40   | 351  | 0    | 31             | 996.0  | 1           | 0           | 0           | 0.0         | NAV       | 0.8                   | 0.7     |                 |      |
| HD 37551       | 4802947444765743104 | ?    | 41   | 364  | 0    | 31             | 975.0  | 1           | 0           | 0           | 0.0         | NAV       | 0.8                   | 0.7     |                 |      |
| V* V1358 Ori   | 3116883781327753216 | ?    | 33   | 290  | 1    | 31             | 0.93   | 0           | 0           | 0           | 0.0         | VAR       | 0.3                   | 0.7     |                 |      |
| * c Eri        | 3205095125321700480 | ?    | 49   | 423  | 0    | 31             | 1145.0 | 1           | 0           | 0           | 0.0         | NAV       | 1.0                   | 0.6     |                 |      |
| CD-57 1054     | 4764027962957023104 | ?    | 35   | 305  | 0    | 31             | 1005.0 | 0           | 0           | 0           | 0.0         | NAV       | 0.8                   | 0.6     |                 |      |

**Table C.1.** Binary status from GaiaPMEX. For a description on the columns, see text.

| Star name            | Gaia DR3 ID         | ZF21 | Nfov | Npts | Dup. | Par. solved | RUWE   | WDS flag | SB9 flag | NSS flag | FMP flag | Phot Var. | $\sigma_{\text{ruwe}}$ | $\sigma_{\text{PMa}}$ | Max sma | Min sma | mass |
|----------------------|---------------------|------|------|------|------|-------------|--------|----------|----------|----------|----------|-----------|------------------------|-----------------------|---------|---------|------|
|                      |                     |      |      |      |      |             |        |          |          |          |          |           |                        |                       |         | (au)    |      |
| HD 32195             | 4622453093418397952 | SB?  | 34   | 295  | 0    | 31          | 957.0  | 0        | 0        | 0        | 0.0      | NAV       | 0.7                    | 0.6                   |         |         |      |
| V* WW PsA            | 6603693881832177792 | ?    | 28   | 247  | 0    | 31          | 1139.0 | 1        | 0        | 0        | 0.0      | NAV       | 1.5                    | 0.5                   |         |         |      |
| V* V479 Car          | 5299141546145254528 | ?    | 38   | 331  | 0    | 31          | 976.0  | 1        | 0        | 0        | 0.0      | VAR       | 1.1                    | 0.5                   |         |         |      |
| HD 13183             | 4743944043046490240 | SB1  | 48   | 418  | 0    | 31          | 983.0  | 1        | 0        | 0        | 0.0      | NAV       | 0.9                    | 0.5                   |         |         |      |
| HD 17250             | 6478258087046528    | SB   | 24   | 211  | 0    | 31          | 965.0  | 1        | 0        | 0        | 0.0      | NAV       | 0.7                    | 0.5                   |         |         |      |
| LP 745-70            | 4338433743723131648 | ?    | 69   | 604  | 0    | 31          | 1.02   | 1        | 0        | 0        | 0.0      | VAR       | 0.3                    | 0.5                   |         |         |      |
| V* V1005 Ori         | 3231945508509506176 | SB   | 56   | 495  | 0    | 31          | 0.9    | 1        | 0        | 0        | 0.0      | NAV       | 0.1                    | 0.5                   |         |         |      |
| V* TW Hya            | 5401795662560500352 | ?    | 45   | 399  | 0    | 31          | 1175.0 | 0        | 0        | 0        | 0.0      | NAV       | 1.7                    | 0.4                   |         |         |      |
| HD 29615             | 4891725758804030208 | ?    | 63   | 554  | 0    | 31          | 1027.0 | 1        | 0        | 0        | 0.0      | NAV       | 0.9                    | 0.4                   |         |         |      |
| HD 6569              | 2371914419569515136 | ?    | 38   | 335  | 0    | 31          | 956.0  | 1        | 0        | 0        | 0.0      | NAV       | 0.8                    | 0.4                   |         |         |      |
| HD 218860            | 652796525898306304  | ?    | 84   | 732  | 1    | 31          | 1011.0 | 1        | 0        | 0        | 1.0      | VAR       | 0.7                    | 0.4                   |         |         |      |
| BD+22 4409           | 1797276382668029440 | ?    | 70   | 605  | 1    | 31          | 1039.0 | 1        | 0        | 0        | 1.0      | VAR       | 0.5                    | 0.4                   |         |         |      |
| * eta Tel            | 6643602576214115584 | ?    | 27   | 238  | 0    | 31          | 1013.0 | 1        | 0        | 0        | 0.0      | NAV       | 0.5                    | 0.4                   |         |         |      |
| HD 61005             | 5592237639209047424 | ?    | 54   | 471  | 0    | 31          | 0.94   | 1        | 0        | 0        | 1.0      | NAV       | 0.3                    | 0.4                   |         |         |      |
| V* CC Phe            | 4916062039935185792 | ?    | 51   | 445  | 0    | 31          | 873.0  | 1        | 0        | 0        | 0.0      | VAR       | 0.2                    | 0.4                   |         |         |      |
| HD 222575            | 2311789825227125632 | ?    | 27   | 234  | 0    | 31          | 1079.0 | 0        | 0        | 0        | 0.0      | VAR       | 1.4                    | 0.3                   |         |         |      |
| HD 35650             | 4819591920506512768 | ?    | 40   | 355  | 0    | 31          | 1081.0 | 0        | 0        | 0        | 0.0      | NAV       | 1.4                    | 0.3                   |         |         |      |
| CD-36 7429A          | 3463395523652894336 | ?    | 42   | 375  | 1    | 31          | 1043.0 | 1        | 0        | 0        | 0.0      | VAR       | 0.9                    | 0.3                   |         |         |      |
| CD-61 1439           | 5479782647926975360 | ?    | 27   | 236  | 0    | 31          | 961.0  | 0        | 0        | 0        | 1.0      | NAV       | 0.8                    | 0.3                   |         |         |      |
| HD 8813              | 4637584916037247488 | ?    | 43   | 380  | 1    | 31          | 957.0  | 0        | 0        | 0        | 1.0      | NAV       | 0.7                    | 0.3                   |         |         |      |
| BD+30 397            | 132362959259196032  | ?    | 23   | 200  | 0    | 31          | 892.0  | 1        | 0        | 0        | 0.0      | VAR       | 0.3                    | 0.3                   |         |         |      |
| HD 987               | 4688292536884945536 | ?    | 36   | 315  | 0    | 31          | 835.0  | 1        | 0        | 0        | 0.0      | NAV       | 0.2                    | 0.3                   |         |         |      |
| V* AU Mic            | 6794047652729201024 | ?    | 46   | 404  | 0    | 31          | 927.0  | 1        | 0        | 0        | 1.0      | NAV       | 0.2                    | 0.3                   |         |         |      |
| Smethells 86         | 6409848126430574592 | ?    | 65   | 561  | 0    | 31          | 1171.0 | 0        | 0        | 0        | 0.0      | NAV       | 1.6                    | 0.2                   |         |         |      |
| HD 224228            | 2307132568850133376 | ?    | 30   | 262  | 0    | 31          | 1.02   | 0        | 0        | 0        | 0.0      | NAV       | 1.1                    | 0.2                   |         |         |      |
| HD 37484             | 2907308172059100544 | ?    | 53   | 470  | 0    | 31          | 1032.0 | 0        | 0        | 0        | 1.0      | NAV       | 0.8                    | 0.2                   |         |         |      |
| HD 25457             | 3256786534197166208 | ?    | 21   | 182  | 0    | 31          | 989.0  | 0        | 0        | 0        | 0.0      | NAV       | 0.7                    | 0.1                   |         |         |      |
| 2M J12164593-7753333 | 5788664871812309376 | ?    | 37   | 319  | 0    | 31          | 1177.0 | 0        | 0        | 0        | 0.0      | NAV       | 1.9                    |                       |         |         |      |
| V* CE Ant            | 5444751795151480320 | ?    | 35   | 302  | 0    | 31          | 1187.0 | 1        | 0        | 0        | 1.0      | NAV       | 1.8                    |                       |         |         |      |
| HD 48370             | 3105749748629384576 | ?    | 25   | 222  | 0    | 31          | 1112.0 | 0        | 0        | 0        | 0.0      | NAV       | 1.7                    |                       |         |         |      |
| CD-47 1999           | 479546683045648768  | ?    | 38   | 328  | 0    | 31          | 1097.0 | 1        | 0        | 0        | 0.0      | NAV       | 1.7                    |                       |         |         |      |
| VXR PSPC 16a         | 5318546822567826944 | ?    | 36   | 322  | 0    | 31          | 1087.0 | 0        | 0        | 0        | 2.0      | VAR       | 1.7                    |                       |         |         |      |
| HD 73777             | 5321190155898133248 | ?    | 44   | 391  | 0    | 31          | 1105.0 | 0        | 0        | 0        | 0.0      | NAV       | 1.7                    |                       |         |         |      |
| BPS CS 22881-0003    | 6571446820698811904 | ?    | 54   | 468  | 0    | 31          | 1128.0 | 0        | 0        | 0        | 0.0      | NAV       | 1.7                    |                       |         |         |      |
| HD 17332B            | 84625630419434496   | ?    | 20   | 175  | 0    | 31          | 1095.0 | 1        | 0        | 0        | 0.0      | NAV       | 1.7                    |                       |         |         |      |
| BD-13 6424           | 2433191886212246784 | ?    | 23   | 202  | 0    | 31          | 1.13   | 0        | 0        | 0        | 0.0      | NAV       | 1.6                    |                       |         |         |      |
| CD-40 1701           | 4814134872498801408 | ?    | 48   | 422  | 0    | 31          | 1087.0 | 0        | 0        | 0        | 0.0      | VAR       | 1.5                    |                       |         |         |      |
| V* TX PsA            | 6603693808817829760 | ?    | 29   | 249  | 0    | 31          | 1.17   | 1        | 0        | 0        | 0.0      | NAV       | 1.5                    |                       |         |         |      |
| HD 223340            | 232825033463289856  | ?    | 24   | 212  | 0    | 31          | 1085.0 | 1        | 0        | 0        | 0.0      | VAR       | 1.4                    |                       |         |         |      |
| HD 24681             | 3256189465023650048 | ?    | 29   | 252  | 0    | 31          | 1102.0 | 0        | 0        | 0        | 0.0      | VAR       | 1.4                    |                       |         |         |      |
| HD 272836            | 4786264859778429824 | ?    | 40   | 352  | 0    | 31          | 1019.0 | 1        | 0        | 0        | 0.0      | NAV       | 1.3                    |                       |         |         |      |
| CI* IC 2391 PMM 756  | 5317884439832479872 | ?    | 36   | 317  | 0    | 31          | 1048.0 | 0        | 0        | 0        | 49.0     | NAV       | 1.3                    |                       |         |         |      |

Limit 0

**Table C.1.** Binary status from GaiaPMEX. For a description on the columns, see text.

| Star name            | Gaia DR3 ID         | ZF21 | Nfov | Npts | Dup. | Par.<br>solved | RUWE   | WDS<br>flag | SB9<br>flag | NSS<br>flag | FMP<br>flag | Phot Var. | $\sigma_{PMa}$ | Max sma<br>(au) | Min sma<br>(au) | mass |
|----------------------|---------------------|------|------|------|------|----------------|--------|-------------|-------------|-------------|-------------|-----------|----------------|-----------------|-----------------|------|
| GSC 08894-00426      | 5481843025342799104 | ?    | 39   | 344  | 0    | 31             | 1101.0 | 1           | 0           | 0           | 2.0         | NAV       | 1.3            |                 |                 |      |
| TYC 7066-1037-1      | 2889149393928673664 | ?    | 44   | 386  | 0    | 31             | 1026.0 | 0           | 0           | 0           | 0.0         | NAV       | 1.2            |                 |                 |      |
| CD-27 2520           | 2904801835303287808 | ?    | 54   | 468  | 0    | 31             | 1084.0 | 0           | 0           | 0           | 1.0         | VAR       | 1.2            |                 |                 |      |
| TYC 486-4943-1       | 4289366113217575424 | ?    | 54   | 471  | 0    | 31             | 1001.0 | 1           | 0           | 0           | 0.0         | NAV       | 1.2            |                 |                 |      |
| V* V1217 Cen         | 5396105586807802880 | ?    | 44   | 381  | 0    | 31             | 1104.0 | 1           | 0           | 0           | 1.0         | NAV       | 1.2            |                 |                 |      |
| CD-48 3199           | 5518068330006200192 | ?    | 40   | 349  | 0    | 31             | 1045.0 | 0           | 0           | 0           | 0.0         | NAV       | 1.2            |                 |                 |      |
| 2M J20013718-3313139 | 6747106443324127488 | ?    | 34   | 297  | 0    | 31             | 1091.0 | 0           | 0           | 0           | 0.0         | NAV       | 1.2            |                 |                 |      |
| BD-09 1108           | 3014411427921646080 | ?    | 69   | 601  | 1    | 31             | 1077.0 | 1           | 0           | 0           | 1.0         | NAV       | 1.1            |                 |                 |      |
| CD-26 8623           | 3485098646237003392 | ?    | 47   | 407  | 0    | 31             | 1071.0 | 1           | 0           | 0           | 2.0         | NAV       | 1.1            |                 |                 |      |
| TYC 7443-1102-1      | 6747467224874108288 | ?    | 34   | 293  | 0    | 31             | 1074.0 | 1           | 0           | 0           | 0.0         | NAV       | 1.1            |                 |                 |      |
| HD 31652             | 3183414542727824896 | ?    | 50   | 435  | 0    | 31             | 1052.0 | 0           | 0           | 0           | 0.0         | NAV       | 1.0            |                 |                 |      |
| TYC 8862-19-1        | 4721546166554166528 | ?    | 38   | 322  | 0    | 31             | 1031.0 | 1           | 0           | 0           | 0.0         | VAR       | 1.0            |                 |                 |      |
| TYC 9217-641-1       | 5218300499165464320 | ?    | 42   | 364  | 0    | 31             | 1009.0 | 0           | 0           | 0           | 0.0         | NAV       | 1.0            |                 |                 |      |
| CD-31 16041          | 6736232346363422336 | ?    | 27   | 238  | 0    | 31             | 961.0  | 1           | 0           | 0           | 0.0         | NAV       | 1.0            |                 |                 |      |
| CD-35 2722           | 2885863400349980288 | ?    | 42   | 365  | 0    | 31             | 1023.0 | 1           | 0           | 0           | 2.0         | NAV       | 0.9            |                 |                 |      |
| BD-08 1195           | 3015216991987620096 | ?    | 46   | 394  | 0    | 31             | 1046.0 | 1           | 0           | 0           | 2.0         | NAV       | 0.9            |                 |                 |      |
| CD-58 553            | 4726518501732727936 | ?    | 41   | 355  | 0    | 31             | 1001.0 | 1           | 0           | 0           | 0.0         | NAV       | 0.9            |                 |                 |      |
| HD 31242             | 4786900244356750976 | ?    | 36   | 309  | 0    | 31             | 976.0  | 1           | 0           | 0           | 0.0         | NAV       | 0.9            |                 |                 |      |
| HD 37551B            | 4802947444765742848 | ?    | 42   | 373  | 0    | 31             | 963.0  | 1           | 0           | 0           | 2.0         | VAR       | 0.9            |                 |                 |      |
| BD-15 705            | 5109911781067864064 | ?    | 46   | 397  | 0    | 31             | 1041.0 | 0           | 0           | 0           | 0.0         | VAR       | 0.9            |                 |                 |      |
| BD-11 648            | 5163141131831884544 | ?    | 24   | 202  | 0    | 31             | 0.97   | 0           | 0           | 2           | 0.0         | VAR       | 0.9            |                 |                 |      |
| BD-20 2977           | 5664853853864480768 | ?    | 25   | 220  | 0    | 31             | 985.0  | 0           | 0           | 0           | 0.0         | NAV       | 0.9            |                 |                 |      |
| CD-69 1055           | 5844573358774024320 | ?    | 43   | 373  | 0    | 31             | 981.0  | 1           | 0           | 0           | 0.0         | VAR       | 0.9            |                 |                 |      |
| IRXS J2054280+090615 | 1750318749306157824 | ?    | 34   | 295  | 0    | 31             | 1006.0 | 0           | 0           | 0           | 0.0         | NAV       | 0.8            |                 |                 |      |
| V* AH Lep            | 2972231722338351360 | ?    | 59   | 514  | 1    | 31             | 1013.0 | 1           | 0           | 0           | 0.0         | NAV       | 0.8            |                 |                 |      |
| HD 42270             | 4621305817457618176 | ?    | 32   | 278  | 0    | 31             | 939.0  | 1           | 0           | 0           | 0.0         | VAR       | 0.8            |                 |                 |      |
| CD-36 1785           | 4867591989673394944 | ?    | 47   | 418  | 0    | 31             | 976.0  | 0           | 0           | 0           | 0.0         | VAR       | 0.8            |                 |                 |      |
| HD 22213             | 5115334331896590208 | SB1  | 34   | 298  | 0    | 31             | 984.0  | 1           | 0           | 0           | 1.0         | NAV       | 0.8            |                 |                 |      |
| V* EO Cha            | 5209135352491538432 | ?    | 36   | 320  | 0    | 31             | 1027.0 | 1           | 0           | 0           | 1.0         | NAV       | 0.8            |                 |                 |      |
| CD-65817             | 5249086141843932544 | ?    | 39   | 343  | 0    | 31             | 921.0  | 1           | 0           | 0           | 2.0         | NAV       | 0.8            |                 |                 |      |
| HD 47875             | 5278895306528592000 | ?    | 36   | 315  | 0    | 31             | 947.0  | 1           | 0           | 0           | 0.0         | NAV       | 0.8            |                 |                 |      |
| HD 51797             | 5557658685702796544 | ?    | 38   | 328  | 0    | 31             | 972.0  | 0           | 0           | 0           | 0.0         | VAR       | 0.8            |                 |                 |      |
| CPD-68 1894          | 5844296281847839232 | SB?  | 46   | 399  | 1    | 31             | 963.0  | 0           | 0           | 0           | 0.0         | VAR       | 0.8            |                 |                 |      |
| BD+20 1790           | 3363049071685181056 | ?    | 21   | 182  | 0    | 31             | 931.0  | 1           | 0           | 0           | 0.0         | VAR       | 0.7            |                 |                 |      |
| GSC 07396-00759      | 4045698732855626624 | ?    | 23   | 200  | 0    | 31             | 0.7    | 0           | 0           | 0           | 0.0         | NAV       | 0.7            |                 |                 |      |
| CD-78 24             | 4635593356881798912 | ?    | 45   | 384  | 0    | 31             | 976.0  | 0           | 0           | 0           | 0.0         | NAV       | 0.7            |                 |                 |      |
| HD 269620            | 4658442922197295232 | ?    | 28   | 249  | 0    | 31             | 795.0  | 0           | 0           | 0           | 0.0         | NAV       | 0.7            |                 |                 |      |
| CD-52 1363           | 4792175838585883904 | ?    | 41   | 353  | 0    | 31             | 932.0  | 0           | 0           | 0           | 0.0         | VAR       | 0.7            |                 |                 |      |
| CD-621197            | 6630890508110702208 | ?    | 55   | 476  | 0    | 31             | 1.03   | 0           | 0           | 0           | 20.0        | NAV       | 0.7            |                 |                 |      |
| CD-52 9381           | 6666178680963755008 | ?    | 41   | 350  | 0    | 31             | 1039.0 | 0           | 0           | 0           | 0.0         | VAR       | 0.7            |                 |                 |      |
| BD-03 4778           | 4222102218052861440 | ?    | 41   | 353  | 0    | 31             | 928.0  | 1           | 0           | 0           | 0.0         | VAR       | 0.6            |                 |                 |      |
| TYC 8098-414-1       | 4793327233418050176 | ?    | 36   | 313  | 0    | 31             | 967.0  | 0           | 0           | 0           | 0.0         | NAV       | 0.6            |                 |                 |      |

**Table C.1.** Binary status from GaiaPMEX. For a description on the columns, see text.

| Star name            | Gaia DR3 ID         | ZF21 | Nfov | Npts | Dup. | Par. solved | RUWE   | WDS flag | SB9 flag | NSS flag | FMP flag | Phot Var. | $\sigma_{\text{PMa}}$ | Max sma | Min sma | mass |
|----------------------|---------------------|------|------|------|------|-------------|--------|----------|----------|----------|----------|-----------|-----------------------|---------|---------|------|
|                      |                     |      |      |      |      |             |        |          |          |          |          |           |                       |         | (au)    |      |
| HD 27679             | 4896343707641120384 | ?    | 89   | 783  | 0    | 31          | 1017.0 | 0        | 0        | 0        | 0.0      | VAR       | 0.6                   |         |         | 0.6  |
| V* V379 Vel          | 5318328676892604800 | SB?  | 42   | 355  | 0    | 31          | 949.0  | 0        | 0        | 0        | 0.0      | VAR       | 0.6                   |         |         | 0.6  |
| 2M J13491293-7549475 | 5789867600093615360 | ?    | 39   | 341  | 0    | 31          | 939.0  | 0        | 0        | 0        | 0.0      | NAV       | 0.6                   |         |         | 0.6  |
| Smethells 20         | 6631685008336771072 | ?    | 34   | 291  | 0    | 31          | 1029.0 | 0        | 0        | 0        | 2.0      | NAV       | 0.6                   |         |         | 0.6  |
| HD 32981             | 2986060653741078784 | ?    | 58   | 509  | 0    | 31          | 993.0  | 0        | 0        | 0        | 0.0      | NAV       | 0.5                   |         |         | 0.5  |
| BD-08 995            | 3183457561120188672 | ?    | 44   | 383  | 0    | 31          | 972.0  | 0        | 0        | 0        | 0.0      | VAR       | 0.5                   |         |         | 0.5  |
| CD-60 416            | 4714764447553568640 | ?    | 35   | 303  | 0    | 31          | 921.0  | 1        | 0        | 0        | 0.0      | VAR       | 0.5                   |         |         | 0.5  |
| CD-69 783            | 5232233789697993728 | ?    | 40   | 350  | 0    | 31          | 893.0  | 0        | 0        | 0        | 0.0      | NAV       | 0.5                   |         |         | 0.5  |
| CD-40 2458           | 5570338906629079936 | ?    | 45   | 394  | 0    | 31          | 942.0  | 1        | 0        | 0        | 0.0      | VAR       | 0.5                   |         |         | 0.5  |
| V* V1249 Cen         | 6150861598484393856 | ?    | 64   | 558  | 1    | 95          | 1007.0 | 1        | 0        | 0        | 0.0      | NAV       | 0.5                   |         |         | 0.5  |
| TYC 9344-293-1       | 6380514358792367232 | ?    | 38   | 332  | 0    | 31          | 965.0  | 0        | 0        | 0        | 0.0      | NAV       | 0.5                   |         |         | 0.5  |
| HD 222259B           | 6387058411482257280 | ?    | 41   | 354  | 0    | 31          | 954.0  | 1        | 0        | 0        | 0.0      | VAR       | 0.5                   |         |         | 0.5  |
| CD-34 2331           | 2900656848263249920 | ?    | 44   | 378  | 0    | 31          | 952.0  | 0        | 0        | 0        | 0.0      | VAR       | 0.4                   |         |         | 0.4  |
| TYC 119-497-1        | 3224017823514705920 | ?    | 44   | 388  | 0    | 31          | 994.0  | 1        | 0        | 0        | 0.0      | VAR       | 0.4                   |         |         | 0.4  |
| HD 86356             | 5202135964549093248 | SB2  | 38   | 321  | 0    | 95          | 998.0  | 0        | 0        | 0        | 0.0      | VAR       | 0.4                   |         |         | 0.4  |
| TYC 8162-1020-1      | 5321517672922567040 | ?    | 43   | 368  | 0    | 31          | 883.0  | 0        | 0        | 0        | 0.0      | NAV       | 0.4                   |         |         | 0.4  |
| HD 35841             | 2958833623399371392 | ?    | 83   | 718  | 0    | 31          | 984.0  | 0        | 0        | 0        | 0.0      | NAV       | 0.3                   |         |         | 0.3  |
| BD-12 943            | 3178069026432500992 | ?    | 71   | 616  | 0    | 31          | 957.0  | 0        | 0        | 0        | 0.0      | VAR       | 0.3                   |         |         | 0.3  |
| CD-46 1064           | 4846466733467661184 | ?    | 44   | 381  | 0    | 31          | 921.0  | 0        | 0        | 0        | 0.0      | VAR       | 0.3                   |         |         | 0.3  |
| CD-35 1167           | 5047124994197379456 | ?    | 53   | 462  | 0    | 95          | 1037.0 | 0        | 0        | 0        | 0.0      | NAV       | 0.3                   |         |         | 0.3  |
| 2M J11401658-8321003 | 5197213279191665920 | ?    | 45   | 386  | 0    | 31          | 926.0  | 0        | 0        | 0        | 0.0      | VAR       | 0.3                   |         |         | 0.3  |
| TYC 9178-284-1       | 5280793308412118656 | ?    | 35   | 306  | 0    | 31          | 882.0  | 0        | 0        | 0        | 0.0      | VAR       | 0.3                   |         |         | 0.3  |
| CPD-54 1712          | 5317655157295238656 | ?    | 42   | 371  | 0    | 31          | 0.88   | 1        | 0        | 0        | 1.0      | NAV       | 0.3                   |         |         | 0.3  |
| CI* IC 2391 PMM 3359 | 5318176875565072768 | ?    | 40   | 350  | 0    | 31          | 841.0  | 0        | 0        | 0        | 0.0      | VAR       | 0.3                   |         |         | 0.3  |
| GSC08162-01222       | 5321275295028390912 | ?    | 40   | 345  | 0    | 31          | 0.89   | 0        | 0        | 0        | 1.0      | VAR       | 0.3                   |         |         | 0.3  |
| UCAC4 189-019053     | 5321280728169745536 | ?    | 45   | 389  | 0    | 31          | 0.88   | 0        | 0        | 0        | 2.0      | VAR       | 0.3                   |         |         | 0.3  |
| HD 298936            | 5356713413789909632 | ?    | 42   | 365  | 0    | 31          | 903.0  | 1        | 0        | 0        | 0.0      | VAR       | 0.3                   |         |         | 0.3  |
| CD-39 5833           | 5431592977432228992 | ?    | 59   | 514  | 1    | 31          | 955.0  | 0        | 0        | 0        | 0.0      | NAV       | 0.3                   |         |         | 0.3  |
| CD-48 2324           | 5552120961029170944 | ?    | 45   | 397  | 0    | 31          | 885.0  | 0        | 0        | 0        | 0.0      | VAR       | 0.3                   |         |         | 0.3  |
| CD-36 3202           | 5578127400323942016 | ?    | 45   | 396  | 0    | 31          | 922.0  | 0        | 0        | 0        | 0.0      | VAR       | 0.3                   |         |         | 0.3  |
| CD-74 712            | 5838361599097855104 | ?    | 43   | 377  | 0    | 31          | 0.9    | 0        | 0        | 0        | 0.0      | VAR       | 0.3                   |         |         | 0.3  |
| 2MJ12194369-7403572  | 5841382846589454080 | ?    | 42   | 365  | 0    | 31          | 914.0  | 0        | 0        | 0        | 1.0      | NAV       | 0.3                   |         |         | 0.3  |
| HD 129496            | 5848129213744138880 | ?    | 58   | 507  | 0    | 31          | 942.0  | 0        | 0        | 0        | 0.0      | NAV       | 0.3                   |         |         | 0.3  |
| CD-54 7336           | 5924485966955008896 | ?    | 46   | 406  | 0    | 31          | 897.0  | 1        | 0        | 0        | 0.0      | VAR       | 0.3                   |         |         | 0.3  |
| CPD-72 2713          | 6382640367603744128 | ?    | 46   | 398  | 0    | 31          | 925.0  | 0        | 0        | 0        | 0.0      | NAV       | 0.3                   |         |         | 0.3  |
| UCAC2 1331888        | 6418631162754209920 | ?    | 57   | 491  | 0    | 31          | 908.0  | 1        | 0        | 0        | 0.0      | VAR       | 0.3                   |         |         | 0.3  |
| HD 201919            | 6834123756346400768 | ?    | 43   | 376  | 0    | 31          | 892.0  | 0        | 0        | 0        | 0.0      | VAR       | 0.3                   |         |         | 0.3  |
| BD-03 5579           | 2638216857371313664 | ?    | 25   | 216  | 0    | 95          | 1.08   | 0        | 0        | 0        | 0.0      | VAR       | 0.2                   |         |         | 0.2  |
| TYC 119-1242-1       | 3224016964521247616 | ?    | 43   | 376  | 0    | 31          | 918.0  | 1        | 0        | 0        | 0.0      | VAR       | 0.2                   |         |         | 0.2  |
| CD-58 860            | 4682151077248467456 | ?    | 36   | 314  | 0    | 31          | 833.0  | 0        | 0        | 0        | 1.0      | NAV       | 0.2                   |         |         | 0.2  |
| HD 274561            | 4799433474323211776 | ?    | 46   | 393  | 0    | 31          | 0.84   | 0        | 0        | 0        | 1.0      | VAR       | 0.2                   |         |         | 0.2  |
| CPD-52 2481          | 5312245422658960768 | ?    | 41   | 355  | 1    | 31          | 852.0  | 0        | 0        | 0        | 0.0      | VAR       | 0.2                   |         |         | 0.2  |

**Table C.1.** Binary status from GaiaPMEX. For a description on the columns, see text.

| Star name          | Gaia DR3 ID         | ZF21 | Nfov | Npts | Dup. | Par.<br>solved | RUWE   | WDS<br>flag | SB9<br>flag | NSS<br>flag | FMP<br>flag | Phot Var. | $\sigma_{\text{ruwe}}$ | $\sigma_{\text{PMa}}$ | Max sma | Min sma<br>(au) | mass |
|--------------------|---------------------|------|------|------|------|----------------|--------|-------------|-------------|-------------|-------------|-----------|------------------------|-----------------------|---------|-----------------|------|
| TYC 8582-3040-1    | 5317269950278675072 | ?    | 43   | 373  | 0    | 31             | 0.81   | 0           | 0           | 0           | 0.0         | VAR       | 0.2                    |                       |         |                 |      |
| CI* IC 2391 D 41   | 5318077507199948672 | ?    | 40   | 344  | 0    | 31             | 0.82   | 0           | 0           | 0           | 0.0         | NAV       | 0.2                    |                       |         |                 |      |
| CD-52 2467         | 5318186221414047104 | ?    | 44   | 384  | 0    | 31             | 0.84   | 0           | 0           | 0           | 0.0         | NAV       | 0.2                    |                       |         |                 |      |
| V* V364 Vel        | 5318545521198976000 | ?    | 39   | 344  | 0    | 31             | 795.0  | 0           | 0           | 0           | 0.0         | VAR       | 0.2                    |                       |         |                 |      |
| TYC 8570-1980-1    | 5319076203049591808 | ?    | 36   | 317  | 0    | 31             | 0.82   | 0           | 0           | 0           | 0.0         | VAR       | 0.2                    |                       |         |                 |      |
| TYC 8174-1586-1    | 5325609711604226048 | ?    | 40   | 351  | 0    | 31             | 0.87   | 0           | 0           | 0           | 0.0         | VAR       | 0.2                    |                       |         |                 |      |
| HD 85151A          | 5412014832876362624 | ?    | 53   | 463  | 0    | 95             | 963.0  | 1           | 0           | 0           | 2.0         | NAV       | 0.2                    |                       |         |                 |      |
| TYC 8557-1251-1    | 5488367737800067072 | ?    | 37   | 320  | 0    | 31             | 0.81   | 0           | 0           | 0           | 0.0         | VAR       | 0.2                    |                       |         |                 |      |
| CD-42 2906         | 5562571883473697152 | ?    | 38   | 326  | 0    | 31             | 833.0  | 0           | 0           | 0           | 0.0         | NAV       | 0.2                    |                       |         |                 |      |
| HD 105923          | 5854812388999707008 | ?    | 36   | 315  | 0    | 31             | 0.82   | 1           | 0           | 0           | 0.0         | NAV       | 0.2                    |                       |         |                 |      |
| CPD-79 1037        | 6362543597150911616 | ?    | 45   | 392  | 0    | 31             | 0.84   | 0           | 0           | 0           | 0.0         | VAR       | 0.2                    |                       |         |                 |      |
| HD 38207           | 2966779995793890560 | ?    | 54   | 474  | 0    | 31             | 905.0  | 0           | 0           | 0           | 0.0         | NAV       | 0.1                    |                       |         |                 |      |
| BD-19 1062         | 2975997549665260416 | ?    | 64   | 558  | 0    | 95             | 1102.0 | 0           | 0           | 0           | 1.0         | VAR       | 0.1                    |                       |         |                 |      |
| HD 274576          | 4799008375640297344 | ?    | 39   | 342  | 0    | 95             | 985.0  | 1           | 0           | 0           | 2.0         | NAV       | 0.1                    |                       |         |                 |      |
| TYC 8561-970-1     | 5295688117557736448 | ?    | 33   | 280  | 0    | 31             | 758.0  | 0           | 0           | 0           | 0.0         | VAR       | 0.1                    |                       |         |                 |      |
| TYC 8927-2035-1    | 5301732820175622912 | ?    | 38   | 320  | 0    | 31             | 785.0  | 1           | 0           | 0           | 0.0         | VAR       | 0.1                    |                       |         |                 |      |
| TYC 8594-58-1      | 5303472350654243712 | ?    | 37   | 321  | 0    | 31             | 753.0  | 0           | 0           | 0           | 0.0         | VAR       | 0.1                    |                       |         |                 |      |
| CI* IC 2391 SMY 23 | 5318093243960659456 | ?    | 44   | 388  | 1    | 31             | 816.0  | 0           | 0           | 0           | 0.0         | NAV       | 0.1                    |                       |         |                 |      |
| CD-49 4008         | 5325281335588219008 | ?    | 44   | 380  | 0    | 31             | 768.0  | 0           | 0           | 0           | 0.0         | VAR       | 0.1                    |                       |         |                 |      |
| CD-48 2972         | 5506101790904438656 | ?    | 44   | 377  | 0    | 31             | 0.82   | 1           | 0           | 0           | 0.0         | VAR       | 0.1                    |                       |         |                 |      |
| CD-42 3328         | 5536071767758647808 | SB2  | 45   | 392  | 0    | 31             | 799.0  | 0           | 0           | 0           | 0.0         | VAR       | 0.1                    |                       |         |                 |      |
| Paranago 2752      | 3016917008762062336 | ?    | 47   | 415  | 0    | 31             | 0.84   | 0           | 0           | 0           | 0.0         | VAR       | 0.0                    |                       |         |                 |      |
| CD-52 381          | 4913138232358905216 | ?    | 42   | 361  | 0    | 95             | 0.87   | 1           | 0           | 0           | 0.0         | VAR       | 0.0                    |                       |         |                 |      |
| TYC 9217-417-1     | 5242190004920798592 | ?    | 47   | 412  | 0    | 31             | 804.0  | 1           | 0           | 0           | 0.0         | VAR       | 0.0                    |                       |         |                 |      |
| CD-66 395          | 5283645647739198464 | ?    | 31   | 273  | 0    | 95             | 828.0  | 0           | 0           | 0           | 0.0         | VAR       | 0.0                    |                       |         |                 |      |
| CD-61 2010         | 5300857711997333120 | ?    | 35   | 304  | 0    | 95             | 0.89   | 0           | 0           | 0           | 0.0         | VAR       | 0.0                    |                       |         |                 |      |
| TYC 8590-1193-1    | 5304374843544543104 | ?    | 39   | 342  | 0    | 31             | 721.0  | 0           | 0           | 0           | 0.0         | VAR       | 0.0                    |                       |         |                 |      |
| CD-57 1709         | 5486699125824396928 | ?    | 35   | 305  | 0    | 95             | 911.0  | 1           | 0           | 0           | 0.0         | NAV       | 0.0                    |                       |         |                 |      |
| HD 358623          | 6882838031333427456 | ?    | 57   | 498  | 0    | 95             | 973.0  | 1           | 0           | 0           | 0.0         | NAV       | 0.0                    |                       |         |                 |      |
| V* PX Vir          | 3677911582262521728 | SB1  | 31   | 270  | 0    | 3              |        | 1           | 1           | 0           | 3.0         | NAV       |                        |                       |         |                 |      |
| CD-2711535         | 4107812485571331328 | SB1  | 47   | 402  | 0    | 3              |        | 1           | 0           | 0           | 19.0        | NAV       |                        |                       |         |                 |      |
| CD-43 1395         | 4839354748662015488 | ?    | 38   | 334  | 0    | 3              |        | 1           | 0           | 0           | 61.0        | NAV       |                        |                       |         |                 |      |
| HD 20121A          | 4850405974392619648 | ?    | 37   | 323  | 0    | 3              |        | 1           | 0           | 0           | 99.0        | NAV       |                        |                       |         |                 |      |
| [K2001c] 17        | 5203033750152434176 | ?    | 35   | 284  | 0    | 3              |        | 1           | 0           | 0           | 81.0        | NAV       |                        |                       |         |                 |      |
| HD 161460          | 5945104490030338432 | SB2  | 42   | 364  | 0    | 3              |        | 1           | 0           | 0           | 35.0        | NAV       |                        |                       |         |                 |      |

**Table D.1.** RV (relative to the median RV) and BVS and associated uncertainties (epsRV, epsBVS) for G80-21.

| JDB-2400000  | RV<br>km/s | epsRV<br>km/s | BVS<br>km/s | epsBVS<br>km/s |
|--------------|------------|---------------|-------------|----------------|
| 57666.692176 | 0.0269     | 0.0072        | 0.0035      | 0.0181         |
| 57666.705881 | 0.0353     | 0.0069        | 0.0346      | 0.0172         |
| 57667.695570 | -0.1006    | 0.0072        | 0.0301      | 0.0180         |
| 57667.706242 | -0.1161    | 0.0075        | 0.0344      | 0.0188         |
| 57668.680072 | 0.0136     | 0.0059        | -0.0311     | 0.0149         |
| 57668.693221 | 0.0219     | 0.0063        | -0.0547     | 0.0158         |
| 57669.745330 | 0.0644     | 0.0053        | -0.0035     | 0.0134         |
| 57669.759729 | 0.0587     | 0.0054        | -0.0477     | 0.0136         |
| 57670.682837 | 0.0216     | 0.0058        | 0.0153      | 0.0147         |
| 57670.696391 | 0.0321     | 0.0060        | -0.0073     | 0.0151         |
| 57671.687117 | -0.0664    | 0.0056        | 0.0223      | 0.0142         |
| 57671.701643 | -0.0762    | 0.0057        | 0.0380      | 0.0143         |
| 57771.563217 | 0.0283     | 0.0074        | -0.0136     | 0.0186         |
| 57771.574096 | 0.0122     | 0.0070        | -0.0563     | 0.0177         |

## Appendix D: Log of observations

### D.1. G80-21

The HARPS data were standard Echelle observations taken as part of program 097.C-0864 B (PI: Lannier). The RV and Bisector velocity spans (BVS) were computed using our SAFIR software (Galland et al. 2005). They are given in Table D.1. Note that the RV are compatible with those found by Trifonov et al. (2020).

### D.2. AB Pic

The coronagraphic SPHERE and GPI data used are described in Table D.2. Additional PSF were recorded prior to and after the coronagraphic observations in the case of SPHERE data. The 2015 AB Pic data were obtained as part of the SPHERE SHINE survey in H2H3 mode. The Oct 2023 data were part of a GO Program (112.25.001, P.I. Alice Zurlo), and were obtained in star-hopping mode.

The RV data of AB Pic were obtained with HARPS as part of a long-term search for RV exoplanets. They are presented in (Grandjean et al. 2020).

### D.3. HD 14082 B

The data were taken as part of the SHARDS survey to search for disks around IR excess stars members of Sco Cen associations (P.I. J. Milli; 096.C-0388(A)). The observing set up and conditions are described in Table D.2. No RV data are available for HD 14082B.

## Appendix E: Data processing and analysis

### E.1. Data processing

The reduction and analysis of SPHERE data are presented in (Chomez et al. 2023). They made use of the PACO algorithm, described in Flasseur et al. (2020a,b) and in (Chomez et al. 2023).

For the GPI data, every raw frame of the archival sequence was dark subtracted, flat-fielded, cleaned of correlated detector noise, and corrected for bad pixel and flexure effects by means of the standard GPI Data Reduction Pipeline (DRP v1.6; Perrin

et al. 2014, 2016). Individual frames were therefore re-centered and combined into a spectral datacube using Pyklip (Wang et al. 2015), which also allowed for a more accurate wavelength and PSF re-calibration. As for SPHERE, post-processing was performed using PACO ASDI (Flasseur et al. 2020b).

### E.2. Detection maps from direct imaging

The  $5\sigma$  detection maps from the DI images expressed in terms of contrast are finally converted in units of Jupiter masses using a suitable routine of the MADYS tool (Squicciarini & Bonavita 2022): the conversion assumes the age of the system and is mediated by the AMES-Cond isochrones.

### E.3. Detection limits from combined data

Finally, (sma, mass) detection limits are derived using the direct imaging detection maps, together with the RV data once corrected from stellar activity to estimate the probability of the presence of other planets in the system. We generate (Monte Carlo approach) planets with various orbital properties and masses and test whether these simulated planets are detected at least for one epoch in direct imaging or are detected in RV (see details in Lannier et al. 2017).

### E.4. MCMC characterization of G80-21

The MCMC tool is based on the emcee 3.0 library (Foreman-Mackey et al. 2013). It uses a mix of custom move functions to alleviate potential multi-modality problems and the cyclicity of angular variables. We consider the RV, ruwe and PMa data. For Gaia data, the logic implemented in the aforementioned GaiaP-MEX tool has been used to compute Gaia-related likelihoods.

The free parameters considered are the orbital parameters (semi-major axis, eccentricity, argument of periastron and phase), the minimum mass(es) of the planet(s), and the RV (global offset due to the star systemic velocity), and a stellar jitter. A value of 200 m/s was adopted for the jitter to account for the observed short term variability. Uniform priors were considered for all parameters. The star RV was between 18 and 18.5 km/s, the range of sma was between 0.001 and 5 au, given the detection limits provided by high contrast imaging (see Section 6.1.2), the mass between 0.1 and 20  $M_{\text{Jup}}$ , and the eccentricity arbitrarily taken 0 and 0.2. The resulting corner plot is given in Figure E.1 (see discussion in Section 6.1).

| Star                       | AB Pic        |                           |              | HD 14082 B    |               |
|----------------------------|---------------|---------------------------|--------------|---------------|---------------|
| instrument                 | SPHERE        | GPI                       | SPHERE       | SPHERE        | SPHERE        |
| OBS night                  | 2015-02-05    | 2018-02-05                | 2023-10-25   | 2015-12-23    | 2016-09-18    |
| DIT(s)×Nframe              | 64×64         | 60×68                     | 64×24        | 16×144        | 16×288        |
| $\Delta$ PA (deg)          | 28.28         | 23.60                     | 22.23        | 11.15         | 22.74         |
| seeing (") <sup>a</sup>    | 1.08          | 0.99                      | 0.49         | 0.84          | 0.67          |
| airmass <sup>a</sup>       | 1.20          | 1.24                      | 1.21         | 1.72          | 1.70          |
| IRDIS filter               | DH_H23        | –                         | DH_H23       | BB_H          | BB_H          |
| $\tau_0$ (ms) <sup>a</sup> | 5.3           | unknown                   | 4.9          | 2.6           | 5.7           |
| coronagraph                | N_ALC_YJH_S   | APO+FPM_H_G6225+080m12_04 | N_ALC_YJH_S  | N_ALC_YJH_S   | N_ALC_YJH_S   |
| program ID                 | 095.C-0298(H) | GS-2017B-Q-500            | 112.25QU.001 | 096.C-0388(A) | 096.C-0388(A) |

**Table D.2.** Observation logs for the SPHERE and GPI observations considered in this work.

**Notes.** DIT = detector integration time per frame,  $\Delta$ PA = amplitude of the parallactic rotation,  $\tau_0$  = coherence time. <sup>a</sup>: for SPHERE, values extracted from the updated DIMM information and averaged over the sequence.

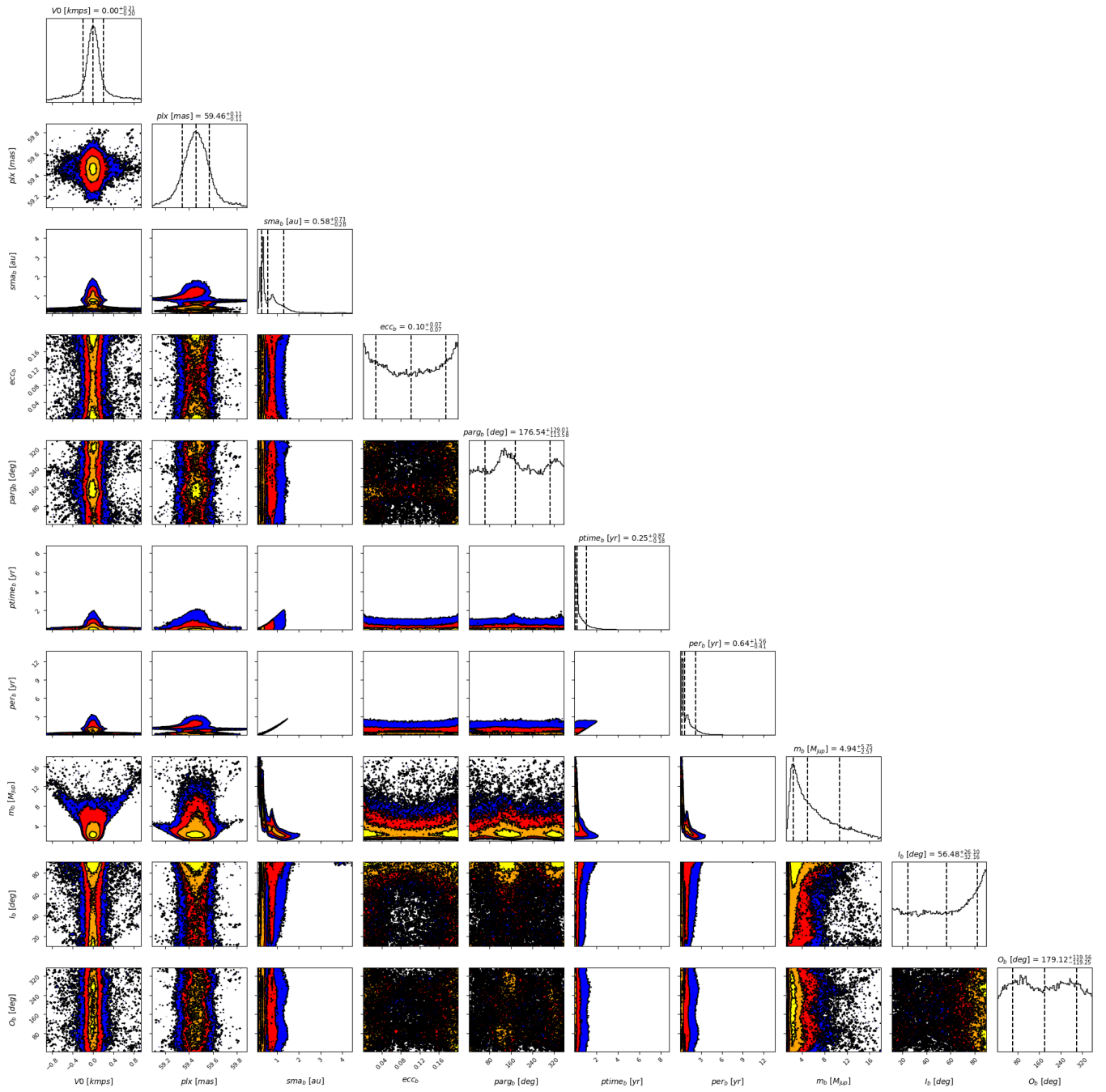


**Fig. E.1.** MCMC results for G80-21. See Text.